University of Iceland
Faculty of Natural Sciences
Department of Physics

RH-09-2004

Grid-Free Ground State of Molecules and Transport in Nanosystems

by

Jens Hjörleifur Bárðarson

A thesis submitted in partial satisfaction of the
requirements for the degree of
Master of Science in Physics at the University of Iceland

Committee in charge:
Prof. Viðar Guðmundsson, Chair
Dr. Andrei Manolescu

Reykjavík
June 2004

Grid-Free Ground State of Molecules and Transport in Nanosystems

Abstract

To model transport through molecules one needs a description of the molecule and a transport formalism. We have implemented a grid-free DFT method to obtain the ground state of a molecule and devised a transport formalism based on the Lippmann-Schwinger equation, the integral equation of scattering. The conductance of a quasi-one-dimensional quantum wire is calculated by connecting the transport formalism with the Landauer equation.

Ágrip

Ef reikna skal straum í gegnum sameind er nauðsynlegt að hafa góða lýsingu á sameindinni sem og lýsingu á flutningi rafeinda. Við höfum notað netfrjálsar þéttnifellafræði (DFT) aðferðir til þess að finna grunnástand sameinda. Einnig höfum við sett saman lýsingu á flutningi sem byggir á heildisjöfnu úr dreififræði, svokallaðri Lippmann-Schwinger jöfnu. Flutningsfræðunum og tengingu þeirra við Landauer jöfnuna er beitt til þess að reikna leiðni í skammtavír.

Acknowledgments

The research presented in this MS thesis was carried out at the University of Iceland under the supervision of Prof. Viðar Guðmundsson. His enthusiasm for, constant interest in and knowledge of many areas of physics has been really inspiring; for that I acknowledge. I would also like to thank other members of the group, Andrei Manolescu and Sigríður Sif Gylfadóttir, with whom I have enjoyed communicating with.

I thank my family for their endless support, my girlfriend for being the best one could have, and Nick Cave for his music.

The research was partly funded by the Icelandic Natural Science Foundation (Rannsóknarsjóður Rannís), the Univeristy of Iceland Reasearch Fund (Rannsóknarsjóður HÍ), the Icelandic Natural Science Education Fund (Rannsóknanámssjóður) and the Nordic Academy for Advanced Study (NorFA).

Contents

Chapter 1

Introduction

Beginning with the invention of the transistor in 1947, the semiconductor industry has developed with almost continuous exponential growth, i.e. according to Moore's law [1, 2]. The original Moore's law [1] states that the number of transistors in the most complex integrated circuit grows exponentially with time. Many other parameters either increase or decrease exponentially with time, often as a consequence of the increased number of transistors (or vice versa), this exponential behavior also often being dubbed as Moore's law. As an important example the minimum feature size in production integrated circuits has decreased exponentially [2].

From the beginning the fact that this exponential growth will come to an end has always been considered a part of Moore's law. In his original paper, for example, Moore claims that "*there is no reason to believe [the rate of increase] will not remain nearly constant for at least 10 years*" [1]. In fact, it has continued at nearly the same rate until today since the industry has been able to find ways to circumvent technological barriers that have arisen. However, to cite Moore again, "*a new and more fundamental barrier must be confronted in the next couple of decades - the fact that materials are made of atoms and the technology is approaching atomic dimensions*" [2]. We are reaching the nanoscale, at which spectacular new effects become important and related fields, such as physics, chemistry and biology, have merged into something new. Something people find interesting enough to give it the name *nanotechnology*.[1] Interestingly enough, Richard P. Feynman had predicted that this field would come into being already in 1959 in a famous talk to the American Physical Society *There's Plenty of Room at the Bottom* [3].

[1] In the most positive sense of this word. The field is actually huge but at the *nano*scale.

Within nanotechnology there are various suggestions on how to keep Moore's law alive, so to speak. One of these has its roots in a paper from 1974 where it is suggested that a molecule can act as a rectifier [4]. As an extension one can imagine an integrated circuit where the building blocks are molecules. In 1997 Reed and coworkers reported measurements of the current through a single (or few) molecule [5], igniting a tremendous interest in what has since become to be known as *molecular electronics*. Throughout the world people began to devise experimental techniques to measure the current through a single molecule [6–9], and to model the conductance of a molecule connected to two leads [10–12].

The field of molecular electronics is still in its infancy and even though the possible applications can be quite important one should not forget that just the physics itself of these systems is interesting enough to warrant further examination. The length scales involved are so small that quantum mechanics is of central importance in modeling the conductance. This is in stark contrast to the semiclassical models often used to model for example the conductance of a macroscopic metal. In combination with the molecule, which by itself constitutes an important nanosystem in which the electron-electron interaction is of paramount interest, we have a system rich of interesting physical effects, yet to be fully understood. In this thesis we report our first steps in a journey towards a complete understanding of these systems.

The ground state of an isolated molecule is usually obtained within the density functional theory (DFT). We have implemented a grid-free version of DFT to obtain the ground state of a molecule, the description of which constitutes the first part of this thesis (cf. Chapter 2). In the second part of the thesis, which concerns itself with conductance, we adapt the successful viewpoint of Landauer, in which conductance is viewed as transmission [13]. In Chapter 3 we therefore describe the Lippmann-Schwinger (LS) equation and how it is used to obtain transmission coefficients. We begin with the simplest 1D case and then extend our discussion to the case where a nanosystem is connected by two semi-infinite wires. The resulting formalism is applied to the special test case of a quasi-one-dimensional quantum wire. The formalism is in principle applicable to the simplest case in molecular electronics, i.e. a molecule bridging two leads. In Chapter 4 we briefly review the field of molecular electronics and discuss how one could possibly use the results of Chapters 2 and 3 to obtain the conductance of a molecule, the problems that could arise and how they might be solved.

Chapter 2

DFT ground state

In this chapter we explain how to obtain the ground state of a molecule. We apply the density functional theory (DFT) using a grid-free method for the exchange and correlation. The theorems of Kohn, Hohenberg and Sham are reviewed in Section 2.1. It can be useful to picture the electronic structure of a molecule as being built up by molecular orbitals. This concept and its validity in DFT is explored in Section 2.2. In the Kohn-Sham scheme the ground state density is obtained by solving a single-particle Schrödinger-like equation which can quite generally be transformed into a matrix eigenvalue equation by expansion in a functional basis set as explained in Section 2.3. Before solving these equations the basis set needs to be specified and the relevant matrices calculated as described in Sections 2.4 and 2.5 respectively. The matrices, however, depend on the solution of the equation, making the resulting equations highly non-linear. This is dealt with by solving these equations self-consistently by iteration as discussed in Section 2.6. In Section 2.7 some results of DFT calculations on a few small molecules are presented.

2.1 Density Functional Theory

Density functional theory is not just an approximate scheme for solving the many-body Schrödinger equation. Rather, DFT is a completely different, rigorous and formally exact approach to electronic structure theory, or more generally to any problem of many interacting particles. In this section we briefly review the basic theorems and approximation of DFT. We do not intend to be complete or self-contained in our discussion (for a good introduction see Ref. [14], for a more rigorous

but clear discussion see Ref. [15]).

2.1.1 The Hohenberg-Kohn Theorem and the Kohn-Sham Equation

According to the Hohenberg-Kohn (HK) theorem [16] the total energy of N Coulomb interacting[1] particles in an external potential $v_{\text{ext}}(\mathbf{r})$ (e.g. electrons in a molecule in the field of the nuclei), is a functional of the density $n(\mathbf{r})$

$$E[n] = G[n] + \frac{e^2}{4\pi\epsilon_0} \iint d^3r d^3r' \, \frac{n(\mathbf{r})n(\mathbf{r}')}{|\mathbf{r} - \mathbf{r}'|} + \int d^3r \, v_{\text{ext}}(\mathbf{r})n(\mathbf{r}), \tag{2.1}$$

and the correct ground state density is the density that minimizes this functional. In the above expression e is the magnitude of the electron charge, ϵ_0 is the permittivity of vacuum and the functional $G[n]$ is the universal functional that gives the sum of the kinetic energy and the non-classical part of the electron-electron interaction energy of electrons with density $n(\mathbf{r})$. The second term is the classical Coulomb interaction energy and the last term gives the energy due to the external potential. The functional $G[n]$ is universal in the sense that given a particle type and particle-particle interaction it is the same functional for all external potentials. The HK-theorem also assures us that the ground state expectation value of any operator is a functional of the ground state density [15]. Minimizing the energy functional would therefore in principle give the solution of the many-body problem. The HK-theorem assures us of the existence of the unknown functional $G[n]$ but does not tell us how to obtain it. It is here that it is paramount that the functional $G[n]$ is universal, since it then becomes practical to device approximations to it.

One could approximate the functional directly and Thomas-Fermi theory can be thought of as a special case of such an approximation. Approaches along these lines usually suffer from inaccurate treatment of the kinetic energy part. Kohn and Sham [17] proposed instead to separate from the functional G the kinetic energy T_s of non-interacting electrons with density $n(\mathbf{r})$, i.e. to write

$$G[n] = T_s[n] + E_{\text{xc}}[n]. \tag{2.2}$$

E_{xc} is called the exchange-correlation (XC) functional. Minimizing the energy func-

[1] The theorems can be generalized to any two particle interaction without complications.

tional using this definition of $G[n]$, one finds that the exact ground state density $n(\mathbf{r})$ of an arbitrary interacting system can be obtained by a self-consistent solution of the Kohn-Sham (KS) equations [15]

$$\left(-\frac{\hbar^2}{2m}\nabla^2 + \frac{e^2}{4\pi\epsilon_0}\int d^3r' \, \frac{n(\mathbf{r}')}{|\mathbf{r}-\mathbf{r}'|} + v_{\text{xc}}([n];\mathbf{r}) + v_{\text{ext}}(\mathbf{r})\right)\psi_i(\mathbf{r}) = \varepsilon_i\psi_i(\mathbf{r}) \tag{2.3}$$

where $\varepsilon_1 \leq \varepsilon_2 \leq \ldots$ and

$$n(\mathbf{r}) = \sum_{i=1}^{\infty} \gamma_i |\psi_i(\mathbf{r})|^2. \tag{2.4}$$

The occupation numbers γ_i satisfy

$$\gamma_i \begin{cases} = 1 & \varepsilon_i < \mu, \\ \in [0,1] & \varepsilon_i = \mu, \\ = 0 & \varepsilon_i > \mu, \end{cases} \tag{2.5}$$

where μ denotes the highest occupied single-particle level and

$$\sum_{i=1}^{\infty} \gamma_i = N. \tag{2.6}$$

The exchange-correlation potential v_{xc} is the functional derivative of the exchange-correlation functional

$$v_{\text{xc}}([n];\mathbf{r}) = \frac{\delta E_{\text{ext}}([n];\mathbf{r})}{\delta n}. \tag{2.7}$$

The wave functions ψ_i are often called Kohn-Sham orbitals. Apart from being the orbitals that make up the density of the system under study, the KS orbitals have no rigorous physical meaning [15].

What the above procedure amounts to is the introduction of an auxiliary system of non-interacting electrons in an external potential

$$V_s(\mathbf{r}) = \frac{e^2}{4\pi\epsilon_0}\int d^3r' \, \frac{n(\mathbf{r}')}{|\mathbf{r}-\mathbf{r}'|} + v_{\text{xc}}([n];\mathbf{r}) + v_{\text{ext}}(\mathbf{r}), \tag{2.8}$$

which has the same ground state density as the system of interacting electrons in the external potential $v_{\text{ext}}(\mathbf{r})$. Even though the ground state density is the same, the total energy is not the same in the two systems. In the auxiliary non-interacting system the total energy is just the sum of the eigenvalues of occupied orbitals, but

in the interacting system the total energy is [15]

$$E_0 = \sum_{i=1}^{\infty} \gamma_i \varepsilon_i - \frac{e^2}{8\pi\epsilon_0} \int d^3r d^3r' \, \frac{n(\mathbf{r})n(\mathbf{r}')}{|\mathbf{r}-\mathbf{r}'|} + E_{\mathrm{xc}}[n] - \int d^3r \, v_{\mathrm{xc}}([n];\mathbf{r})n(\mathbf{r}). \quad (2.9)$$

The unknown functional is now the XC-functional $E_{\mathrm{xc}}[n]$ and to proceed we need to make approximations to it. There exist many different methods for approximations. The oldest and most widely used approximation is the local density approximation (LDA) presented in Section 2.1.2. Methods that try to go beyond the LDA include nonlocal methods, inclusion of self-interaction corrections and gradient expansions. Gradient corrected functionals are in common use in chemistry but since we are really not interested in chemical accuracy we do not go further than using the simplest type of an LDA-approximation.

The Kohn-Sham equation is made abstract by defining a Kohn-Sham Hamiltonian by

$$\hat{H}_{\mathrm{KS}} = \hat{T} + \hat{V}_{\mathrm{Har}} + \hat{V}_{\mathrm{xc}} + \hat{V}_{\mathrm{ext}}. \quad (2.10)$$

The Kohn-Sham equation (2.3) is then seen to be the $\{|\mathbf{r}\rangle\}$-representation of the abstract Kohn-Sham equation

$$\hat{H}_{\mathrm{KS}} \, |\psi_i\rangle = \varepsilon_i \, |\psi_i\rangle \, . \quad (2.11)$$

This form of the equation will be useful in later manipulations.

There are subtle issues regarding the domain of the functionals and their exact definition. The density has of course to be positive, but not all positive functions are ground states of some Hamiltonian. Functions that are a ground state of some Hamiltonian are called *v-representable*. Since not all positive functions are v-representable one has to ask if one can extend the domain of the functionals to non v-representable functions. These are two examples of these subtle points that arise when one seeks to make DFT more rigorous. We will not go into these details but refer the interested reader to the book of Dreizler and Gross [15].

2.1.2 The Local Density Approximation

The local density approximation (LDA), a commonly applied approximation to the XC-functional, is defined by

$$E_{\mathrm{xc}}^{\mathrm{LDA}}[n] = \int \mathrm{d}^3 r \, n(\mathbf{r}) \epsilon_{\mathrm{xc}}(n(\mathbf{r})), \tag{2.12}$$

where ϵ_{xc} is the exchange and correlation energy per particle of a uniform electron gas of density n. The corresponding XC-potential becomes

$$v_{\mathrm{xc}}^{\mathrm{LDA}}([n];\mathbf{r}) = \left. \frac{\partial(n\epsilon_{\mathrm{xc}}(n))}{\partial n} \right|_{n \to n(\mathbf{r})}. \tag{2.13}$$

The local density approximation amounts to assuming that the XC-energy of a non-uniform system can be obtained by applying results from many-body theory of uniform electron gas to infinitesimal $\mathrm{d}^3 r$ portions of space and integrating. Kohn and Sham argued that this procedure is exact in the limit of slowly varying density and in the limit of high density [17]. Additionally, rather favorable results are obtained for highly inhomogeneous densities such as for atoms and molecules. This has partly to do with the fact that only the spherical average of the exchange-correlation hole enters the XC-energy, and LDA describes this spherical average quite well even though the overall description of the exchange-correlation hole is poor [15].

Long before the advent of density functional theory, Slater had introduced a local approximation to the Hartree-Fock equations that can be thought of as a special case of the local density approximation [18]; the difference being that Slater made his local approximation in the XC-potential rather than the XC-energy as Kohn and Sham [17]. Both these approximations give a local $X\alpha$ potential

$$v_{X\alpha}([n];\mathbf{r}) = -3\frac{e^2}{4\pi\epsilon_0}\alpha \left(\frac{3n(\mathbf{r})}{8\pi} \right)^{1/3} \tag{2.14}$$

where in Slaters approach $\alpha = 1$ but Kohn and Sham obtained $\alpha = \frac{2}{3}$. This ambiguity in where to apply the LDA approximation has led to use of α as an adjustable parameter. For atoms and molecules the value $\alpha \approx 0.75$ gives better results than both $\alpha = 1$ and $\alpha = \frac{2}{3}$ [14].

Many parameterizations of the XC-functional exist, most of them specified for the spin-polarized case [15]. These different parameterizations are based on various

approximations obtained in many-body or Monte-Carlo calculations. Even though use of a more advanced parameterizations is straightforward we have in this work only used the Slater $X\alpha$-potential and will thus not discuss these different parameterizations further.

2.2 The Concept of Molecular Orbitals in DFT

We now take a small detour to discuss the concept of molecular orbitals. Assuming for a moment that the electrons in a molecule do not interact with each other but only with the nuclei, the exact many-particle wave function would be a Slater determinant of single-particle functions (ignoring spin):

$$\Psi(\mathbf{r}_1, \ldots, \mathbf{r}_N) = \frac{1}{\sqrt{N!}} \begin{vmatrix} \psi_1(\mathbf{r}_1) & \psi_1(\mathbf{r}_2) & \ldots & \psi_1(\mathbf{r}_N) \\ \psi_2(\mathbf{r}_1) & \psi_2(\mathbf{r}_2) & \ldots & \psi_2(\mathbf{r}_N) \\ \vdots & \vdots & \ddots & \vdots \\ \psi_N(\mathbf{r}_1) & \psi_N(\mathbf{r}_2) & \ldots & \psi_N(\mathbf{r}_N) \end{vmatrix}, \tag{2.15}$$

where ψ_i is an eigenfunction of the single-particle Schrödinger equation describing an electron in the field of the nuclei. We can thus picture the electron distribution of the molecule as being built up of orbitals, each containing a single electron (two in case of spin). This is of course the same picture as the atomic orbital picture that Bohr had of the atom. In correspondence, we therefore call the eigenfunctions ψ_i *molecular orbitals*.

There is of course no such thing as molecules with non-interacting electrons. If we, however, search for the Slater-determinant that minimizes the energy of interacting electrons in a molecule, we obtain the Hartree-Fock (HF) equations for the single particle wave functions. These equations can be thought of as describing the electrons as non-interacting but moving in an effective single-particle potential which is a mean field of the electron-electron interaction. By construction there corresponds a single occupied wave function ψ_i to each electron and the concept of molecular orbitals is therefore still well-defined.

Now, we know that the exact wave function of an interacting many-particle system can not in general be written as a single Slater determinant, but is rather a linear combination of such determinants. In this case we need more single-particle wave functions to construct the ground state wave function than there are electrons,

and the concept of molecular orbitals becomes ill-defined.

So, what about the concept of molecular orbitals in DFT? Well, DFT is not a wave function approach but rather a completely different approach. However, in the Kohn-Sham scheme the single-particle Kohn-Sham orbitals are well defined, and are the single-particle orbitals that, if doubly occupied, give the correct density of the system. We can therefore assign a single electron to a given Kohn-Sham orbital and the concept of molecular orbitals becomes well-defined again. There are small conceptual differences since the Kohn-Sham orbitals do not have a rigorous physical meaning, but by our definition the concept of molecular orbitals is rigorous and exact. In the literature the Kohn-Sham orbitals are often used, without real justification, as the real molecular orbital. Comparison with experiments can justify this procedure in some cases, but debate remains on this.

In the following we use the concept of molecular orbital extensively. Note also, that if the molecule contains only one nucleus, i.e. the molecule is an atom, we talk of *atomic orbitals* as usual.

2.3 Expansion in a Basis

We will now show how we can generally transform an abstract eigenvalue equation

$$\hat{H} \left|\psi_i\right\rangle = \varepsilon_i \left|\psi_i\right\rangle , \tag{2.16}$$

where $\hat{H}$ is a Hermitian operator, into a matrix equation by expansion in a basis. Later we will set the operator $\hat{H}$ to the Kohn-Sham Hamiltonian but generally it could be any Hermitian operator (or actually any operator, but Hermitian operators have good properties like real eigenvalues etc.).

We introduce a complete basis $\{\left|\phi_\mu\right\rangle \left|\mu = 1, 2, \ldots\right.\}$ which is not restricted to be orthogonal, but rather the basis elements are allowed to overlap with an overlap matrix

$$S_{\nu\mu} = \left\langle\phi_\nu\right| \left.\phi_\mu\right\rangle. \tag{2.17}$$

The overlap matrix is Hermitian and can be shown to be positive-definite [19].

Expanding the ket $\left|\psi_i\right\rangle$ in our basis

$$\left|\psi_i\right\rangle = \sum_\mu c_{\mu,i} \left|\phi_\mu\right\rangle , \tag{2.18}$$

substituting into the eigenvalue equation (2.16) and projecting onto $\langle\phi_\nu|$ we obtain

$$\sum_\mu c_{\mu,i} H_{\nu\mu} = \varepsilon_i \sum_\mu c_{\mu,i} S_{\nu\mu}, \qquad \mu = 1, 2, \ldots \tag{2.19}$$

where

$$H_{\nu\mu} = \langle\phi_\nu| \hat{H} |\phi_\mu\rangle . \tag{2.20}$$

These equations can be seen to be a generalized matrix eigenvalue problem

$$H\mathbf{c}_i = \varepsilon_i S\mathbf{c}_i \tag{2.21}$$

of infinite dimension and is equivalent to the original eigenvalue equation (2.16).

In practice we have to cut the basis at some value $\mu_{\max} = K$. The matrices H and S truncate to $K \times K$ square matrices and $\mathbf{c}_i$ is the $K \times 1$ column matrix of expansion coefficients. The resulting finite dimensional generalized eigenvalue equation can be solved by standard methods of linear algebra [19].

In the case of molecules the $|\psi\rangle$-s are the molecular orbitals. As discussed in Section 2.4, one would like to use atomic orbitals as a basis. The whole procedure above is then commonly called *Linear Combination of Atomic Orbitals* (LCAO). Since one rarely uses real atomic orbitals but at most atomic-like orbitals this terminology is somewhat inaccurate. When using Gaussian orbitals (cf. Section 2.4) a more accurate term would be *Linear Combination of Gaussian Type Orbitals* (LCGTO).

2.4 Gaussian Basis Set

When choosing a basis set, several things need to be considered, two important ones being accuracy and speed. The perfect basis should incorporate in some sense the behavior of the system and therefore converge with relatively small number of elements. It should be easily obtained, well defined, easily extended and matrix elements analytically doable. By easily extended we mean that one can easily enlarge it to test basis set convergence.

Plane waves, a common choice, satisfies many of the requirements of a perfect basis but in the case of atoms and molecules it has at least one important deficiency. Plane waves are delocalized and one therefore needs very many elements to describe the inhomogeneities of a molecule and this large number can limit the size of the

system to be treated.

A more physical choice is to use the observation that since molecules are made of atoms, one would expect the molecular orbitals to resemble the union of the atomic orbitals of its constituents. That is, a linear combination of atomic orbitals, each centered on the corresponding atomic center, should describe the system quite well.[2]

The real atomic orbitals are not easily obtained since they are solutions of a many-particle Schrödinger equation. Instead, one could think of using non-interacting atomic orbitals, i.e. the solutions of the Schrödinger equation of a single electron in the field of a nucleus with atomic number Z. These are the well known hydrogenic functions which in spherical coordinates centered at the nucleus can be written as

$$\phi_{nlm}^{\mathrm{Hyd}}(\mathbf{r}) = Y_{lm}(\theta,\phi)R_{nl}^{\mathrm{Hyd}}(r), \tag{2.22}$$

where Y_{lm} are the spherical harmonics and the radial functions are given by

$$R_{nl}^{\mathrm{Hyd}}(r) = \left[\frac{4Z^3}{a_0^3 n^4}\frac{(n-l-1)!}{(n+l)!}\right]^{l/2}\left(\frac{2Zr}{na_0}\right)^l \exp\left(-\frac{Zr}{na_0}\right) L_{n-l-1}^{2l+1}\left(\frac{2Zr}{na_0}\right). \tag{2.23}$$

L_{n-l-1}^{2l+1} are the associated Legendre polynomials, a_0 the Bohr radius and n, l and m the conventional hydrogenic quantum numbers. The hydrogenic basis is well defined and easily extended but matrix elements between basis elements on different atoms include many different centers (in the Hartree term one can have up to four different centers) and can be impossible to do analytically. This makes the hydrogenic basis unfeasible.

The complicated nodal structure of the Legendre polynomials makes the basis orthogonal on a single center, but since we have multiple centers the elements do overlap anyhow. There is therfore no need to keep this complicated nodal structure, and one can retain only the highest power of r and allow the exponent in the exponential to vary. This procedure leads to the Slater type orbitals (STO) [20]. Even with their simplified structure the STO's matrix elements are difficult to do analytically.

In 1950 Boys proposed the use of Gaussian functions (Gaussian times a polynomial) and showed that with their use all Hartree-Fock matrix elements could be done analytically [21]. We will not try to review the large number of Gaussian basis sets

[2]Even though the Kohn-Sham orbitals do not have a rigorous physical meaning, resemblance with the Hartree equation and results from calculations indicate that this is also a good idea in LDA DFT calculations.

available in the literature but rather only describe the general features of the kind of basis we have chosen to use (for a general review of Gaussian basis set see Ref. [20] and [22], a good review of the basis set we use along with general considerations in molecular orbital theory can be found in Ref. [23]).

For each atom in a molecule we define a set of Cartesian Gaussian functions that in a coordinate system centered on the corresponding atom can be written

$$g(\mathbf{r};\mathbf{n},\zeta) = \mathcal{N}(\mathbf{n},\zeta)x^{n_x}y^{n_y}z^{n_z}\exp(-\zeta r^2), \tag{2.24}$$

where $\mathbf{n} = (n_x, n_y, n_z)$ is a set of nonnegative integers and ζ is the exponent of the Gaussian. $\mathcal{N}$ is a normalization constant. The sum $n_x + n_y + n_z$ is closely related to the total angular momentum quantum number and is therefore often refered to as *the angular momentum*. Correspondingly $\mathbf{n}$ is refered to as the *the angular momentum index*. In the spirit of the above, Cartesian functions with angular momentum $0, 1, 2, \ldots$ are termed $s-, p-, d-, \ldots$ type functions respectively.

Explicitly, the Cartesian Gaussian functions of the lowest angular momentum are

$$g_s(\zeta,\mathbf{r}) = \left(\frac{2\zeta}{\pi}\right)^{3/4}\exp(-\zeta r^2), \tag{2.25}$$

$$g_{p_x}(\zeta,\mathbf{r}) = \left(\frac{128\zeta^5}{\pi^3}\right)^{1/4} x\exp(-\zeta r^2), \tag{2.26}$$

$$g_{d_{x^2}}(\zeta,\mathbf{r}) = \left(\frac{2048\zeta^7}{9\pi^3}\right)^{1/4} x^2\exp(-\zeta r^2) \tag{2.27}$$

and so on for g_{p_y}, g_{p_z}, $g_{d_{y^2}}$, $g_{d_{z^2}}$, $g_{d_{xy}}$, $g_{d_{xz}}$ and $g_{d_{yz}}$. Here, we have replaced the angular momentum index with the commonly used spectroscopic notation. Note that the six d-type Gaussian orbitals do not have the same angular symmetry as the hydrogenic orbitals (i.e. as the spherical harmonics) but can be linearly combined to obtain the set of five d-type spherical harmonics. The sixth linear combination

$$g_{r^2} = \sqrt{5}(g_{x^2} + g_{y^2} + g_{z^2}) \tag{2.28}$$

yields an s-type function.

A single Gaussian does not mimic the behavior of an atomic orbital very well and many elements are needed if one uses single Gaussians as basis elements. Instead

one can use a fixed linear combination of Gaussian type orbitals as basis functions. An s-type function would then be expanded in terms of s-type Gaussians, p-type in terms of p-type Gaussians etc., such that our basis elements become

$$\phi_{nl}(\mathbf{r}) = \sum_{k=1}^{N_{nl}} d_{nl,k} g_l(\zeta_{n,k}, \mathbf{r}), \tag{2.29}$$

where N_{nl} is the number of Gaussians. The terminology used for this combination is *contracted* Gaussian and N_{nl} is called the *length of the contraction*. In this context, a single Gaussian is sometimes called a *primitive* Gaussian. Throughout the calculations the coefficients $d_{nl,k}$ and $\zeta_{n,k}$ are kept fixed. We should note that neither single Gaussians or any finite linear combination of Gaussians have the correct exponential tail or satisfy the nuclear cusp condition [20]. In spite of this, relatively few contracted Gaussians are needed for a given level of accuracy, in fact even fewer than the number of Slater type orbitals needed [22].

A minimal basis set would contain one s-type function for each hydrogen (H) and helium (He) atom and two s-type and three p-type functions for the first row elements lithium (Li) to neon (Ne). In such a minimal basis there is only a single function of each symmetry (e.g. $1s$, $2s$ and $2p_x$) and the basis cannot expand and contract in response to different molecular environments. Since it is mostly the valence electrons that are responsible for bonding in a molecule, we give the basis more adaptability by using two valence functions of each symmetry (see Figure 2.1(a)), one that is more *contracted* and one more *diffuse*. Only one function is used to describe the quite inert core electrons. Basis sets of this kind are in the literature termed *split-valence basis set*.

The basis elements are all centered on the atoms but in a molecule the charge can move non-uniformly from the atoms, i.e. the molecule can polarize. To allow the basis to take this effect into account we add basis functions of higher symmetry; three p-type functions for H and He and the six d-type functions for the first row elements. In the case of hydrogen, for example, one can see that a mixture of say a s-type function and a p_x-type displaces the center of the basis function along the x-axis (cf. Figure 2.1(b)). Basis functions like these are called *polarization functions* and the basis a *polarization basis set*.

We are now in position to completely specify the basis sets we use. They are polarization split-valence basis sets introduced by Pople *et al.* [24–26], called 6-

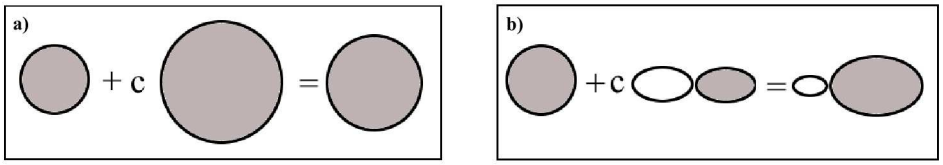

Figure 2.1: Schematic view of a) how split-valence set allow the basis set to expand and contract in response to different molecular environments and b) how addition of polarization functions can allow for displacement of the center of the basis functions.

31G, 6-31G* and 6-31G**. The number 6 means that the core basis functions are contractions of six primitive Gaussians ($N_{nl} = 6$), 31 means that one of the split valence functions is a contraction of three Gaussians ($N_{nl} = 3$) and the other a single Gaussian ($N_{nl} = 1$). The first star stands for addition of polarization functions on the heavier elements and the second star denotes addition of polarization functions for H and He. So, for hydrogen and helium, which have only valence electrons, the basis elements are

$$\phi'_{1s}(\mathbf{r}) = \sum_{k=1}^{3} d'_{1s,k} g_s(\zeta'_{1k}, \mathbf{r}) \tag{2.30}$$

$$\phi''_{1s}(\mathbf{r}) = g_s(\zeta''_{1s}, \mathbf{r}) \tag{2.31}$$

with three single Gaussians as polarization functions

$$\phi_{2p_{x/y/z}}(\mathbf{r}) = g_{p_{x/y/z}}(\zeta_p, \mathbf{r}). \tag{2.32}$$

Note that all the polarization functions have the same exponent. The first row elements have basis set functions

$$\phi_{1s}(\mathbf{r}) = \sum_{k=1}^{6} d_{1s,k} g_s(\zeta_{1k}, \mathbf{r}), \tag{2.33}$$

$$\phi'_{2s}(\mathbf{r}) = \sum_{k=1}^{3} d'_{2s,k} g_s(\zeta'_{2k}, \mathbf{r}), \tag{2.34}$$

$$\phi'_{2p_{x/y/z}}(\mathbf{r}) = \sum_{k=1}^{3} d'_{2p,k} g_{p_{x/y/z}}(\zeta'_{2k}, \mathbf{r}), \tag{2.35}$$

$$\phi''_{2s}(\mathbf{r}) = g_s(\zeta''_{2k}, \mathbf{r}), \tag{2.36}$$

$$\phi''_{2p_{x/y/z}}(\mathbf{r}) = g_{p_{x/y/z}}(\zeta''_{2k}, \mathbf{r}). \tag{2.37}$$

Note that $2s$ and $2p$ share Gaussian exponents ζ'_{2k} and ζ''_{2k}. The polarization functions for the first row elements are

$$\phi_{3d_{x^2/y^2/z^2/xy/xz/yz}}(\mathbf{r}) = g_{d_{x^2/y^2/z^2/xy/xz/yz}}(\zeta_d, \mathbf{r}). \tag{2.38}$$

All the polarization functions have, again, the same exponent.

We could use the atomic ϕ functions directly, but to take account of changes in the size of the atoms in a molecular environment the valence shell atomic orbitals are rescaled

$$\phi^{\text{molecule}}(\mathbf{r}) = \gamma^{3/2}\phi^{\text{atom}}(\gamma\mathbf{r}). \tag{2.39}$$

Inner shells remain unscaled.

To complete our specification of the basis we need the values of the scaling factors γ, the contraction coefficients d and exponents ζ. The values for the unpolarized basis are obtained by minimizing the spin-unrestricted Hartree-Fock energy of a single atom over the parameter space of d and α [24, 25]. The polarization exponents are then found by using these values, adding polarization functions and finding the optimum value of the polarization exponent for a set of small molecules. A suitable average, that gives good results in most molecules, is then chosen [26]. The scaling factors are also obtained by optimizing the scaling factor on some representive small molecules and choosing a suitable average [24].

Since much of our work is done in an abstract state space we define kets for the basis set,

$$|\phi_{nl}\rangle = \sum_{k=1}^{N_{nl}} d_{nl,k} \left|g_l(\zeta_{n,k})\right\rangle . \tag{2.40}$$

The $\{\mathbf{r}\}$-representation of these kets are the Gaussian functions described above.

2.4.1 A Closer Look at the 6-31G Family of Basis Sets

To get a better feel for the basis set we will now compare it with the more familiar hydrogenic basis set. We begin by reminding ourselves of the explicit form of the

first few spherical harmonics [20]

$$\begin{aligned} Y_0^0(\theta,\varphi) &= \frac{1}{2\sqrt{\pi}}, \\ Y_1^{\pm 1}(\theta,\varphi) &= \mp\frac{1}{2}\sqrt{\frac{3}{2\pi}}\sin\theta\exp(\pm i\varphi), \\ Y_1^0(\theta,\varphi) &= \frac{1}{2}\sqrt{\frac{3}{\pi}}\cos\theta. \end{aligned} \tag{2.41}$$

By use of these the Gaussian primitives become

$$\begin{aligned} g_s(\zeta,\mathbf{r}) &= Y_0^0(\theta,\varphi)2\frac{(2\zeta)^{3/4}}{\pi^{1/4}}\exp(-\zeta r^2) \\ &= Y_0^0(\theta,\varphi)R_s^{\mathrm{GTO}}(\zeta,r), \\ g_{p_x}(\zeta,\mathbf{r}) &= \frac{1}{\sqrt{2}}\left(Y_1^{-1}(\theta,\varphi) - Y_1^1(\theta,\varphi)\right)\left(\frac{2048\zeta^5}{9\pi}\right)^{1/4} r\exp(-\zeta r^2) \\ &= \frac{1}{\sqrt{2}}\left(Y_1^{-1}(\theta,\varphi) - Y_1^1(\theta,\varphi)\right)R_p^{\mathrm{GTO}}(\zeta,r), \\ g_{p_y}(\zeta,\mathbf{r}) &= \frac{i}{\sqrt{2}}\left(Y_1^{-1}(\theta,\varphi) + Y_1^1(\theta,\varphi)\right)\left(\frac{2048\zeta^5}{9\pi}\right)^{1/4} r\exp(-\zeta r^2) \\ &= \frac{i}{\sqrt{2}}\left(Y_1^{-1}(\theta,\varphi) + Y_1^1(\theta,\varphi)\right)R_p^{\mathrm{GTO}}(\zeta,r), \\ g_{p_z}(\zeta,\mathbf{r}) &= Y_1^0(\theta,\varphi)\left(\frac{2048\zeta^5}{9\pi}\right)^{1/4} r\exp(-\zeta r^2) \\ &= Y_1^0(\theta,\varphi)R_p^{\mathrm{GTO}}(\zeta,r). \end{aligned} \tag{2.42}$$

The Gaussian and hydrogenic basis functions differ effectively only in the radial part, the angular part of the Gaussians being a simple linear combination of the spherical harmonics. The contracted Gaussians can now be written

$$\begin{aligned} \phi_{1s}(\mathbf{r}) &= Y_0^0(\theta,\varphi)\sum_{k=1}^{6} d_{1s,k}R_s^{\mathrm{GTO}}(\zeta_{1k},r) \\ &= Y_0^0(\theta,\varphi)R_{1s}^{\mathrm{GTO}}(r), \\ \phi'_{2p_x}(\mathbf{r}) &= \frac{1}{\sqrt{2}}\left(Y_1^{-1}(\theta,\varphi) - Y_1^1(\theta,\varphi)\right)\sum_{k=1}^{3} d'_{2p,k}R_p^{\mathrm{GTO}}(\zeta'_{2k},r) \\ &= \frac{1}{\sqrt{2}}\left(Y_1^{-1}(\theta,\varphi) - Y_1^1(\theta,\varphi)\right)R_{2p}^{\mathrm{GTO}'}(r). \end{aligned} \tag{2.43}$$

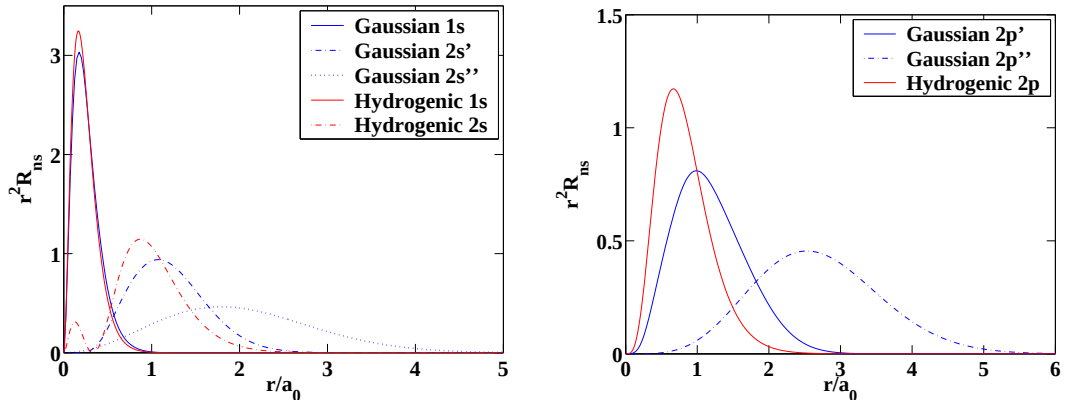

Figure 2.2: Comparison of the radial distribution function $r^2R_{nl}^2$ for the 6-31G family of basis sets and the hydrogenic basis. This specific example is for the basis elements of carbon.

Similar definitions hold for other basis elements.

With these definitions we can graphically compare the radial distribution functions $r^2R_{nl}^2$ of the 6-31G basis and the hydrogenic basis (cf. Figure 2.2). The first thing to notice is the absence of the nodal structure in the Gaussian basis set. As we have already mentioned, the main purpose of this structure is to make the basis elements orthogonal. If nodal structure would really be needed it could be reintroduced into the wave function by the linear combination. The second thing to notice is that the core functions are quite similar to their hydrogenic counterparts reflecting the inertness of the core electrons in a molecular environment. The valence orbitals are quite different, however, and not only in the sense that we have split-valence. One should remember that the Gaussian basis elements are obtained by minimizing the Hartree-Fock energy and therefore incorporate in some sense the electron-electron interaction. This interaction is seen to push the electrons a little bit further out from the nuclei making the valence functions more diffuse than in the noninteracting hydrogenic case.

2.5 Obtaining the Kohn-Sham Matrix

Having specified the basis we can use the procedure described in Chapter 2.3 with the Kohn-Sham Hamiltonian (2.10) to solve the Kohn-Sham equation (2.11) for a molecule. To avoid getting lost in the notation we simplify it even further, using

only one Greek index to number the basis elements

$$|\phi_\mu\rangle = \sum_{k=1}^{N_\mu} d_{\mu,k} \, |g_\mu(\zeta_{\mu,k})\rangle \, , \tag{2.44}$$

where there is a one-to-one map between the index μ and the basis element type (i.e. $1s$, $2s$ etc.) and atomic center.

The matrix elements of the Kohn-Sham Hamiltonian are written in terms of matrix elements of primitive Gaussians by inserting the contraction of the basis elements. For single particle operators $\hat{V}$ (such as $\hat{T}$ and $\hat{V}_{\text{ext}}$) we obtain

$$\langle \phi_\mu | \, \hat{V} \, | \phi_\nu \rangle = \sum_{k=1}^{N_\mu} \sum_{l=1}^{N_\nu} d_{\mu,k} d_{\nu,l} \, \langle g_\mu(\zeta_{\mu,k}) | \, \hat{V} \, | g_\nu(\zeta_{\nu,l}) \rangle \, , \tag{2.45}$$

since the contraction coefficients d are real. In the case of molecules we apply the Born-Oppenheimer approximation which amounts to assuming that the nuclei are kept fixed in space while solving for the electronic structure. The external potential is then the field of the fixed nuclei

$$U_{\text{nucl}} = \sum_\alpha \frac{Z_\alpha}{4\pi\epsilon_0} \frac{-e^2}{|\mathbf{r} - \mathbf{R}_\alpha|} = \sum_\alpha U_{\text{nucl}}(\mathbf{R}_\alpha), \tag{2.46}$$

where Z_α is the atomic number of nucleus with center $\mathbf{R}_\alpha$. The sum is over all the nuclei in the molecule. The matrix elements of the nuclear attraction potential become

$$\langle \phi_\mu | \, \hat{U}_{\text{nucl}} \, | \phi_\nu \rangle = \sum_{k=1}^{N_\mu} \sum_{l=1}^{N_\nu} d_{\mu,k} d_{\nu,l} \sum_\alpha \langle g_\mu(\zeta_{\mu,k}) | \, \hat{U}_{\text{nucl}}(\mathbf{R}_\alpha) \, | g_\nu(\zeta_{\nu,l}) \rangle \, . \tag{2.47}$$

The classical part of the electron-electron interaction is described by the Hartree operator

$$V_{\text{Har}}(\mathbf{r}) = \frac{e^2}{4\pi\epsilon_0} \int d^3r' \, \frac{n(\mathbf{r}')}{|\mathbf{r} - \mathbf{r}'|}. \tag{2.48}$$

Assuming zero temperature the electron density is given by

$$n(\mathbf{r}) = \sum_{i,\text{occ}} |\psi_i(\mathbf{r})|^2 \, , \tag{2.49}$$

which through expansion (2.18) becomes

$$n(\mathbf{r}) = \sum_{i,\mathrm{occ}} \sum_{\lambda\sigma} c_{\lambda,i} c_{\sigma,i} \phi_\lambda(\mathbf{r}) \phi_\sigma(\mathbf{r}), \tag{2.50}$$

where we have used the fact that the expansion coefficients and basis elements are real. The matrix elements of $\hat{V}_{\mathrm{Har}}$ can by use of the contraction therefore be written in terms of primitive Cartesian Gaussians as

$$\begin{aligned} \langle \phi_\mu | \hat{V}_{\mathrm{Har}} | \phi_\nu \rangle = \sum_{i,\mathrm{occ}} \sum_{\lambda\sigma} c_{\lambda,i} c_{\sigma,i} \sum_{k=1}^{N_\mu} \sum_{l=1}^{N_\nu} \sum_{m=1}^{N_\lambda} \sum_{n=1}^{N_\sigma} d_{\mu,k} d_{\nu,l} d_{\lambda,m} d_{\sigma,n} \\ \times \langle g_\mu(\zeta_{\mu,k}) g_\nu(\zeta_{\nu,l}) | \, | g_\lambda(\zeta_{\lambda,m}) g_\sigma(\zeta_{\sigma,n}) \rangle \, , \end{aligned} \tag{2.51}$$

where we have introduced the Gaussian electron repulsion integral (ERI)

$$\begin{aligned} &\langle g_\mu(\zeta_{\mu,k}) g_\nu(\zeta_{\nu,l}) | \, | g_\lambda(\zeta_{\lambda,m}) g_\sigma(\zeta_{\sigma,n}) \rangle = \\ &\frac{e^2}{4\pi\epsilon_0} \iint d^3r d^3r' \, \frac{g_\mu(\zeta_{\mu,k}, \mathbf{r}) g_\nu(\zeta_{\nu,l}, \mathbf{r}) g_\lambda(\zeta_{\lambda,m}, \mathbf{r}') g_\sigma(\zeta_{\sigma,n}, \mathbf{r}')}{|\mathbf{r} - \mathbf{r}'|}. \end{aligned} \tag{2.52}$$

By introduction of a density-matrix

$$P_{\lambda\sigma} = \sum_{i,\mathrm{occ}} c_{\lambda,i} c_{\sigma,i}, \tag{2.53}$$

the matrix element is reduced to

$$\begin{aligned} \langle \phi_\mu | \hat{V}_{\mathrm{Har}} | \phi_\nu \rangle = \sum_{\lambda\sigma} P_{\lambda\sigma} \sum_{k=1}^{N_\mu} \sum_{l=1}^{N_\nu} \sum_{m=1}^{N_\lambda} \sum_{n=1}^{N_\sigma} d_{\mu,k} d_{\nu,l} d_{\lambda,m} d_{\sigma,n} \\ \times \langle g_\mu(\alpha_{\mu,k}) g_\nu(\alpha_{\nu,l}) | \, | g_\lambda(\alpha_{\lambda,m}) g_\sigma(\alpha_{\sigma,n}) \rangle \, . \end{aligned} \tag{2.54}$$

We have so far managed to reduce the first three terms of the Kohn-Sham matrix to a sum of matrix elements of primitive Gaussians which, as Boys had shown, can be done analytically. Instead of doing the integrals directly the matrix elements are obtained with recursive relations by Obara and Saika [27] which are reviewed in Appendix A.

The remaining term in the KS-matrix is the XC-potential. This potential is usually quite a complicated function of the density (the leading term is the density to power one third) and a straightforward insertion of the expansion of the density in

the basis elements will lead to powers of large sums which are not easily treated. Instead, people often either do the integration numerically or expand the XC-potential in an auxiliary basis. Neither of these methods are ideal (no method is), the former can suffer from numerical noise and be time consuming. In the latter one needs to introduce an auxiliary basis but might still have to do difficult integrals. Ideally, one would like to do the XC-matrix elements analytically as all the other elements. This can actually be done by using matrix manipulations, described in the next subsection, which only require integrals of primitive Gaussians. We have thereby managed to obtain the KS-matrix by analytical methods by the use of contracted Gaussians.

2.5.1 Grid-free Method

The grid-free method described here was advocated in 1993 by Zheng and Almlöf [28] and later taken up by Berghold *et al.* [29]. We will begin by discussing the method generally and end with the specific case of our basis.

Assume we want to calculate matrix elements of the form

$$\langle \chi_\mu | \, f(\hat{n}) | \chi_\nu \rangle = \int d^3r \, \chi_\mu(\mathbf{r}) f(n(\mathbf{r})) \chi_\nu(\mathbf{r}) \tag{2.55}$$

where f is any function of n, for example the Slater Xα-potential

$$f(n(\mathbf{r})) = v_{\mathrm{X}\alpha}(\mathbf{r}) = -3\frac{e^2}{4\pi\epsilon_0}\alpha \left(\frac{3n(\mathbf{r})}{8\pi} \right)^{1/3}, \tag{2.56}$$

and the kets $\{|\chi\rangle\}$ can belong to any complete basis.

Think of the density as a multiplicative operator, such that

$$M_{\mu\nu}[n] = \langle \chi_\mu | \hat{n} | \chi_\nu \rangle = \int d^3r \, \chi_\mu(\mathbf{r}) n(\mathbf{r}) \chi_\nu(\mathbf{r}). \tag{2.57}$$

Note that the matrix of density M is not the same thing as the density matrix. Transforming our basis into an orthogonal basis with a transformation matrix X, satisfying

$$X^\dagger S X = 1, \tag{2.58}$$

the matrix of density transforms as

$$\tilde{M}[n] = X^{\dagger} M[n] X. \tag{2.59}$$

In the orthogonal basis $\tilde{M}$ is diagonalized by a unitary matrix U, such that

$$\tilde{M}[n] = U \Lambda U^{\dagger}, \tag{2.60}$$

where Λ is a diagonal matrix of eigenvalues of $\tilde{M}$. By standard linear algebra[3]

$$f(\tilde{M}[n]) = U f(\Lambda) U^{\dagger}. \tag{2.61}$$

Transforming back to the original basis we obtain

$$f(M[n]) = SXU f(\Lambda)(SXU)^{\dagger} \tag{2.62}$$

where we have used that $S^{\dagger} = S$ and from (2.58) that

$$X^{-1} = X^{\dagger} S. \tag{2.63}$$

Now, one can show (assuming that f can be written as a Taylor series, cf. Appendix B) that since the basis is complete

$$M[f(n)] = f(M[n]), \tag{2.64}$$

and we obtain our final result

$$M[f(n)] = SXU f(\Lambda)(SXU)^{\dagger}. \tag{2.65}$$

In the above derivation we have often used the fact that the basis is complete. In molecular electronic structure calculations the basis sets used are usually especially made to describe the electronic structure of the molecules and there is no *a priori* reason for them to be also good in the above manipulations. Experience, however, shows that good results are obtained using the same basis sets [28, 30]. In the case of a contracted basis set it can be advantageous to uncontract it and carry on the

[3] In principle the matrices are infinite, which is not the case in standard linear algebra, but in practice they are truncated.

matrix manipulations in the uncontracted basis. At the end of the calculations one contracts the basis again to obtain the correct matrix elements [30]. This is the route we have chosen to follow.

In the uncontracted basis the elements of the matrix of density are

$$M_{\mu\nu}[n] = \langle g_\mu(\zeta_\mu)|\, \hat{n}\, |g_\nu(\zeta_\nu)\rangle = \int d^3r\, g_\mu(\zeta_\mu, \mathbf{r}) n(\mathbf{r}) g_\nu(\zeta_\nu, \mathbf{r}). \tag{2.66}$$

Inserting the density with the density matrix and using the contraction expansion this becomes

$$M_{\mu\nu}[n] = \sum_{\lambda\sigma} P_{\lambda\sigma} \sum_{m=1}^{N_\lambda} \sum_{n=1}^{N_\sigma} d_{\lambda,m} d_{\sigma,n} \left\langle g_\mu(\zeta_\mu) g_\lambda(\zeta_{\lambda,m}) g_\sigma(\zeta_{\sigma,n}) g_\nu(\zeta_\nu) \right\rangle, \tag{2.67}$$

where

$$\begin{aligned} &\langle g_\mu(\zeta_\mu) g_\lambda(\zeta_{\lambda,m}) g_\sigma(\zeta_{\sigma,n}) g_\nu(\zeta_\nu)\rangle = \\ &\qquad \int d^3r\, g_\mu(\zeta_\mu, \mathbf{r}) g_\lambda(\zeta_{\lambda,m}, \mathbf{r}) g_\sigma(\zeta_{\sigma,n}, \mathbf{r}) g_\nu(\zeta_\nu, \mathbf{r}) \end{aligned} \tag{2.68}$$

is a four center overlap matrix element. The four center overlap matrix is calculated by the same method as other matrix elements of primitive Gaussians (cf. Appendix A.1).

All that remains is to specify how we obtain the transformation matrix X. There are of course many solutions to Equation (2.58) corresponding to the many choices one has in orthogonalizing a given basis set. There are two ways that are in common use [19], *symmetric orthogonalization* that uses the inverse square root of S

$$X = S^{-1/2} \tag{2.69}$$

and *canonical orthogonalization*

$$X = U_S {\Lambda_S}^{-1/2} \tag{2.70}$$

where U_S is a matrix that diagonalizes S and Λ_S is the corresponding diagonal matrix of eigenvalues of S. It is easy to see by straightforward insertion that both of these choices are solutions. We have chosen to use the former one. If the basis is nearly linearly independent some of the eigenvalues of S can approach zero and

the procedure can be unstable. Our basis seems not to include these near linear dependencies.

2.6 A Self-consistent Solution of the Kohn-Sham Equation

We have shown how to obtain the Kohn-Sham matrix by analytical methods. The overlap matrix S is obtained similarly by insertion of the contraction

$$\langle \phi_\mu | \, \phi_\nu \rangle = \sum_{k=1}^{N_\mu} \sum_{l=1}^{N_\nu} d_{\mu,k} d_{\nu,l} \, \langle g_\mu(\zeta_{\mu,k}) | \, g_\nu(\zeta_{\nu,l}) \rangle. \tag{2.71}$$

All matrices needed for the solution of the Kohn-Sham equation (2.11) have therefore been obtained.

The Kohn-Sham matrix depends through the Hartree and XC-potential on the electron density n, i.e. it depends on the solution of the Kohn-Sham equation. We have therfore to solve the equation self-consistently (cf. Figure 2.3). We begin by obtaining an initial guess for the density matrix by solving the Kohn-Sham equation without electron-electron interaction for the molecule. This is not always a good guess and one could sometimes obtain a better result by using more advanced method to obtain an initial guess, like semi-empirical extended Hückel-type calculation [19]. Our non-interacting guess seems to be sufficient in the molecules we have calculated. Having obtained an initial guess, we calculate the Kohn-Sham matrix and solve the Kohn-Sham equation. If the solution is different from the initial guess, by some measure, we calculate a new Kohn-Sham matrix using the new solution or a blend of the new and old solution. This is repeated until convergence is obtained. We have used the mean square difference between eigenvalues in consecutive iterations as a measure of the convergence. Other measures can be used, such as the mean square difference of the density matrix.

2.7 Simple Test Cases for DFT

To confirm our DFT calculations we have tested it on some small molecules. Our main test was the water molecule were the total energy was minimized by par-

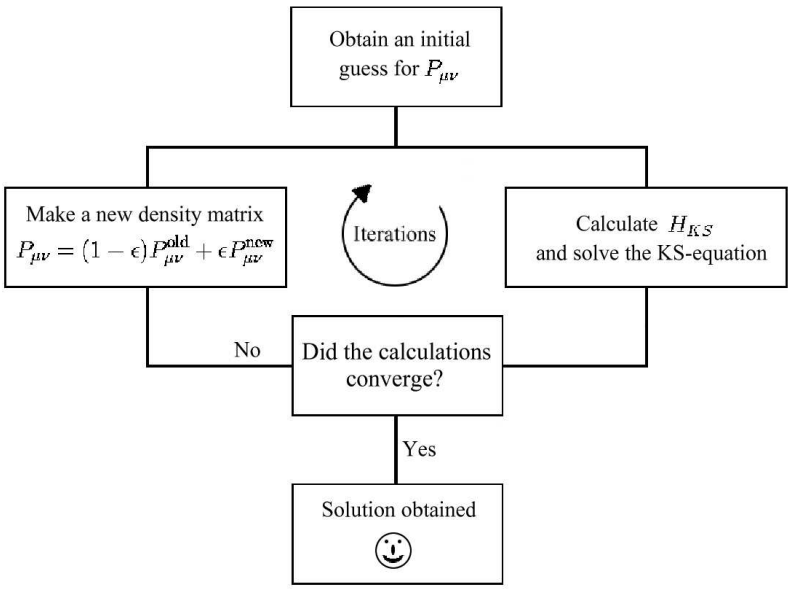

Figure 2.3: A schematic view of the self-consistency process. The process is described in more detail in the text.

tial geometrical optimization (cf. Section 2.7.1). In Section 2.7.2 we present total energy calculations on a couple of small molecules and compare them with other calculations. Finally, in Section 2.7.3 the ground state electron density, the highest occupied molecular orbital (HOMO) and the lowest unoccupied molecular orbital (LUMO) of a benzene molecule are visualized and analyzed.

2.7.1 Water as a Benchmark Molecule

As a reasonable benchmark for our DFT calculations we have chosen the water molecule (H_2O). The total energy at the experimental geometry falls between the energy obtained with Hartree-Fock and coupled cluster calculations (cf. Table 2.1). This is a trend that is also seen in other molecules and discussed in Section 2.7.2

Partial geometry optimizations were performed by minimizing the energy as a function of one of the degrees of freedom (R_{OH} or θ_{HOH}) keeping the other fixed at its experimental value. Figure 2.4 shows a plot of the energy as a function of the geometrical variables; exact values of the minima are found in Table 2.1. The experimental values fall between the values found using the 6-31G basis and the 6-31G** basis, the former giving higher values and the latter lower in both cases.

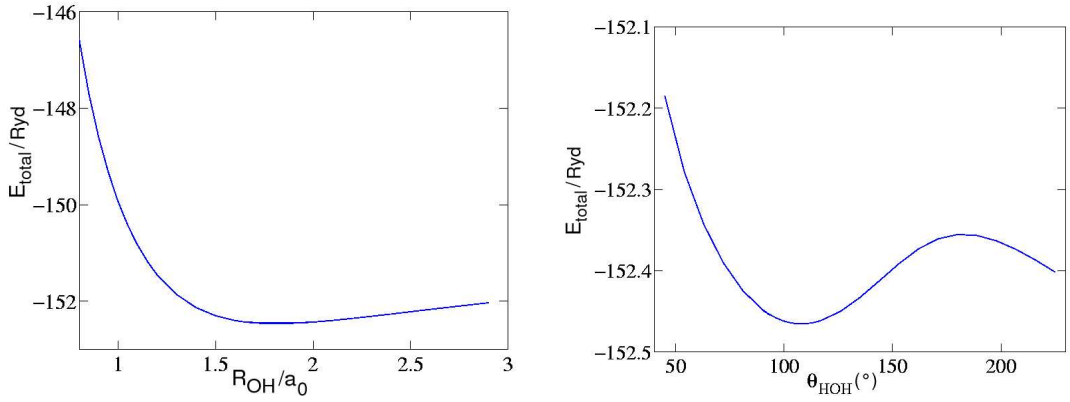

Figure 2.4: The total energy of a water molecule as a function of hydrogen-oxygen bond length (left) and as a function of bond angle (right). Only one geometrical variable is varied at a time, the other being held fixed at its experimental value. All calculations are made using the Slater $X\alpha$-potential with $\alpha = 0.75$.

Polarization functions are seen to be important to obtain the geometry reasonably, but we are still bit off in the bond length. Considering the simple approximation used for the XC-potential the results are acceptable.

It can be interesting to see how the electrons distribute themselves around the molecule, i.e. to visualize the electron density. Since the density is a function of the three spatial variables one has to either plot the density in a plane or plot an isosurface. In Figure 2.5 we have plotted a contour plot of the density of water in the plane of the nuclei using both the density and the density times the squared distance from the origin. The latter quantity includes the volume element of the spherical coordinates in the given plane.

The molecular orbitals of the water can be analyzed further by calculating the weight of the atomic orbitals in it. Since the atomic orbitals are non-orthogonal this

Table 2.1: Total energy, equilibrium bond angle and bond length of water. Calculation are made with the $X\alpha$-potential with $\alpha = 0.75$. The experimental values, Hartree-Fock and coupled cluster calculations are from Ref. [20].

	6-31G	6-31G**	HF	CCSD(T)	Exp.
Total energy (Ryd)	-152.390	-152.418	-152.135	-152.878	
Bond angle (θ_{HOH}) (°)	110.3	104.4	106.2	104.2	104.52
Bond length (R_{OH}) (a_0)	1.833	1.785	1.776	1.808	1.809

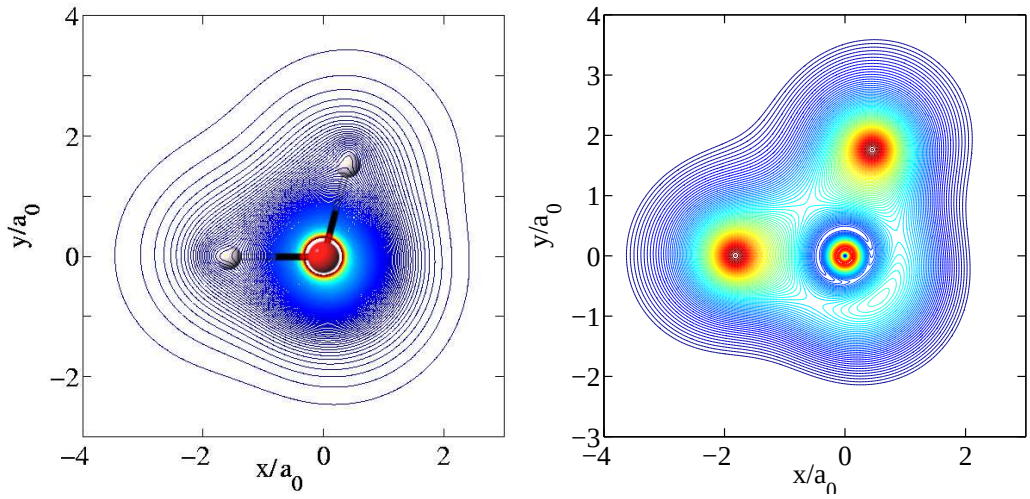

Figure 2.5: Contour plot of the density (left) and the density times the squared distance from the origin (right). In the former a schematic of the experimental structure has been superimposed. Both plots are in the plane of the water molecule. The contours are cut at a given maximum value, otherwise all one would see were the core electrons.

is not a uniquely defined concept. We define it as

$$W_\nu = \frac{|\langle\phi_\nu|\psi\rangle|^2}{\sum_\mu |\langle\phi_\mu|\psi\rangle|^2}. \tag{2.72}$$

In Figure 2.6 we have plotted a histogram of the orbital weights for the molecular orbital with the lowest eigenvalue and of the HOMO corresponding to the highest eigenvalue of an occupied state. We should remember that the eigenvalues do not have a rigorous meaning as single-particle energies even though we continue to use concepts such as the HOMO and LUMO. The molecular orbital with lowest eigenvalue is mainly made of the $1s$ atomic orbital on the oxygen as expected of a molecular orbital with the lowest energy. The HOMO is made out of p_z-orbitals on all atoms, mainly on the oxygen though, building up a π-orbital. The other molecular orbitals are made from higher s-functions or a mixture of s and $p_{x/y}$, the $p_{x/y}$ components mainly coming from the oxygen.

2.7.2 Total Electron Energy of Some Small Molecules

To further check our calculations we have calculated the total energy of few small molecules at their experimental geometry and compared with both Hartree-Fock and

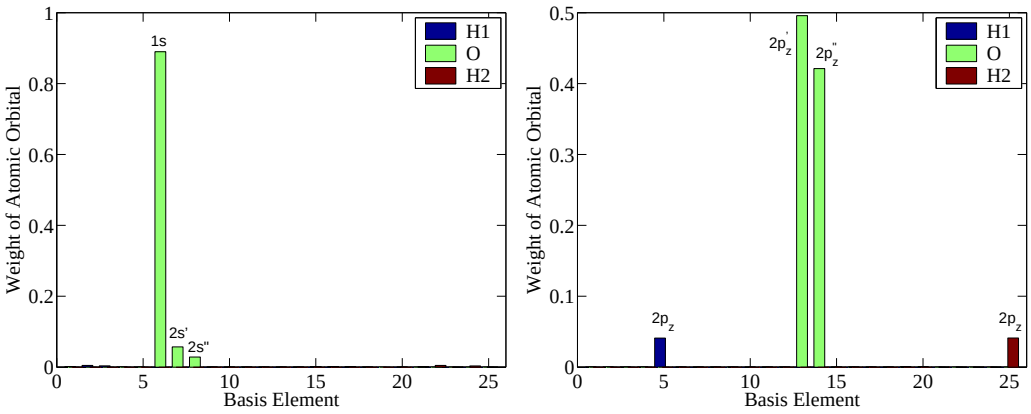

Figure 2.6: A histogram of orbital weights for the lowest (left) and highest (right) occupied molecular orbital.

coupled cluster calculations (cf. Table 2.2). Our results are always lower in energy than Hartree-Fock but higher than the coupled cluster calculations. The addition of polarization functions does not seem to have so much effect. One would perhaps expect that the polarization function are important to describe correlation effects. The results might be interpreted such that the correlation energy is a small portion of the total energy but we should also remember that we are using the $X\alpha$-Slater potential description of the XC-potential which is not an accurate description. In spite of differences in methodology and basis set the overall comparison with other calculations are quite good.

In the comparison one should keep in mind that both HF and the coupled cluster calculations are variational methods and therefore give upper bounds for the total energy. Due to the approximate functional DFT can give results that are lower than the correct total energy.

Table 2.2: Total energy in Rydbergs of a few molecules calculated with the $X\alpha$-Slater potential with $\alpha = 0.75$. The geometry is kept fixed at the experimental values. We compare with Hartree-Fock calculations in the pV6Z basis and coupled cluster calculations carried out in the pcV(56)Z basis [20].

	6-31G	6-31G*	6-31G**	HF	CCSD(T)
HF	-200.525	-200.562	-200.575	-200.1416	-200.920
HOF	-350.426	-350.464	-350.474	-349.6460	-351.106
NH_3	-112.602	-112.631	-112.648	-112.4498	-113.128

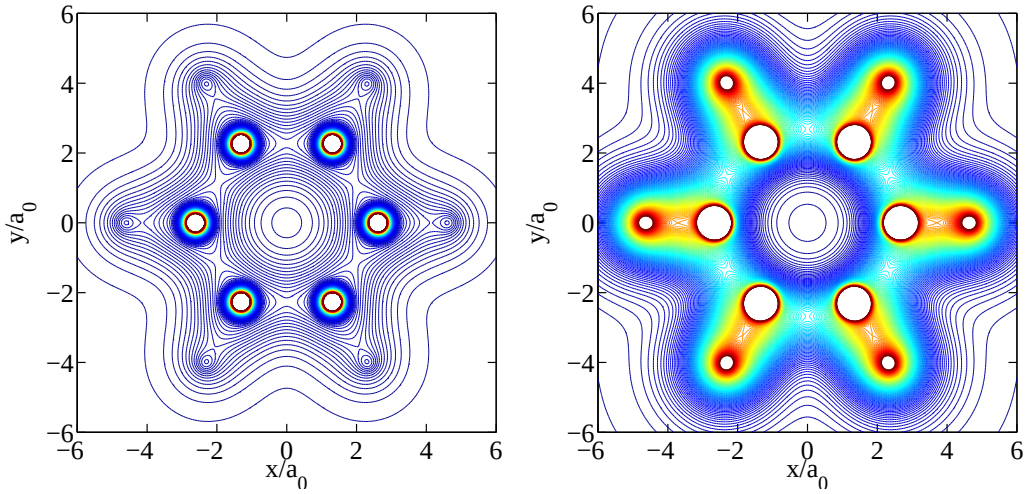

Figure 2.7: A contour plot of the total ground state electron density of benzene in the plane of the benzene molecule (left) and the total density times the squared distance from the origin (right). The contours have been cut at some high value since most of the density is near the nuclei, and that would be the only density visible on a contour plot with equally spaced contours. Because of this the nuclei appear as white circles.

2.7.3 Electron Density of Benzene

In this section we explore the density of the benzene molecule. The main reason for examining this molecule is that it is the base of the most common molecules used in studies of transport through molecules. It is also a bit larger than the molecules that we have been exploring so far and therfore gives us an indication of the capabilities, in terms of size of the system studied, of our program.

We have calculated the ground state density of Benzene using the 6-31G basis set. To visualize the density we have projected it onto the plane of the molecule and plotted a contour plot of it in Figure 2.7. We have plotted both the density and the density tine the distance square from the origin.

The pictures of the total density do not convey much information. It is more interesting to examine the density of the HOMO and the LUMO. If we look at the value of the eigenvalue corresponding to the HOMO and the LUMO we find that in both cases there are actually two molecular orbitals that are nearly degenerate. Instead of picking either one of them we have made a simple linear combination of them when visualizing the HOMO and the LUMO. In Figure 2.8 we have plotted a single isosurface of both the HOMO and the LUMO. The π-conjugated electron system is quite clear, being made of the p_z-orbitals of the carbon nuclei. We can

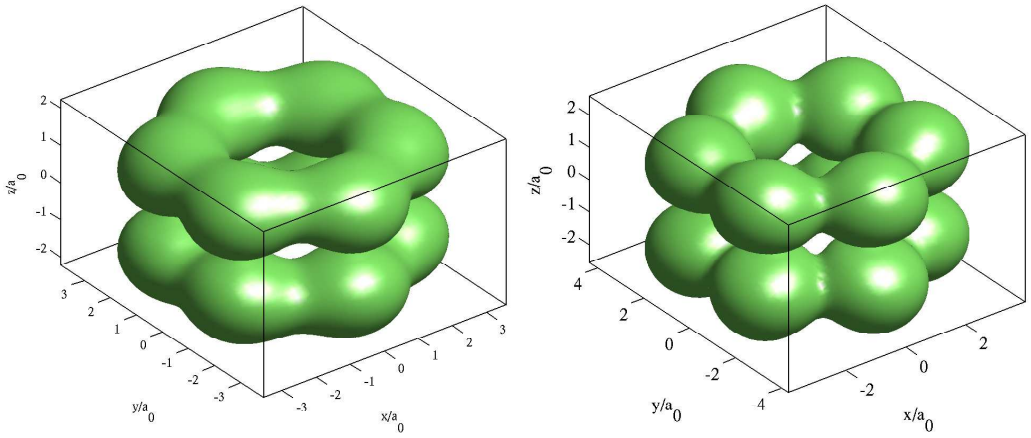

Figure 2.8: An isosurface of the electron density of the HOMO (left) and the LUMO (right) in a benzene molecule.

also see that the HOMO is a bonding state (i.e. a π-state) and the LUMO an antibonding state (i.e. π^*-state). This can be seen from the fact that the orbitals add up in between their maximums in the HOMO case but subtract in the LUMO case.

Just by looking at the density of the HOMO and the LUMO we can speculate that the transmission resonance of an electron would be similar for the HOMO and the LUMO and the current through benzene should behave similarly and be of similar amplitude whether the transport is through the HOMO or the LUMO. However one should remember that in the most common experiments measuring current through molecules the benzene molecules have thiol groups attached to them. Sulfur-based states can then alter the picture [10].

The atomic orbital weight analysis introduced in Section 2.7.1 can also be used here. The six lowest eigenvalues of the Kohn-Sham Hamiltonian are nearly degenerate and therefore we add up the atomic orbital weights from these six lowest occupied molecular orbitals. As seen in Figure 2.9 these molecular orbitals are mainly made from the $1s$ orbitals on each carbon as expected for the lowest energy orbitals. The orbitals next in energy are found to be a mixture of mainly $2s$, $2p_x$ and $2p_y$. In transport considerations, we are most interested in the HOMO and the LUMO. The isosurfaces in Figure 2.8 suggested that those were π-orbitals. The atomic weight analysis also shows that these orbitals are almost exclusively made out of the p_z orbitals of the carbon atoms as expected for π-orbitals. In the atomic orbital weight

analysis of the HOMO and the LUMO we have added together the contribution of the two near degenerate molecular orbitals at that energy, just as when Figure 2.8 was obtained.

The schematic view of the benzene molecule in Figure 2.9 also shows how the nuclei are numbered in the basis. The first elements in the basis are the elements of C1, then C2 etc. until C6 followed by H1 to H6. For each atom the basis elements are numbered from low angular momentum to high, i.e. first comes $1s$ then $2s'$, $2s''$, $2p'_x$, $2p''_x$ and so on.

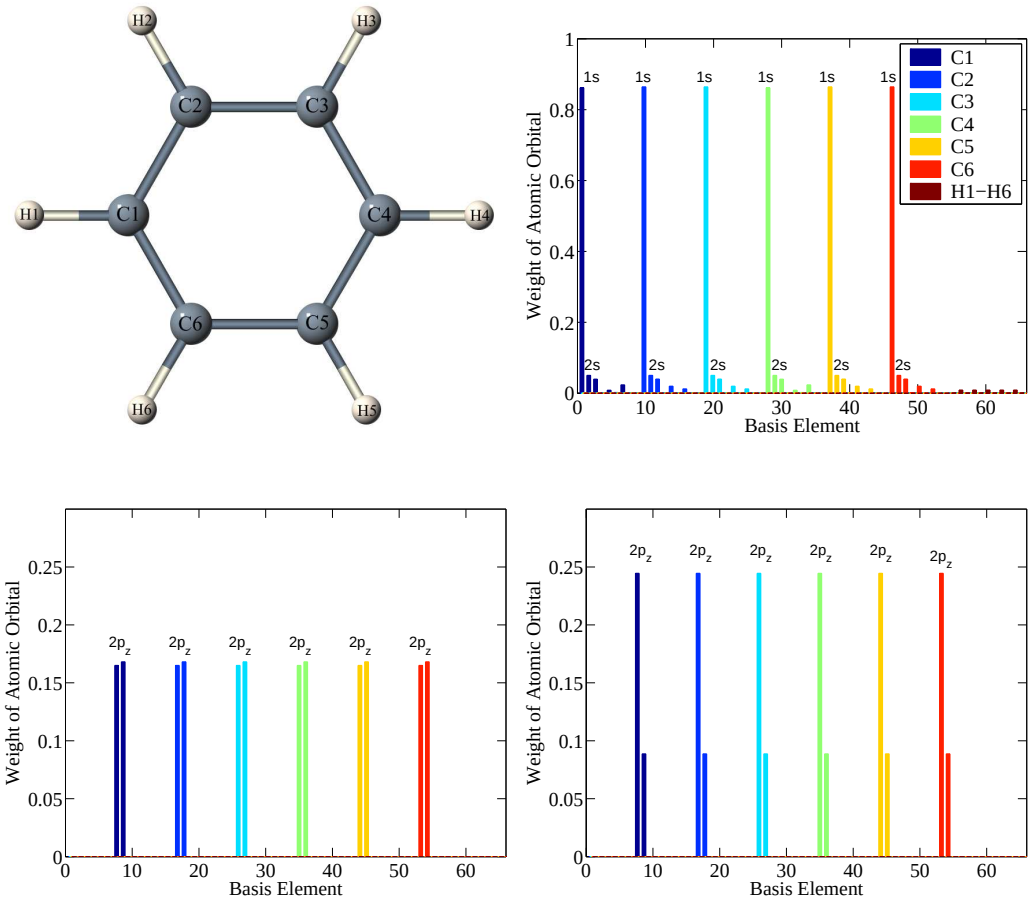

Figure 2.9: A schematic view of a benzene molecule (top left) numbering the atoms in the same order as in the basis. Histogram of the weights of the atomic orbitals in the six lowest occupied molecular orbitals (top right), the two highest occupied orbitals (HOMO, bottom left), and the two lowest unoccupied molecular orbitals (LUMO, bottom right). The legend in the top right histogram refers to all the histograms. $2p_z$ and $2s$ refer to the two spilt-valence orbitals $2p'_z$ and $2p''_z$ and $2s'$ and $2s''$ respectively.

Chapter 3

Transport through Nanoscale Systems

In the Landauer scheme conductance is viewed as transmission, i.e. the ease at which an electron can transverse a sample is a measure of the conductance [13]. This viewpoint is important in systems which are so small that the wave function is coherent throughout the whole system. In such cases one can obtain the transmission by solving the Schrödinger equation. A description in terms of scattering is evident, since one is interested in the transmission probability of an electron impinging on a nanosystem. A convenient way to discuss scattering is to transform the Schrödinger equation into an integral equation called the Lippman-Schwinger (LS) equation (cf. Section 3.1). In 1D, this equation has a simple structure and one can learn valuable things about it solutions by solving it for special 1D scattering potential as done both numerically and analytically in Section 3.2. To describe a more complicated system, such as a molecule connected to two leads, one has to go to three dimensions. How one models the system in this case depends on the physical setup of the system. In Section 3.3 we describe a formalism where the contacts to a nanosystem are modeled by two long wires connected to reservoirs. In doing so we introduce the so called scattering states, in terms of which on can connect the scattering formalism to the Landauer formalism to obtain the conductance of the system (cf. Section 3.4). The resulting formalism is used in Section 3.5 to calculate the conductance of a quasi-one-dimensional quantum wire in the presence of a single elastic impurity.

3.1 The Lippmann-Schwinger Equation

In the conventional textbook scattering setup a particle in the form of a plane wave is incident from infinity and is scattered by a finite range scattering potential, inducing a spherical scattered outgoing wave. In some cases it can be advantageous to generalize our notion of scattering to the case where a scattering potential scatters the state of the system from one eigenstate to another. Assume therefore that we want to solve the single particle Schrödinger equation

$$\hat{H}\left|\psi_E\right\rangle = E\left|\psi_E\right\rangle, \tag{3.1}$$

with

$$\hat{H} = \hat{H}_0 + \hat{V}, \tag{3.2}$$

in an open system. What is included in $\hat{H}_0$ and what in $\hat{V}$ is sometimes quite arbitrary. One has however to assume that the potential $\hat{V}$ has a finite range or falls off fast enough at infinity. The eigenfunctions of $\hat{H}_0$ are assumed to be known

$$\hat{H}_0\left|\psi_E^0\right\rangle = E\left|\psi_E^0\right\rangle, \tag{3.3}$$

and we think of $\hat{V}$ as a perturbative scattering potential. Since we are considering an open system the eigenvalues E are continuous and for each E there exists an eigenfunction for both $\hat{H}$ and $\hat{H}_0$.

By defining the Green's functions $\hat{G}_0(E)$ as the solution to

$$(E - \hat{H}_0 + i\eta)\hat{G}_0(E) = 1, \tag{3.4}$$

the solution to the single particle Schrödinger equation can be seen to satisfy the Lippmann-Schwinger equation

$$\left|\psi_E\right\rangle = \left|\psi_E^0\right\rangle + \hat{G}_0(E)\hat{V}\left|\psi_E\right\rangle. \tag{3.5}$$

This can be confirmed by applying the operator $\hat{G}_0^{-1} = (E - \hat{H}_0)$ to both sides of the solution (3.5)

$$\hat{G}_0^{-1}\left|\psi_E\right\rangle = \hat{V}\left|\psi_E\right\rangle \tag{3.6}$$

leading to

$$(E - \hat{H}_0)\,|\psi_E\rangle = \hat{V}\,|\psi_E\rangle\,, \tag{3.7}$$

i.e. $|\psi_E\rangle$ is a solution to the Schrödinger equation (3.1). The infinitesimal $\eta \to 0^+$ has been introduced to incorporate the boundary conditions as will be seen in the following.

We can learn more about the Green's function by looking at the special case of a free particle, $\hat{H}_0 = \hat{p}^2/2m$, in three dimensional space. In $\{\mathbf{r}\}$-space the Green's functions satisfies

$$(E - H_0 + i\eta)G_0(\mathbf{r}, \mathbf{r}'; E) = \delta(\mathbf{r} - \mathbf{r}'). \tag{3.8}$$

This equation is similar to the Schrödinger equation for the same system, except for the source term $\delta(\mathbf{r} - \mathbf{r}')$. One can therefore think of the Green's function as the field at $\mathbf{r}$ of a unit point source in $\mathbf{r}'$. The solution of Equation (3.8) is [31]

$$G(\mathbf{r}, \mathbf{r}'; E) = -\frac{m}{2\pi\hbar^2}\frac{e^{ik|\mathbf{r}-\mathbf{r}'|}}{|\mathbf{r} - \mathbf{r}'|}, \tag{3.9}$$

where $E = \hbar^2 k^2/2m$. In the following we will interchange k and E freely in our notation. The Green's function is an outgoing spherical wave corresponding to the boundary condition that a particle comes in and is scattered out. Using $-i\eta$ instead of $+i\eta$ one obtains

$$G_0^{(-)}(\mathbf{r}, \mathbf{r}'; E) = -\frac{m}{2\pi\hbar^2}\frac{e^{-ik|\mathbf{r}-\mathbf{r}'|}}{|\mathbf{r} - \mathbf{r}'|}, \tag{3.10}$$

i.e. an incoming wave [31]. The outgoing Green's function, which we denote by G_0 is sometimes denoted by $G_0^{(+)}$. We will not use this notation.

In configuration space the LS equation becomes

$$\psi_E(\mathbf{r}) = \psi_E^0(\mathbf{r}) + \int d^3r'\, G_0(\mathbf{r}, \mathbf{r}'; E)V(\mathbf{r}')\psi_E(\mathbf{r}'), \tag{3.11}$$

and can be interpreted such that the potential $V(\mathbf{r})$ induces an outgoing spherical wave at $\mathbf{r}$ that is proportional to both the strength of the potential and the amplitude of the wave function. The total wave function is the sum of the incoming wave and all the induced waves. This view, that we have an incoming part and a scattered part, is strengthened by writing the LS equation (3.11) as

$$\psi_E(\mathbf{r}) = \psi_E^0(\mathbf{r}) + \psi_{\mathrm{sc},E}(\mathbf{r}), \tag{3.12}$$

where $\psi_{\mathrm{sc},E}(\mathbf{r})$ is the scattered wavefunction.

Continuing with a free particle in three dimensions we introduce the concept of the T-matrix. If one is only interested in the solution in the far zone, i.e. outside the range of the scattering potential, one can use the expansion

$$|\mathbf{r}-\mathbf{r}'| \approx r - \frac{\mathbf{r}\cdot\mathbf{r}'}{r} \tag{3.13}$$

such that

$$G_0(\mathbf{r},\mathbf{r}';E) \approx -\frac{m}{2\pi\hbar^2}\frac{e^{ik\left(r-\frac{\mathbf{r}\cdot\mathbf{r}'}{r}\right)}}{r}. \tag{3.14}$$

The LS equation thus becomes

$$\psi_E(\mathbf{r}) = \psi_E^0(\mathbf{r}) - \frac{m}{2\pi\hbar^2}\frac{e^{ikr}}{r}\int d^3r'\, e^{-ik\hat{r}\cdot\mathbf{r}'}V(\mathbf{r}')\psi_E(\mathbf{r}'). \tag{3.15}$$

where $\hat{r}$ is a unit vector in the direction of $\mathbf{r}$. Let $\mathbf{k}' = k\hat{r}$ be the wave vector of the scattered wave. Since the integral depends only on the direction of the scattering and the energy E through k, one can define a scattering amplitude $f_E(\mathbf{k}' \leftarrow \mathbf{k})$ for scattering from $\mathbf{k}$ to $\mathbf{k}'$ such that

$$\psi_E(\mathbf{r}) = \psi_E^0(\mathbf{r}) + f_E(\mathbf{k}' \leftarrow \mathbf{k})\frac{1}{(2\pi)^{3/2}}\frac{e^{ikr}}{r} \tag{3.16}$$

where

$$f_E(\mathbf{k}' \leftarrow \mathbf{k}) = -\frac{4\pi^2 m}{\hbar^2}\langle\psi_{\mathbf{k}'}^0|\hat{V}|\psi_{\mathbf{k}}\rangle. \tag{3.17}$$

The T-matrix, defined as

$$T_E(\mathbf{k}',\mathbf{k}) = \langle\psi_{\mathbf{k}'}^0|\hat{T}|\psi_{\mathbf{k}}^0\rangle = \langle\psi_{\mathbf{k}'}^0|\hat{V}|\psi_{\mathbf{k}}\rangle, \tag{3.18}$$

is through Equation (3.17) directly related to the scattering amplitude and can through the LS equation be shown to satisfy the operator relation [31]

$$\hat{T} = \hat{V} + \hat{V}\hat{G}_0(E)\hat{T}. \tag{3.19}$$

In momentum space this becomes

$$T(\mathbf{k}',\mathbf{k}) = V(\mathbf{k}',\mathbf{k}) + \int d^3p\, V(\mathbf{k}',\mathbf{p})G_0(\mathbf{p};E)T(\mathbf{p},\mathbf{k}). \tag{3.20}$$

The Green's function is diagonal in momentum space for a translationally invariant H_0. Notice that the scattering amplitude f_E is related to the T-matrix *on the energy-shell*, i.e. where $|\mathbf{k}'| = |\mathbf{k}|$, but the LS equation (3.20) for the T-matrix connects $T(\mathbf{k}', \mathbf{k})$ to matrix elements $T(\mathbf{p}, \mathbf{k})$ for all possible $\mathbf{p}$ both on and off the energy shell. We also see from Equation (3.16) that the on-shell matrix elements of the T-matrix give us all the information about the wavefunction in the far zone and is thus equivalent to it.

In the following we will discuss the LS equation in various forms, for different dimensions and systems.

3.2 Transport in 1D

We begin by studying the LS equation and its solution in an infinite one dimensional system. The main reason for doing so is that the equations are simpler in 1D than in 3D since we only have one index instead of three. The structure of the equations and the solutions is therefore clearer. We will also learn about the complications that arise in an infinite system as compared to a finite system. The delta function potential is one of the simplest scattering potential we can think of. The LS equation with this potential can be solved analytically both in configuration and momentum space, the latter being much more difficult as one needs to introduce distribution functions. These analytical solutions are derived in Subsection 3.2.1. Examining these solutions we find that it is favorable to introduce the T-matrix as discussed for a general scattering potential in Subsection 3.2.2 and the resulting LS equation for the T-matrix is solved analytically for the delta function potential in Subsection 3.2.3. In the general case we need to solve the LS equation for the T-matrix numerically. The results of such numerical calculations are presented in Subsection 3.2.4.

3.2.1 Transmission through a Delta Function Potential Barrier

The delta function potential barrier is defined by

$$V(x) = V_0 \delta(x). \tag{3.21}$$

The solution of scattering by such a potential using the Schrödinger equation is a common textbook exercise [32].

Solution in Configuration Space

The physical setup is such that an electron coming from the right is scattered by the delta function potential at the origin, part of the wavefunction is transmitted and part reflected

$$\psi_k(x) = \begin{cases} \frac{1}{\sqrt{2\pi}} e^{ikx} + \frac{r}{\sqrt{2\pi}} e^{-ikx} & x < 0, \\ \frac{t}{\sqrt{2\pi}} e^{ikx} & x > 0. \end{cases} \tag{3.22}$$

Our problem is to find the unknown transmission and reflection amplitudes t and r. These are readily obtained using the LS equation in $\{\mathbf{r}\}$-space. With $\psi_k^0(x) = e^{ikx}/\sqrt{2\pi}$ and [33]

$$G_0(x, x'; k) = -\frac{im}{\hbar^2 k} e^{ik|x-x'|}, \tag{3.23}$$

the LS equation becomes

$$\begin{aligned} \psi_k(x) &= \frac{1}{\sqrt{2\pi}} e^{ikx} - \frac{im}{\hbar^2 k} \int dx'\, e^{ik|x-x'|} V_0 \delta(x') \psi_k(x') \\ &= \frac{1}{\sqrt{2\pi}} e^{ikx} - \frac{imV_0}{\hbar^2 k} e^{ik|x|} \psi_k(0). \end{aligned} \tag{3.24}$$

Putting $x = 0$ in the above equation gives

$$\psi_k(0) = \frac{1}{\sqrt{2\pi}} \frac{\hbar^2 k}{\hbar^2 k + imV_0}, \tag{3.25}$$

hence we obtain the form (3.22) with

$$t = \frac{\hbar^2 k}{\hbar^2 k + imV_0} \tag{3.26}$$

and $r = t - 1$ by continuity of the wave function.

The transmission probability is obtained as the squared absolute value of the transmission amplitude.

$$T = |t|^2 = \frac{k^2}{k^2 + \frac{m^2 V_0^2}{\hbar^4}} \tag{3.27}$$

and will be discussed in more detail later.

Solution in Momentum Space

The configuration space solution demonstrated the use of the LS equation but did not bring up anything new. By solving the same problem in momentum space we will learn valuable things regarding scattering in infinite systems. We could proceed by Fourier transforming the solution of the last section but that is not a very enlightening process so we start from scratch.

Expand $|\psi_k\rangle$ in plane waves

$$|\psi_k\rangle = \int dq\, \bar{\psi}_k(q)\, |q\rangle\,, \tag{3.28}$$

where

$$\langle x|k\rangle = \frac{1}{\sqrt{2\pi}} e^{ikx}. \tag{3.29}$$

The quantum number k is continuous since we have an infinite system. The plane waves are normalized such that

$$\langle k|k'\rangle = \frac{1}{2\pi}\int_{-\infty}^{\infty} dx\, e^{-i(k-k')x} = \delta(k-k'). \tag{3.30}$$

Introducing this expansion in the LS equation and projecting onto $\langle p|$ we obtain

$$\bar{\psi}_k(p) = \delta(k-p) + \int dq\ \langle p|\, \hat{G}_0\hat{V}\, |q\rangle\, \bar{\psi}_k(q). \tag{3.31}$$

The matrix element is obtained by using the Green's function (3.23)

$$\begin{aligned}\langle p|\, G_0 V\, |q\rangle &= \frac{1}{2\pi}\int dx dx'\, e^{-ipx} G_0(x,x';E) V(x') e^{iqx'} \\ &= -\frac{imV_0}{\hbar^2 k 2\pi}\int_{-\infty}^{\infty} dx\, e^{-ipx+ik|x|} \\ &= -\frac{imV_0}{\hbar^2 k 2\pi}(i\zeta(k+p) + i\zeta(k-p)),\end{aligned} \tag{3.32}$$

where we have introduced the function

$$i\zeta(k) = \lim_{K\to\infty}\int_0^K dx\, e^{ikx} = \frac{P}{k} - i\pi\delta(k), \tag{3.33}$$

where P denotes the Cauchy principal value. For the lack of a better name we have chosen to call this function the Heitler zeta function [34]. This is not a real function

but rather a distribution function, as of course the delta function. Notice that in this special case of the delta function potential the matrix element does not depend on q, and can therefore be taken out of the integral

$$\bar{\psi}_k(p) = \delta(k-p) + \frac{mV_0}{\sqrt{2\pi}\hbar^2 k}(\zeta(k+p) + \zeta(k-p))\psi_k(0), \tag{3.34}$$

since

$$\frac{1}{\sqrt{2\pi}} \int dq\, \bar{\psi}_k(q) = \psi_k(0). \tag{3.35}$$

By integrating Equation (3.34) with respect to p and using (cf. Appendix C)

$$\int_{-\infty}^{\infty} dp\, \zeta(k \pm p) = -i\pi, \tag{3.36}$$

one obtains

$$\psi_k(0) = \frac{1}{\sqrt{2\pi}} \frac{\hbar^2 k}{\hbar^2 k + imV_0}, \tag{3.37}$$

as in Equation (3.25). The wave function in momentum space follows

$$\bar{\psi}_k(p) = \delta(k-p) + \frac{1}{2\pi} \frac{mV_0}{\hbar^2 k + imV_0}(\zeta(k+p) + \zeta(k-p)). \tag{3.38}$$

The Fourier transform of the Heitler zeta function can be shown to be (cf. Appendix C)

$$\frac{1}{\sqrt{2\pi}} \int_{-\infty}^{\infty} dp\, e^{ipx} \zeta(k \pm p) = -\sqrt{2\pi} i e^{\mp ikx} \theta(\mp x), \tag{3.39}$$

where $\theta(x)$ is the Heaviside step function. The wave function in configuration space is therefore

$$\psi_k(x) = \frac{1}{\sqrt{2\pi}} e^{ikx} + \frac{1}{\sqrt{2\pi}}(t-1)e^{ikx}\theta(x) + \frac{1}{\sqrt{2\pi}} r e^{-ikx}\theta(-x) \tag{3.40}$$

where

$$t = \frac{\hbar^2 k}{\hbar^2 k + imV_0}, \tag{3.41}$$

and $r = t - 1$. This is of course the same solution as obtained by considerably less labor in configuration space. There is, however, an important lesson to be learned from the momentum space solution (3.38). In an infinite system the momentum space wave function for the delta function potential is not an analytic function but rather a distribution function. One can be convinced that, at least when the

scattering potential has a finite range, this will always be the case. This should not of course come as a surprise since similar things come up when using as basis in wave function space functions that do not belong to it, a case in hand being the plane waves [32]. In the case of an infinite system a straightforward expansion of the wave function in plane waves is therefore unfeasible in numerical calculations. One can then either make the system finite by some means, but the formulation of scattering can be tricky in this case, or one can try to avoid the distribution functions by reformulating the problem e.g. in terms of the T-matrix.

3.2.2 Transmission and the T-matrix

To obtain the transmission coefficient for a general finite range potential one only needs the wave function in the far zone. As already seen in the conventional 3D case, the T-matrix gives us this information. In 1D the LS equation (3.5) in configuration space, the only space where the far zone can easily be defined, is

$$\psi_k(x) = \psi_k^0(x) + \int dx'\, G_0(x, x'; k) V(x') \psi_k(x'). \tag{3.42}$$

Assuming that the potential V has a finite range R we obtain for $|x| \gg R$

$$|x - x'| \approx |x| - \mathrm{sgn}(x) x', \tag{3.43}$$

hence

$$\psi_k(x) \underset{|x|\gg R}{=} \psi_k^0(x) - \frac{im}{\hbar^2 k} e^{ik|x|} \int dx'\, e^{-ik\mathrm{sgn}(x)x'} V(x') \psi_k(x'). \tag{3.44}$$

Note that $k > 0$. Defining

$$k' = \mathrm{sgn}(x) k \tag{3.45}$$

we obtain

$$\psi_k(x) \underset{|x|\gg R}{=} \psi_k^0(x) + \frac{1}{\sqrt{2\pi}} f_E(k' \leftarrow k) e^{ik|x|}, \tag{3.46}$$

where

$$\begin{aligned} f_E(k' \leftarrow k) &= -\frac{im\sqrt{2\pi}}{\hbar^2 k} e^{ik|x|} \int dx'\, e^{-ik'x'} V(x') \psi_k(x') \\ &= -\frac{im2\pi}{\hbar^2 k} \langle \psi_{k'}^0 | V | \psi_k \rangle. \end{aligned} \tag{3.47}$$

As before the T-matrix is defined by

$$T_E(k',k) = \langle \psi^0_{k'}|\hat{T}|\psi^0_k\rangle = \langle \psi^0_{k'}|\hat{V}|\psi_k\rangle. \tag{3.48}$$

Using the LS equation

$$\begin{aligned}\langle \psi^0_{k'}|\hat{T}|\psi^0_k\rangle &= \langle \psi^0_{k'}|\hat{V}\left(|\psi^0_k\rangle + \hat{G}_0(E)\hat{V}\,|\psi_k\rangle\right)\\ &= \langle \psi^0_{k'}|\hat{V}|\psi^0_k\rangle + \langle \psi^0_{k'}|\hat{V}\hat{G}_0(E)\hat{T}|\psi^0_k\rangle,\end{aligned} \tag{3.49}$$

since

$$\langle \psi^0_{k'}|\hat{V}\hat{G}_0(E)\hat{V}|\psi_k\rangle = \langle \psi^0_{k'}|\hat{V}\hat{G}_0(E)\hat{T}|\psi^0_k\rangle. \tag{3.50}$$

Since $|\psi^0_k\rangle$ is an arbitrary state vector we obtain the operator LS equation for $\hat{T}$

$$\hat{T} = \hat{V} + \hat{V}\hat{G}_0(E)\hat{T}. \tag{3.51}$$

This is of course the same equation as in the 3D case, since it is valid regardless of dimension.

In momentum space $\hat{G}_0(E)$ is diagonal since $\hat{H}_0$ is translationally invariant. The LS equation for $\hat{T}$ therefore takes the form

$$T(k',k) = V(k'-k) + \int dp\, V(k'-p)G_0(p;E)T(p,k). \tag{3.52}$$

We have also assumed that the potential V is local and its Fourier transform does thus only depend on the difference of the momenta. The transmission amplitude is related to the on-shell matrix elements of the T-matrix through

$$t = 1 + f(k \leftarrow k) = 1 - \frac{im2\pi}{\hbar^2 k}T(k,k). \tag{3.53}$$

3.2.3 The T-matrix and the Delta Function Potential

In the case of a delta function potential the integral equation for the T-matrix can be solved analytically. The Fourier transform of the potential

$$V(k',k) = \frac{1}{2\pi}\int dx\, e^{i(k-k')x}V_0\delta(x) = \frac{V_0}{2\pi}, \tag{3.54}$$

is a constant. The T-matrix is therefore independent of k' as can be seen from iteration (Born series)

$$\begin{aligned} T(k',k) = V(k',k) + \int dp\, V(k',p) G_0(p;E) V(p,k) \\ + \int dpdq\, V(k',p) G_0(p;E) V(p,q) G_0(q;E) V(q,k) + \dots . \end{aligned} \tag{3.55}$$

From this series it is evident that $T(k',k)$ only depends on the energy of the electron (or equivalently only on k), in other words the scattering is isotropic. The T-matrix LS equation (3.52) can therefore be written

$$T(k) = \frac{V_0}{2\pi} + \frac{V_0}{2\pi} T(k) \int dp\, G_0(p;k). \tag{3.56}$$

The integral over G can be performed by the residue theorem, giving

$$\int dp\, G_0(p;k) = \frac{2m}{\hbar^2} \int_{-\infty}^{\infty} dp\, \frac{1}{k^2 - p^2 + i\eta} = \frac{-2\pi i m}{\hbar^2 k}, \tag{3.57}$$

hence

$$T(k) = \frac{V_0/2\pi}{1 + \frac{imV_0}{\hbar^2 k}}. \tag{3.58}$$

The transmission amplitude becomes through Equation (3.53)

$$t = \frac{\hbar^2 k}{\hbar^2 k + imV_0}, \tag{3.59}$$

as before.

A similar derivation using momentum space partial-wave expansion of matrix elements can be found in Ref. [35].

3.2.4 Numerical Solution of the Lippman-Schwinger Equation for the T-matrix

Rarely can we solve the Lippman-Schwinger equation analytically as in the case of the delta function potential. For more complicated potentials we might be interested in, a numerical scheme for the solution needs to be devised. One such scheme [31, 36] transforms the integral equation into a matrix equation by performing the integral using a Gaussian quadrature. Special care has to be taken in treating the singu-

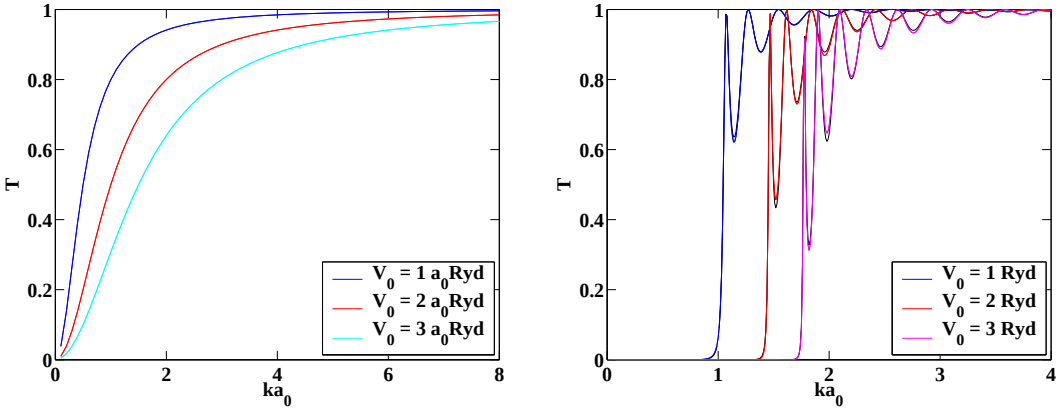

Figure 3.1: The transmission probability of an electron as a function of energy for different strengths of the potential. The plot on the left is for a delta function and the plot on the right for a rectangular potential barrier. In the latter case the length of the potential is kept fixed at $b = 4a_0$ but the height is varied. For each numerical solution we have plotted the corresponding analytical solution in a dotted black line. The number of intervals is $n_{\text{intervals}} = 12$ and $n_{\text{intervals}} = 40$ for the delta and rectangular potential respectively. $p_{\max} = 30a_0^{-1}$ in both cases.

larities of the Green's function. Our version of the method is described in detail in Appendix D, here we only present the results. There are though two parameters we need to define since they are used in the discussion. The integral in the momentum space LS equation has its limits in the infinity. These limits are changed to some maximum denoted by $p_{\max}$. The remaining integral over positive momenta is divided into $n_{\text{intervals}}$ subintervals and four point Gaussian quadrature is used in each interval.

Delta Function Potential

As a first example, we calculate the transmission through a delta function potential yet again. We have already seen that in this case the T-matrix elements only depend on k. The Gaussian quadrature is therefore exact, the only approximation coming from the introduction of $p_{\max}$. The numerical solution cannot be distinguished from the analytical solution, even at low values of $p_{\max}$ (cf. Figure 3.1). The transmission probability is rather characterless, growing steadily from zero to one as the energy of the incident electron is increased.

The Rectangular Potential Barrier

A more interesting case is the rectangular potential barrier, defined by

$$V_{\text{rectangular}} = \begin{cases} V_0 & -b < x < b, \\ 0 & \text{elsewhere.} \end{cases} \tag{3.60}$$

The transmission probability can be obtained by solving the Schrödinger equation in the different intervals and matching the solution at their interfaces ($x = \pm b$), leading to [37]

$$T_{\text{rectangular}} = \frac{1}{\cosh^2 2\kappa b + (\varepsilon^2/4)\sinh^2 2\kappa b}, \tag{3.61}$$

where

$$\varepsilon = \frac{\kappa}{k} - \frac{k}{\kappa}, \tag{3.62}$$

$\hbar k = \sqrt{2mE}$ and $\hbar\kappa = \sqrt{2m(V_0 - E)}$. In Figure 3.1 we have plotted the results of the numerical solution to the LS equation and compared with the analytical solution (3.61). The numerical solution is quite accurate; only in the valleys are there differences. Classically the transmission probability would be a step function. In the quantum mechanical case resonances and oscillations appear as the energy is increased. These are well known an exhibit clearly the wave nature of the electron.

Gaussian Potential

A simple case to examine is the case of a Gaussian potential

$$V_{\text{Gauss}} = V_0 \exp\left[-\left(\frac{x}{b}\right)^2\right]. \tag{3.63}$$

We have calculated the transmission probability for both attractive and repulsive Gaussian potential (cf. Figure 3.2). In both cases the transmission is rather characterless, growing steadily from zero to perfect transmission as the energy is increased. There are no resonances or oscillations as in the rectangular potential barrier case.

3.3 Wires Connected to a Nanostructure

Having considered scattering from a finite potential in one dimension we extend the discussion to a nanostructure connected by two infinite wires. Depending on

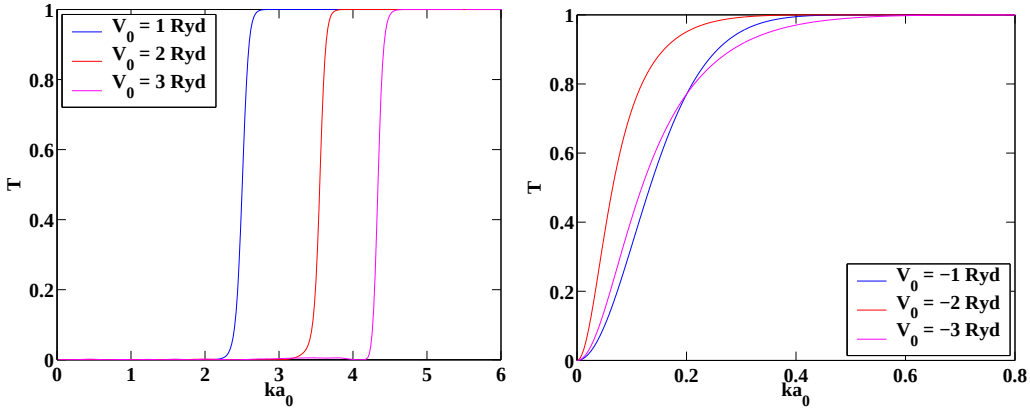

Figure 3.2: Transmission through a repulsive (left) and attractive (right) Gaussian potential of varying strength. In both cases the width of the potential is given by $b = 4a_0$. The number of intervals used are 12 and 30 respectively while $p_{\max} = 30a_0^{-1}$ in both cases.

how we model the wires, the number of dimensions is thus increased to two or three. The scattering is not the conventional scattering of free particles discussed in relation with the LS equation in Section 3.1 since the electrons are confined to the wires. In this case it will become important to carefully distinguish between the propagating direction (which in our case is always the z-direction) and the transverse directions where the motion of the electrons is confined by the wire. We begin by discussing scattering states and the scattering matrix which are defined by means of the transverse modes (Section 3.3.1), and then show how we can obtain them with the LS equation (Section 3.3.2) and the T-matrix (Section 3.3.3).

3.3.1 Scattering States and the Scattering Matrix

We divide the system into the two leads and the nanosystem (finite range potential) as in Figure 3.3. Electrons are fed into the leads by two reservoirs characterized by the quasi chemical potentials μ_L and μ_R. The leads are assumed to be ideal, i.e. there is no scattering. We will discuss the population of electrons in the leads in Section 3.4 but we assume here that we can have an electron with energy E in a well defined eigenstate of the system. As before in our discussion of scattering we neglect electron-electron interaction in the leads.

The leads are described by a rectangular waveguide, modeled with the confine-

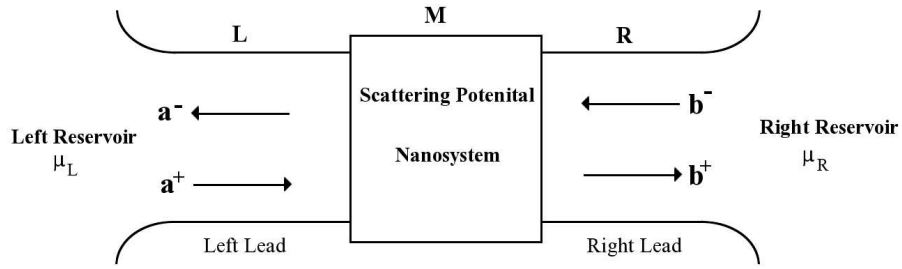

Figure 3.3: A schematic view of the nanosystem connected by two ideal leads to two reservoirs. The reservoirs are assumed reflectionless. Adapted from [38].

ment potential

$$V_C(x,y) = \begin{cases} 0 & 0 < x < L_x, 0 < y < L_y, \\ \infty & \text{elsewhere.} \end{cases} \tag{3.64}$$

The normalized eigenfunctions of the transverse Hamiltonian in the leads

$$H_\perp = \frac{p_x^2}{2m} + \frac{p_y^2}{2m} + V_C(x,y) \tag{3.65}$$

can be written

$$\chi_{n_x n_y}(x,y) = \frac{2}{\sqrt{L_x L_y}} \sin\left(\frac{n_x \pi}{L_x} x\right) \sin\left(\frac{n_y \pi}{L_y} y\right), \quad n_x, n_y = 1, 2, \ldots \tag{3.66}$$

with eigenvalues

$$E_\perp(n_x, n_y) = \frac{\hbar^2 \pi^2}{2m} \left[\left(\frac{n_x}{L_x}\right)^2 + \left(\frac{n_y}{L_y}\right)^2 \right]. \tag{3.67}$$

In the following we simplify the notation by using just a single index n to number the channels corresponding to n_x and n_y. The eigenvalues will be denoted by $\varepsilon_n = E_\perp(n_x, n_y)$. By doing so the formalism becomes identical to the case of a 2D wire and this will be useful later.

Eigenfunctions of the total Hamiltonian

$$H = \frac{p^2}{2m} + V_C(x,y) + V(\mathbf{r}) = H_0 + V(\mathbf{r}) \tag{3.68}$$

approach the solution of H_0 outside the range of the scattering potential, i.e.

$$\phi^{\pm}_{LnE}(\mathbf{r}) = \frac{1}{\sqrt{k_n(E)}} e^{\pm i k_n(E) z} \chi_n(\mathbf{r}_\perp), \quad \mathbf{r} \in L, \tag{3.69}$$

$$\phi^{\pm}_{RnE}(\mathbf{r}) = \frac{1}{\sqrt{k_n(E)}} e^{\pm i k_n(E) z} \chi_n(\mathbf{r}_\perp), \quad \mathbf{r} \in R, \tag{3.70}$$

where

$$E = \frac{\hbar^2 k_n^2(E)}{2m} + \varepsilon_n. \tag{3.71}$$

The eigenfunctions have been normalized such that they all carry the same current in anticipation of later development (cf. Section 3.4). If $\varepsilon_n < E$, $k_n(E)$ is real and the eigenfunctions $\phi^{\pm}_{L/RnE}$ are propagating and the channel is correspondingly called a transverse propagation mode. If on the other hand $\varepsilon_n > E$, $k_n(E)$ is purely imaginary and the eigenfunctions must be exponentially decaying to satisfy boundary conditions. We will write $k_n(E) = i\kappa_n(E)$ and denote these so called evanescent modes by

$$\phi^{\mathrm{ev}}_{LnE}(\mathbf{r}) = \sqrt{\kappa_n(E)} e^{-\kappa_n(E) z} \chi_n(\mathbf{r}_\perp), \quad \mathbf{r} \in L, \tag{3.72}$$

$$\phi^{\mathrm{ev}}_{RnE}(\mathbf{r}) = \sqrt{k_n(E)} e^{+\kappa_n(E) z} \chi_n(\mathbf{r}_\perp), \quad \mathbf{r} \in R. \tag{3.73}$$

The evanescent modes are normalized to unity in the absence of a scattering potential.

A general eigenfunction of the total Hamiltonian with energy E, can be written as a linear combination of $\phi^{\pm}_{L/RnE}$ and $\phi^{\mathrm{ev}}_{L/RnE}$, i.e. in the left and right lead they take the form

$$\psi_E(\mathbf{r}) = \begin{cases} \sum_{n,\mathrm{prop}} a_n^+ \phi^+_{LnE} + \sum_{n,\mathrm{prop}} a_n^- \phi^-_{LnE} + \sum_{n,\mathrm{ev}} a_n^{\mathrm{ev}} \phi^{\mathrm{ev}}_{LnE} & \mathbf{r} \in L, \\ \sum_{n,\mathrm{prop}} b_n^+ \phi^+_{RnE} + \sum_{n,\mathrm{prop}} b_n^- \phi^-_{RnE} + \sum_{n,\mathrm{ev}} b_n^{\mathrm{ev}} \phi^{\mathrm{ev}}_{RnE} & \mathbf{r} \in R, \\ \psi_M(\mathbf{r}) & \mathbf{r} \in M. \end{cases} \tag{3.74}$$

We collect the coefficients into a vector $\mathbf{a}^+ = (a_1^+, a_2^+, \ldots, a^+_{N_{\mathrm{prop}}})$, and similarly for $\mathbf{a}^-$, $\mathbf{b}^{\pm}$, $\mathbf{a}^{\mathrm{ev}}$ and $\mathbf{b}^{\mathrm{ev}}$ (Figure 3.3 shows only the vectors of propagating modes). Note that since there are only finite number N_{prop} of propagating modes, the corresponding vectors are finite. The number of evanescent modes are on the other hand infinite and the corresponding vectors are therefore of infinite dimensions. In calculations one has to limit the number of evanescent modes used.

We now define the scattering matrix, or the S-matrix, as the matrix that connects ingoing and outgoing propagating modes,

$$\mathbf{c}_{\text{out}} = \begin{pmatrix} \mathbf{a}^- \\ \mathbf{b}^+ \end{pmatrix} = \begin{pmatrix} r & t' \\ t & r' \end{pmatrix} \begin{pmatrix} \mathbf{a}^+ \\ \mathbf{b}^- \end{pmatrix} = S\mathbf{c}_{\text{in}}. \tag{3.75}$$

One can see, for example by matching the wave function in different regions, that the coefficients in the expansion (3.74) must be linearly dependent. One could however doubt that the transmission and reflection amplitudes of the propagating modes are linearly dependent independent of the evanescent modes. If not, the above definition of the scattering matrix would not be applicable. Far enough from the scattering potential, however, the evanescent modes are exponentially small and can therefore be neglected as can their coefficients. In this case the scattering matrix as defined above becomes well defined. By use of current conservation the scattering matrix can be shown to be unitary [38, 39]. Comparing with the 1D case we have now instead of the transmission and reflection amplitudes t and r, $N_{\text{prop}} \times N_{\text{prop}}$ matrices of transmission and reflection amplitudes, also denoted by t and r respectively. t_{mn} is the probability amplitude for a particle in state n in the left lead to scatter out in state m in the right lead. t'_{mn} is the same amplitude for scattering in the other direction. r_{mn} and r'_{mn} give similarly the probability amplitude for reflection into state m.

We are now in position to define the so called scattering states. These are states with an incoming wave in a single channel, such that $\mathbf{c}_{\text{in}} = (0, 0, \ldots, 0, 1, 0, \ldots)$, and are denoted

$$\psi^+_{nE}(\mathbf{r}) = \begin{cases} \phi^+_{LnE} + \sum_{m,\text{prop}} r_{mn}\phi^-_{LmE} + \sum_{m,\text{ev}} r_{mn}\phi^{\text{ev}}_{LmE} & \mathbf{r} \in L, \\ \sum_{m,\text{prop}} t_{mn}\phi^+_{RmE} + \sum_{m,\text{ev}} t_{mn}\phi^{\text{ev}}_{RmE} & \mathbf{r} \in R, \\ ? & \mathbf{r} \in M, \end{cases} \tag{3.76}$$

and

$$\psi^-_{nE}(\mathbf{r}) = \begin{cases} \sum_m t'_{mn}\phi^-_{LmE} + \sum_{m,\text{ev}} t'_{mn}\phi^{\text{ev}}_{LmE} & \mathbf{r} \in L, \\ \phi^-_{RnE} + \sum_m r'_{mn}\phi^+_{RmE} + \sum_{m,\text{ev}} r'_{mn}\phi^{\text{ev}}_{LmE} & \mathbf{r} \in R, \\ ? & \mathbf{r} \in M. \end{cases} \tag{3.77}$$

In the above expression n must be a propagating mode. The exact form of the

wave function in the region of the scattering potential is not important since we are only interested in the transmission probability. We have also used the scattering matrix notation for the coefficient of the evanescent modes even though they are not included in the scattering matrix. These amplitudes do however have a very similar physical meaning and are therefore denoted as above. To obtain the conductance only the matrix of transmission amplitudes t is needed (cf. Section 3.4), i.e. we only need to examine the scattering state ψ^+_{nE}. This scattering state corresponds to the usual boundary condition of scattering, i.e. an electron impinging from the left is scattered by a finite scattering potential into all directions (modes in our case).

An important difference between the scattering of free particles and the partially bound ones we are looking at, is that the latter can scatter into evanescent modes that are localized around the scatterer. If we would turn off the influx the evanescent modes would soon be depleted since the scattering potential couples them with the propagating modes. With the flux on these modes will however get occupied and can have important effects on the transmission and conductance [40].

3.3.2 Scattering States and the Lippmann-Schwinger Equation

We will now show how we can find the scattering states ψ^+_{nE}, or rather the matrix of transmission amplitudes t. The scattering state ψ^+_{nE} is a solution to the Schrödinger equation

$$\left(-\frac{\hbar^2\nabla^2}{2m} + V_C(x,y) + V(\mathbf{r})\right)\psi^+_{nE} = E\psi^+_{nE}, \tag{3.78}$$

where $V(\mathbf{r})$ is the finite range scattering potential. Expanding the scattering states in the basis $\{\chi_m\}$ [41]

$$\psi^+_{nE}(\mathbf{r}) = \sum_m \varphi_{mE}(z)\chi_m(x,y), \tag{3.79}$$

and introducing this expansion into the Schrödinger equation one obtains

$$\sum_m \left(-\frac{\hbar^2}{2m}\frac{\partial^2}{\partial z^2} + \varepsilon_m + V(\mathbf{r})\right)\varphi_{mE}(z)\chi_m(x,y) = E\sum_m \varphi_{mE}(z)\chi_m(x,y). \tag{3.80}$$

Note that the sum over m must contain both propagating and evanescent modes. Multiplying with $\chi^*_{m'}$, integrating over $\mathbf{r}_\perp$ and using the orthogonality of the χ-s

(and let $m \leftrightarrow m'$) one obtains

$$\left(\frac{d^2}{dz^2} + k_m^2(E)\right)\varphi_{mE}(z) = \sum_{m'} \mathcal{V}_{mm'}(z)\varphi_{m'E}(z), \tag{3.81}$$

where we have defined

$$\mathcal{V}_{mm'}(z) = \frac{2m}{\hbar^2}\int d^2r_\perp\, \chi_m^*(\mathbf{r}_\perp)V(\mathbf{r})\chi_{m'}(\mathbf{r}_\perp). \tag{3.82}$$

For evanescent modes we replace $k_m(E)$ by $i\kappa_m(E)$ in the above equation. The potential $\mathcal{V}_{mm'}(z)$ couples different modes, both propagating and evanescent.

By use of the Green's function $G_{nE}^0(z,z')$ defined by

$$\left(\frac{d^2}{dz^2} + k_n^2(E)\right)G_{nE}^0(z,z') = \delta(z-z'), \tag{3.83}$$

the solution to Equation (3.81) can be written

$$\varphi_{mE}(z) = \varphi_{mE}^0(z) + \sum_{m'}\int dz'\, G_{mE}^0(z,z')\mathcal{V}_{mm'}(z')\varphi_{m'E}(z'), \tag{3.84}$$

where $\varphi_{mE}^0(z)$ is a solution to the homogeneous equation

$$\left(\frac{d^2}{dz^2} + k_m^2(E)\right)\varphi_{mE}^0(z) = 0, \tag{3.85}$$

decided by the scattering boundary conditions. An evanescent mode can not have an incoming wave and therefore $\varphi_{mE}^0(z) = 0$ for these modes. This is similar to the case of bound states [31], even though the evanescent states are not real bound states. One can be convinced that (3.84) is a solution by acting on it by $d^2/dz^2 + k_n^2(E)$, thereby obtaining the Scrödinger Equation (3.81). Note the difference between definition (3.83) for the Green's function and the one given in Equation (3.8). The only difference being the normalization of the Green's function, which in this case becomes

$$G_{nE}^0(z,z') = -\frac{i}{2k_n(E)}e^{ik_n(E)|z-z'|}. \tag{3.86}$$

For evanescent modes we get the correct Green's function by replacing k_n with $i\kappa_n$ as before.

In the above the transverse directions have been described by a conventional

solution of the Schrödinger equation through the χ_m-s but the z-direction, in which we have propagating waves, has been described by a LS equation using the 1D Green's function.

By choosing

$$\varphi^0_{mE}(z) = \delta_{nm}\phi^+_{mE}(z), \tag{3.87}$$

where n is a propagating mode

$$\phi^+_{nE}(z) = \frac{1}{\sqrt{k_n(E)}} e^{ik_n(E)z}, \tag{3.88}$$

we will obtain the scattering states as we will now show. Using this boundary condition and inserting the Green's functions (3.86), Equation (3.84) becomes

$$\varphi_m(z) = \delta_{nm}\phi^+_{nE}(z) - \frac{i}{2k_m(E)} \sum_{m'} \int dz'\, e^{ik_m(E)|z-z'|} \mathcal{V}_{mm'}(z')\varphi_{m'}(z'). \tag{3.89}$$

If we now look at the limit of this equation for $z \gg R$, where R is the range of the potential, such that the absolute value in the integrand becomes $|z - z'| = z - z'$, we obtain

$$\begin{aligned} \varphi_m(z) = \frac{1}{\sqrt{k_m(E)}} e^{ik_m(E)z} \Bigg(& \delta_{nm} + \\ & \frac{1}{2i} \sum_{m'} \int dz' \, \frac{1}{\sqrt{k_m(E)}} e^{-ik_m(E)z'} V_{mm'}(z')\varphi_{m'}(z') \Bigg). \end{aligned} \tag{3.90}$$

Since we are looking at the far zone the prefactor (or equivalently the Green's function) is exponentially small for evanescent modes and we can ignore them as already discussed. Through the expansion (3.79) the solution therefore takes the form of a scattering state without all evanescent modes

$$\psi^+_{nE}(\mathbf{r}) = \sum_{m,\text{prop}} t_{mn}\phi^+_{RmE}(\mathbf{r}) \tag{3.91}$$

for all $\mathbf{r} \in R$, where

$$t_{mn} = \delta_{mn} + \frac{1}{2i} \sum_{m'} \int dz' \, \frac{1}{\sqrt{k_m(E)}} e^{-ik_m(E)z'} \mathcal{V}_{mm'}(z')\varphi_{m'}(z'). \tag{3.92}$$

The sum in the above expression does however include all modes, propagating and

evanescent. Similarly by taking the limit $z \ll -R$, we obtain

$$\psi^+_{nE}(\mathbf{r}) = \phi^+_{LnE}(\mathbf{r}) + \sum_{m,\text{prop}} r_{mn}\phi^-_{LmE}(\mathbf{r}) \tag{3.93}$$

for all $\mathbf{r} \in L$, where

$$r_{mn} = \frac{1}{2i}\sum_{m'}\int dz' \, \frac{1}{\sqrt{k_m(E)}} e^{-ik_m(E)z'} \mathcal{V}_{mm'}(z')\varphi_{m'}(z'). \tag{3.94}$$

We have thus obtained the scattering states and the transmission and reflection amplitudes of the scattering matrix. When solving for $\varphi_{m'}(z')$ used to obtain t_{mn} we need to solve the system of integral equations (3.84), which couples both propagating and evanescent modes.

3.3.3 Scattering States and the T-matrix

Having obtained the transmission amplitudes in terms of the configuration space wave function we now find them in terms of matrix elements of a transition operator. Inserting the definition (3.82) of $\mathcal{V}_{mm'}$ into relation (3.92) one obtains

$$\begin{aligned} t_{mn} &= \delta_{mn} + \frac{m}{i\hbar^2}\int d^3r' \, \frac{1}{\sqrt{k_m(E)}} e^{-ik_m(E)z'} \chi^*_m(\mathbf{r}'_\perp) V(\mathbf{r}') \sum_{m'} \varphi_{m'}(z')\chi_{m'}(\mathbf{r}'_\perp) \\ &= \delta_{mn} + \frac{m}{i\hbar^2}\langle mk_m|\hat{V}|\psi^+_{nE}\rangle, \end{aligned} \tag{3.95}$$

where we have used the expansion (3.79). Using the LS equation (3.84) in the same expansion

$$\begin{aligned} \psi^+_{nE}(\mathbf{r}) &= \sum_m \varphi^0_{mE}(z)\chi_m(\mathbf{r}_\perp) + \sum_{m,m'}\int dz' \, G^0_{mE}(z,z')\mathcal{V}_{mm'}(z')\varphi_{m'E}(z')\chi_m(\mathbf{r}_\perp) \\ &= \phi^+_{nE}(\mathbf{r}) + \int d^3r' \, G_0(\mathbf{r},\mathbf{r}';E)V(\mathbf{r}')\psi^+_{nE}(\mathbf{r}') \end{aligned} \tag{3.96}$$

where

$$G_0(\mathbf{r},\mathbf{r}';E) = \frac{2m}{\hbar^2}\sum_m \chi^*_m(\mathbf{r}_\perp)G^0_{mE}(z,z')\chi_m(\mathbf{r}'_\perp). \tag{3.97}$$

This is just the LS equation in 3D and therefore if we define a T-matrix by the relation

$$\langle mk'|\hat{T}|nk\rangle = \langle mk'|\hat{V}|\psi^+_{nE}\rangle, \tag{3.98}$$

both on and off the energy shell, it satisfies the operator LS equation

$$\hat{T} = \hat{V} + \hat{V}\hat{G}_0(E)\hat{T}, \tag{3.99}$$

as discussed in the 1D case. In the eigenfunction basis of $\hat{H}_0$ this becomes

$$\langle mk|\hat{T}|nk_n\rangle = \langle mk|\hat{V}|nk_n\rangle + \sum_l \int dq\, \frac{q^2}{(2\pi)^2}\langle mk|\hat{V}|lq\rangle G^0_l(q;E)\langle lq|\hat{T}|nk_n\rangle \tag{3.100}$$

where we have used that in our current normalization the unity operator is

$$\hat{1} = \sum_l \int dq\, \frac{|q|}{2\pi}\, |lq\rangle\, \langle lq|\,, \tag{3.101}$$

and that the Green's function becomes

$$\begin{aligned}\langle lq|\,\hat{G}_0(E)\,|l'q'\rangle &= \langle lq|\,\frac{1}{E-\hat{H}_0+i\eta}\,|l'q'\rangle = \frac{1}{E-\frac{\hbar^2q^2}{2m}-\varepsilon_l+i\eta}\langle lq|l'q'\rangle \\ &= \frac{2m}{\hbar^2}\frac{1}{k_l^2-q^2+i\eta}\delta_{ll'}\frac{2\pi}{|q|}\delta(q-q') = G^0_l(q;E)\delta_{ll'}\delta(q-q').\end{aligned} \tag{3.102}$$

Hence the T-matrix satisfies

$$T_{mn}(k,k_n) = V_{mn}(k,k_n) + \frac{m}{\pi\hbar^2}\sum_l \int dq\,|q|\frac{V_{ml}(k,q)T_{ln}(q,k_n)}{k_l^2-q^2+i\eta}. \tag{3.103}$$

The integral can be treated the same way as we did in the 1D case. The transformation of the above equation to a matrix equation is more complicated but can be done (cf. Appendix D).

We have therefore managed to link the transmission amplitudes to matrix elements of the transition operator $\hat{T}$. The result is intuitively appealing, transmission from one channel to another is related to the transition from an eigenstate in one channel to an eigenstate in another. This is of course the reason for the definition and the name of the transition operator.

3.4 The Landauer Formula

Having introduced the scattering states formalism in the last section there are only few steps we need to obtain the celebrated Landauer formula. We assume that the contacts are reflectionless, i.e. that an electron incident from the leads to the contact is transmitted into the reservoir without reflection. This is a good approximation when the energy of the electron is not near a bottom of an energy band in the contact [33]. We assume also that the leads are ideal, i.e. the electrons suffer no scattering. The latter assumption was also used in Section 3.3. The two reservoirs have different quasi-Fermi energies or chemical potentials μ_L and μ_R, where $\mu_L = \mu_R + eV$, where V is the potential applied between the two contacts. Because of the assumption of reflectionless contacts the scattering states in the leads are occupied according to these chemical potentials, i.e. ψ^+_{nE} is occupied with the chemical potential μ_L and ψ^-_{nE} according to μ_R. Calculating the current of each scattering state and summing over occupied state one can derive the Landauer formula[1] [33, 38, 42]

$$I = \frac{2e}{h} \int_0^\infty dE\, T(E) \left[f(E - \mu_L) - f(E - \mu_R) \right], \tag{3.104}$$

where f is the Fermi function and

$$T(E) = \mathrm{Tr}[t^\dagger_E t_E]. \tag{3.105}$$

For the above formula for $T(E)$ to be correct the equal current normalization used earlier is essential. We have denoted explicitly that the matrix of transmission amplitudes depends on the energy. Since the evanescent modes carry no current the trace is only over propagating modes [39]. Note also that a factor of 2 has been included to count for spin, and the trace does therefore not include trace over spin.

It is interesting to note that the Landauer formalism says nothing about how one obtains the transmission probability. In Section 3.3 we discussed explicitly how we could use the LS equation and scattering states to obtain the transmission probability. We could also have used the 1D calculation of the transmission probability to obtain the current in those systems. There is however one important point we have

[1] This formula is sometimes called the Landauer-Büttiker formula. We have adapted the view that the multi-probe version of this formula is the Landauer-Büttiker formula while the two probe version shown here is the Landauer formula.

not discussed. When defining the different chemical potential we introduce a potential that is applied between the two contacts. The scattering potential is changed because of this additional electrostatic potential and the transmission probability does therefore depend on the applied voltage. A more explicit notation would therefore be

$$I(V) = \frac{2e}{h} \int dE\, T(E,V) \left[f(E-\mu_L) - f(E-\mu_R) \right]. \tag{3.106}$$

We will discuss this point in more detail in Chapter 4.

In the limit of small potential and low temperature one can assume that the transmission probability is independent of energy in the Fermi window and the integral for the current can be done, leading to

$$G = \frac{I}{V} = \frac{2e^2}{h} T(E_F), \tag{3.107}$$

where E_F is the Fermi energy and G is the conductance.

3.5 The Conductance of a Quantum Wire

The transport formalism we have been introducing will now be used to obtain the conductance of a quantum wire with a single elastic impurity. A quantum wire can be obtained by imposing an extra confinement on one of the free directions of a two dimensional electron gas (2DEG), such that free motion is possible in only one direction [42, 43]. The confinement is achieved e.g. by patterning the heterostructure of the 2DEG by etching, applying a negative bias to a split gate on top of the heterostructure pushing electrons from underneath the gates, or by growing a heterostructure on a vicinal surface [43].

We need two model potentials for the systems, one for the confinement potential and the other for the impurity potential. The confinement potential the electrons see is in most cases rather smooth but as a first approximation we can use the 2D version of the hard wall potential of Section 3.3. A more accurate model of the confinement might be parabolic walls. The transverse eigenfunctions are a little bit more complicated in this case but their inclusion in the transport formalism of last chapter is straightforward. The results are however qualitatively the same so we use the hard wall potential. The third type of confinement sometimes used is the saddle-point potential [44, 45]. The impurity potential is most often modeled

by a delta function potential [40, 46] but the main reason for this choice seems to be simplification of analytic calculations. In our approach we can use any local potential, but we focus mainly on a Gaussian potential.

The physical setup is the same as as schematically shown in Figure 3.3. Our procedure to obtain the conductance of a quantum wire is thus the following. Solving the system of Equations (3.103) for the T-matrix, using the scheme in Appendix D, we obtain the matrix of transmission amplitudes t. The trace of t is proportional to the conductance through the Landauer formula (3.107). We assume that the wire and the setup satisfies all the conditions necessary for the Landauer formula to be valid.

In the case of a perfectly ballistic wire (no impurities), the Landauer formula tells us that as we increase the energy and more and more modes become propagating, the conductance increases in steps of height equal to the unit of conductance $G_0 = 2e^2/h$. In the presence of a impurity in the wire, there will be scattering and the conductance will not vary in this steplike way. If there were no coupling between the modes we would expect the conductance of each mode to rise gradually to one, with perhaps some oscillations, just as in the 1D case already discussed in Section 3.2. When there is coupling between modes the structure can be drastically different from the one we see in the 1D case. In the next subsections we will examine the conductance of a quantum wire in the presence of a single impurity of Gaussian type (Section 3.5.1) and delta function potential type (Section 3.5.2).

3.5.1 Scattering by a Gaussian Potential

The first model potential for the impurity potential we examine is the Gaussian potential

$$V(x,z) = V_0 e^{-\alpha((x-x_i)^2 - z^2)}, \tag{3.108}$$

where V_0 gives the strength of the potential, α^{-1} is a measure of the range of the potential and $(x_i, 0)$ is the location of the center of the potential. Unless otherwise noted we have chosen $x_i = L_x/2$, i.e. the center of the potential is in the middle of the wire. In Figure 3.4 we have plotted this kind of potential for a wire of length $L_x = 4a_0$ using $V_0 = \pm 1$ Ryd and $\alpha = 2a_0^{-2}$. For definiteness we note that a 2DEG is often formed at the GaAs side of the interface between AlGaAs and GaAs. In GaAs $a_o = 9.79$ nm and Ryd $= 5.93$ meV, hence a wire with $L_x = 4a_0$ is approximately 39 nm wide, an experimentally plausible width.

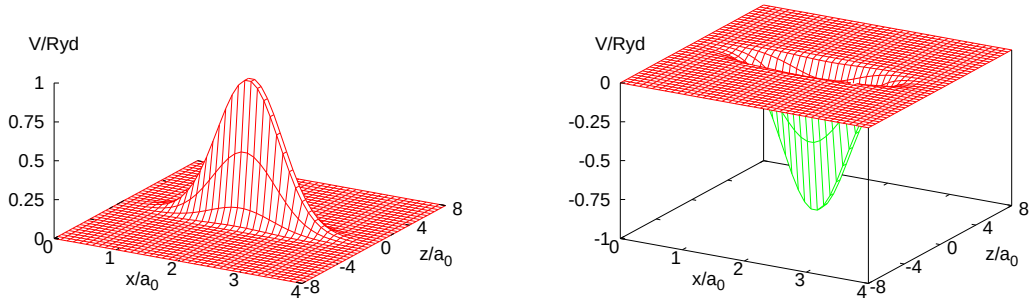

Figure 3.4: Gaussian scattering potential in the middle of a quantum wire. Infinite walls at the edges of the wire ($x = 0$ and $x = 4a_0$) are not shown. The potential on the left (right) is repulsive (attractive) of strength $V_0 = 1$ Ryd ($V_0 = -1$ Ryd) and the exponent α is in both cases equal to $2a_0^{-2}$.

The conductance of a repulsive Gaussian potential is shown in the left panel of Figure 3.5. Comparing with the transmission of a 1D Gaussian in Figure 3.2 we observe that qualitatively the conductance is the same for each channel. As the energy is increased more and more channels contribute to the conductance, each channel contributing one quantum of conductance G_0 when completely open. Coupling between transverse modes does not seem to alter qualitatively the picture we would expect for independent channels in a repulsive potential. The smoothing of the steps due to inelastic scattering is similar to what was seen in the first measurement of the quantizes conductance effect [47]. There are more effects that can cause smoothing but our results show that inelastic scattering is one of them.

Figure 3.5 also shows the conductance of an attractive Gaussian potential which is qualitatively very different from the 1D case since resonance dips appear in the conductance. These can be understood from a simple mode coupling model which we will now briefly review.

The coupled-channel equation (3.81), which in the present case we write as

$$\left(-\frac{\hbar^2}{2m}\frac{d^2}{dz^2} - E + \varepsilon_n\right)\varphi_{nE}(z) = -\sum_m V_{nm}(z)\varphi_{mE}(z) \tag{3.109}$$

where $V_{nm}(z) = \int dx\, \chi_n(x) V(\mathbf{r}) \chi_m(x)$, is an exact description of our system and has been solved accurately using the LS equation in Section 3.3.2 and 3.3.3. We now take a different route, focusing on the resonances (dips) [44, 45, 48]. Choosing

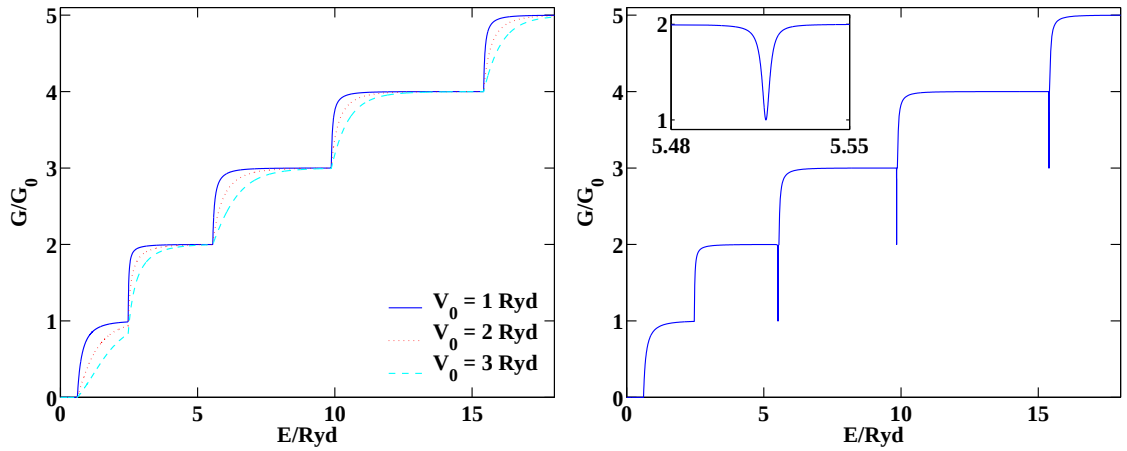

Figure 3.5: Conductance in units of $G_0 = 2e^2/h$ as a function of energy for a repulsive Gaussian potential of varying strength (left) and attractive Gaussian potential with $V_0 = -1$ Ryd (right). The inset in the latter has the same units on its axes as the main plot and shows the first resonance in more detail. In both cases the quantum wire has $L_x = 4a_0$ and the scattering potential has $\alpha = 2a_0^{-2}$. Calculations were performed with total number of modes $N_{\text{modes}} = 8$, number of intervals $n_{\text{intervals}} = 12$ and $p_{\text{max}} = 30a_0^{-1}$.

an energy in the range $\varepsilon_1 \leq E \leq \varepsilon_2$, only channel $n = 1$ will have a propagating solution in the absence of off-diagonal coupling (i.e. if $V_{nm} = 0$ for $m \neq n$), given by

$$\left(-\frac{\hbar^2}{2m}\frac{d^2}{dz^2} + V_{11}(z) + \varepsilon_1\right)\Psi_E^{\pm}(z) = E\Psi_E^{\pm}(z). \tag{3.110}$$

$\Psi_E^{\pm}(z)$ is defined similarly as $\phi_{nE}^{\pm}$ (Equation (3.88)) except for the potential term $V_{11}(z)$. Since the range of the potential is finite the asymptotic form is the same

$$\Psi_E^{\pm}(z) = \begin{cases} t^{\text{bg}} e^{\pm ik_1 z} & z \to \pm\infty, \\ e^{\pm ik_1 z} + r_{\pm}^{\text{bg}} e^{\mp ik_1 z} & z \to \mp\infty. \end{cases} \tag{3.111}$$

We have changed the normalization in agreement with the literature [45, 48]. The transmission and reflection coefficients t^{bg} and r^{bg} are the ones that a 1D system in the potential V_{11} would have, i.e. they describe non-resonant scattering in the channel.

Since the energy is lower than ε_2 and we are assuming that the potential is attractive, and thus V_{nn} are negative, the uncoupled channel $n = 2$ has at least one

bound state with energy E_0 given by

$$\left(-\frac{\hbar^2}{2m}\frac{d^2}{dz^2} + V_{22}(z) + \varepsilon_2\right)\Phi_0(z) = E_0\Phi_0(z). \tag{3.112}$$

Further assuming E to be close to the bound state energy E_0 and that no other channel has a bound state near E_0, we can neglect all the other channels in the coupled-channel equation (3.109), which then reduces to the system of equations

$$\left[E - \varepsilon_1 + \frac{\hbar^2}{2m}\frac{d^2}{dz^2} - V_{11}(z)\right]\varphi_1(z) = V_{12}\varphi_2(z), \tag{3.113}$$

$$\left[E - \varepsilon_2 + \frac{\hbar^2}{2m}\frac{d^2}{dz^2} - V_{22}(z)\right]\varphi_2(z) = V_{21}\varphi_1(z). \tag{3.114}$$

At least two routes have been taken in solving these equations and both lead to the same result. Nöckel and Stone [48] use the ansatz

$$\varphi_2(z) = A\Phi_0(z), \tag{3.115}$$

i.e. they assume that even in the presence of off-diagonal coupling the electron distribution of the second channel resembles the density of the bound state closely. The system of equations is then solved by introducing mode Green's functions defined by

$$G_n = \left[E - \varepsilon_n + \frac{\hbar^2}{2m}\frac{d^2}{dz^2} - V_{nn}(z) + i\eta\right]^{-1}, \tag{3.116}$$

and using a LS equation for each channel. Gurvitz and Levinson [45] use the spectral representation of $\hat{G}_2$, but close to the resonance $E \to E_0$, assume that the contribution of the bound state Φ_0 dominates such that

$$\hat{G}_2 = \frac{|\Phi_0\rangle\langle\Phi_0|}{E - E_0}. \tag{3.117}$$

Both approximations lead effectively to the same answer, i.e. that the conductance near the resonance is given by

$$G = G_0|t^{\mathrm{bg}}|^2\frac{(E - E_0 - \Delta - \delta)^2}{(E - E_0 - \Delta)^2 + \Gamma^2}, \tag{3.118}$$

where $E_0 + \Delta$ is a shifted quasi-bound state energy, the width of the resonance Γ is given by

$$\langle \Phi_0 | \hat{V}_{21} \hat{G}_1 \hat{V}_{12} | \Phi_0 \rangle = \Delta - i\Gamma, \tag{3.119}$$

and δ is similarly due to coupling between the bound state Φ_0 and the propagating states $\Psi_E^{\pm}$. Observe that the conductance goes to zero at $E = E_0 + \Delta - \delta$.

The physical meaning of the above model is that due to the bound state from channel 2 the propagating mode is resonantly backscattered causing a decrease in the conductance. Qualitatively the same behavior is obtained if one includes more evanescent modes [45]. This model has not, to our knowledge, been extended to energies were more than one mode is propagating. However, using symmetries and the scattering matrix, Nöckel and Stone [48] have obtained similar results. One can therefore generalize and say that the dips in the conductance of Figure 3.5 are due to coupling with quasi-bound states.

The above model is applicable for energies in the first step but as clearly seen in Figure 3.5 there is no dip there in our results. This is not in contradiction to the model because of symmetry reasons. The width Γ and the energy shifts Δ and δ are related to matrix elements of the operator $V_{12}(z)$ as explained above. The normal modes χ_n have a definite parity with respect to the center of the wire, χ_{2n+1} are even and χ_{2n} are odd. Since the Gaussian potential is even the operator $V_{12}(z) = 0$. The conductance at the resonance (3.118) therefore reduces to the non-resonant conductance $G = G_0 |t^{\mathrm{bg}}|^2$.

The absence of the dip in the first subband is of course a special case for a Gaussian potential with center in the middle of the wire. If the center of the potential is moved closer to the edge of the wire, the coupling between the modes will become different from zero and the resonance will reappear. Examining the coupling matrix element V_{12} we observe that its amplitude will increase as the center is moved from the middle, reach a maximum approximately between the middle of the wire and the edge and then decrease again. According to the simple mode coupling model, this would mean that the resonance should broaden and then become narrow again as the center is moved. Similarly the matrix element V_{22} responsible for bonding has a maximum approximately between the center and the edge of the wire, and a minimum at the edge. The resonance should therefore get lower in energy as it broadens, and then move to higher energy as it narrows again. The left panel of Figure 3.6 shows the conductance as the center of the Gaussian potential is varied.

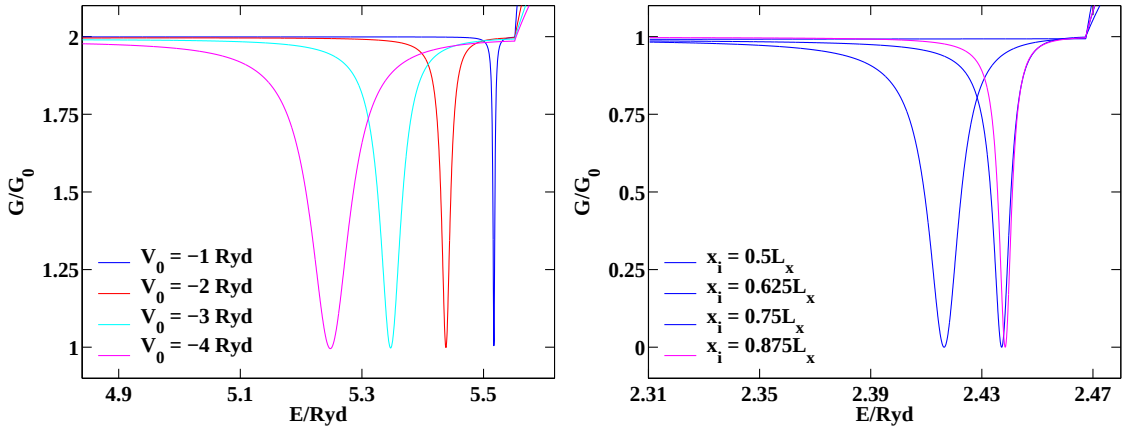

Figure 3.6: A closer look at a the first resonance as the center of the Gaussian potential is varied (left) and at the second resonance as the strength of the attractive potential is varied (right). In the former case the strength is kept fixed at $V_0 = -1$ Ryd. Both cases are for $4a_0$ wide wire and the potential has $\alpha = 2a_0^{-2}$. Calculations were performed with total number of modes $N_{\text{modes}} = 8$, number of intervals $n_{\text{intervals}} = 12$ and $p_{\text{max}} = 30a_0^{-1}$.

The behavior is exactly the one described above.

The resonances in the conductance of the attractive potential in Figure 3.5 are extremely narrow. The resonance in the inset has for example full width at half maximum on the order of 4 mRyd, i.e. around 21 μeV. Seeing resonances of this width in experiments is most likely a formidable task. As already mentioned, the width of the resonance depends on the coupling strength. Hence, increasing the strength of the potential while keeping all other parameter fixed the resonance should broaden. The binding energy of the quasi bound state will also increase and as an effect the resonance should move away from the energy of the next mode, i.e. to lower energy. Both of these effects can be clearly seen in the right panel of Figure 3.6 where we have plotted a close up of the resonance just before the third transverse mode.

3.5.2 Delta Function Potential

The delta function potential

$$V(x, z) = V_0 \delta(x - x_i)\delta(z), \tag{3.120}$$

is, in spite of its singular nature, very common in the literature. This is most likely because it can simplify analytical calculations, but numerically it can be a nuisance. We mainly study it as a comparison with the literature. We chose the

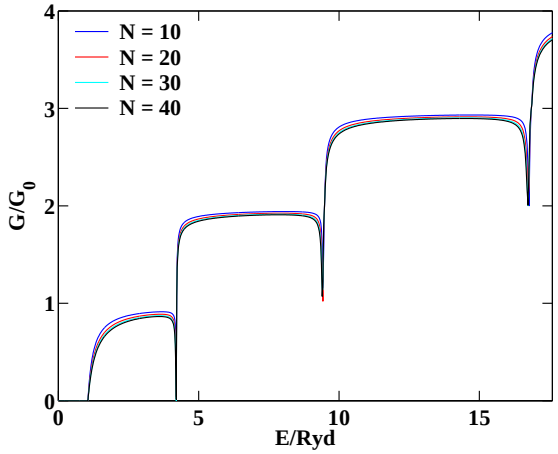

Figure 3.7: Conductance through a quantum wire with a delta function impurity potential as a function of energy. The total number of modes N_{modes} used in the calculation is varied but the number of intervals and maximum momentum in the LS integral is kept fixed at $n_{\text{intervals}} = 12$ and $p_{\text{max}} = 30a_0^{-1}$ respectively.

same parameters as Bagwell [40], i.e. $L_x = 3.06a_0$ and $V_0 = 1.055$ Ryda_o^2. In Figure 3.7 the conductance as a function of energy is plotted for these parameters, using more and more total number of modes. The overall correspondence with the results of Bagwell is quite good except that the conductance is perhaps a little bit lower in his case. Increasing the number of evanescent modes in the calculation decreases the conductance and we have only gone up to 50 total number of modes. Increasing the number of modes more than that increases the computing time and memory consumption very fast, and we have therefore not done it. Bagwell argues that one needs 100 modes so that the contribution of the next evanescent modes are negligible [40]. This is a case of the numerical nuisance of the delta potential mentioned above, and should be compared to the Gaussian potential. There we only use eight total number of modes and increasing the number of modes has very small, negligible effect.

Chapter 4

Molecular Electronics

In the last two chapters we have discussed the two main parts of this work, grid-free ground state of molecules and a Lippmann-Schwinger transport formalism. In a project inspired by the interesting field of molecular electronics it seems fitting to discuss briefly the field and its relation to our work. This chapter serves twofold purpose. Firstly, it ties the two parts of our work together. Secondly, we can look forward and examine how one would take the next steps towards understanding transport through molecules using the LS formalism. We also briefly compare our approach to the most common approaches in the literature. By no means is the discussion in this chapter intended to be thorough or detailed.

4.1 The Birth of a Field

Already in 1974 Aviram and Ratner suggested the use of molecules as active devices in molecular electronics and showed that a particular molecule could function as a diode [4]. The field did not catch on though, since experimental techniques were not advanced enough to measure the effect and the interest of the community lay elsewhere. In 1997 the breakthrough came, when Reed *et al.* [5], building upon the mechanically controllable break junction (MCB) method of Van Ruitenbeek and coworkers [49], were able to measure the current through potentially one (or at most few) molecule. More measurements followed, using the MCB method [7, 50], scanning tunneling probe measurements [51] and other methods [6, 8, 52]. Ruitenbeek and coworkers have even managed to measure the conductance of a hydrogen molecule using MCB [9].

Having something exciting to understand and explain such as transport through molecules, the theory part took off. Simplified models have been used but all the *ab initio* calculations are DFT based. Most often people use non-equilibrium Green's functions (NEGF) methods to obtain the current [12, 33, 51]. Another approach is the scattering formalism through the Lippmann-Schwinger equation, a simple variation of which we have already discussed and whose ideas originate with N.D. Lang and coworkers [11, 53]. This approach has not been taken up by many and is not nearly as popular as the non-equilibrium Green's function methods.

The rapid advance of the field of molecular electronics has aroused much interest from physics, chemistry and related fields, who have merged in a new field of molecular electronics. It is a young field and in spite of the rapid advances, theory and experiment do not agree completely. There are many open questions to be answered, and things to be explored. In the following sections we will discuss the most important questions related to our project and approach.

4.2 Obtaining the Current Through Molecules

The basic idea of the LS approach is to use the field of the molecule as a scattering potential in the equations of chapter 3 to obtain the current. The realization of this is not as straightforward as it sounds. In this section we will discuss some of the conceptional issues involved in a full scale calculation based on this approach.

4.2.1 The Contacts

How do we model the contacts? This is an important question, and perhaps the most important one in the field at the moment since the exact geometry of the contacts is not known experimentally. Calculations have shown that both the geometry, the number and type of atoms in the contacts can alter the shape and absolute value of the current quite extensively [11, 50, 54]. In the NEGF methods the semi-infinite contacts are taken into account by inclusion of extra self-energies [33]. In the LS approach the contacts are usually described by the jellium model. This is implicit in our approach. Often, a part of the contact is included in the molecule, making a so called extended molecule. This can be advantageous since the the contacts will not have reached their bulk values right at the molecule lead interface, but these bulk values are used to obtain the lead self-energies. Similar things can of course be

done in the LS approach.

As a first approximation we would most likely use only the molecule and devise some potential barriers to imitate the work function for electrons to go from the metals to the molecule. These would then be a part of the scattering potential. In a full scale calculations the effect of the contacts would be included self-consistently, thereby obtaining the electrostatic potential barriers as a part of the solution.

4.2.2 The Applied Voltage

The exact electrostatic profile is an active issue of discussion [55]. The simplest model assumes that the electrostatic potential drops linearly from one lead to the other, from zero to the applied voltage V. Ideally one should calculate the electrostatic potential profile self-consistently [11]. But even using the simplified linear model, the applied voltage raises some questions in our scattering approach, which in chapter 3 was only at zero applied voltage.

It should be clear that one can not include this applied potential as a part of the scattering potential since it would then not fall rapidly enough at infinity for the scattering formalism to be applicable. To only include it as a difference in the chemical potential of the right and left reservoir seems to crude an approximation, but might serve as a starting point. The only way seems to be to include it as a part of $\hat{H}_0$ in the LS approach. How this would be done is not unique. One can include all the electrostatic potential in $\hat{H}_0$ [11, 54] or one could only include a step function, the rest being a part of the scattering potential. Either way, this induces some changes in the analytic work of chapter 3. The most obvious one being that the Green's function corresponding to $\hat{H}_0$ is not as analytically simple as in the case of zero potential. Otherwise, the procedure is the same, the only question being how soon one has to introduce numerical work.

Chapter 5

Conclusions and Summary

We have applied grid-free DFT methods to obtain the ground state of molecules. In this method the molecular orbitals are expanded in a Gaussian type basis set and matrix elements of the exchange-correlation potential are obtained by matrix manipulations (diagonalization etc.). One thereby avoids any use of numerical grids often used in DFT calculations. We have used our method to calculate ground state energies of various small molecules, water, HF, HOF and NH_3, the results usually being in between Hartree-Fock and coupled-cluster calculations. These are reasonable results especially since we use the simple Slater $X\alpha$ functional as an approximation to the unknown exchange-correlation energy functional. Geometrical optimizations of water also give results comparable with experiments. We thus conclude that we have an working DFT implementation, capable of obtaining the ground state of smaller molecules (the largest molecule we have calculated is benzene) as an expansion in an analytical basis set.

In the second part of the thesis we discussed transport and its relation to scattering theory. We have shown that in an infinite system the k-space solution of the Lippmann-Schwinger equation, the integral equation of scattering, includes distribution functions, as could have been expected by comparison with the use of plane waves as a basis set. This can cause problems in numerical calculations and one therefore introduces the T-matrix (transition operator) which is related to the wave function outside the range of the potential. The T-matrix satisfies a LS like equation, free of the difficult singularities of the wave function LS equation. In a 2D and 3D system were the electron is confined in all but one direction (such as a nanosystem connected by two semi-infinite wires) one can use the conventional

Schrödinger equation to describe the transverse modes (confinement modes) but a 1D LS equation for the propagating part. Thereby one obtains scattering states in which an electron in a definite mode impinges from one direction and is transmitted and reflected by the scattering potential into different modes. From these transmission amplitudes one can read off the conductance of the system by help of the Landauer formula.

We have applied the transport formalism described above to a quasi-one-dimensional quantum wire. The calculated conductance shows steps as function of energy as more and more modes become propagating; the conductance of a completely open channel being equal to the quantum of conductance $G_0 = 2e^2/h$. If the scattering potential is attractive dips appear in the conductance due to resonant backscattering by means of quasi-bound states in the scattering potential. All the above is in complete agreement with what has been seen before in the literature. We therefore conclude that we have devised a transport formalism capable of describing many different systems.

Being interested in obtaining the current through molecules we have laid two important cornerstones in building a theory capable of achieving that goal. We have shown how to obtain the ground state density of a molecule and how one can model transport in a nanosystem. The next step would be to try to combine these two and we have briefly discussed how one could approach it and what the potential difficulties are. A realistic description of the contacts is of central importance, but how this is done is something people do not agree upon. The applied voltage also causes complications such as in the Green's function and how one should model screening of the electrostatic potential. The key word is self-consistency but there are still unanswered questions that remain. In due time people will find answers to these questions and at that we find it appropriate the end this thesis.

Appendix A

The Obara and Saika Scheme

In the Obara and Saika scheme recursive relations are used to obtain integrals over Cartesian Gaussian functions. In this appendix this scheme will be discussed. In Section A.1 we will derive in detail recursive relations for four center integrals, all other recursive relations used being collected without prove in Section A.2. We have chosen to do this since the four center overlap integrals are not mentioned in the original paper [27] but all the other relations are there. In this appendix all energies are scaled in Rydbergs and all lengths are scaled in Bohr radii.

A.1 Four Center Overlap Integrals

The material in this chapter follows closely the derivations in the original paper of Obara and Saika [27].

In the grid-free method we need the four center overlap integrals

$$\langle g_\mu(\zeta_\mu) g_\lambda(\zeta_{\lambda,m}) g_\sigma(\zeta_{\sigma,n}) g_\nu(\zeta_\nu)\rangle = \int d^3r\, g_\mu(\zeta_\mu, \mathbf{r}) g_\lambda(\zeta_{\lambda,m}, \mathbf{r}) g_\sigma(\zeta_{\sigma,n}, \mathbf{r}) g_\nu(\zeta_\nu, \mathbf{r}). \quad (2.68)$$

In the following we need to be a little bit more explicit, and therefore we write unnormalized Cartesian Gaussian functions with origin at $\mathbf{A}$ as

$$\tilde{g}(\mathbf{r}; \zeta_a, \mathbf{a}, \mathbf{A}) = (x - A_x)^{a_x} (y - A_y)^{a_y} (z - A_z)^{a_z} \exp[-\zeta_a (\mathbf{r} - \mathbf{A})^2] \quad (A.1)$$

where $\mathbf{r} = (x, y, z)$ represents the coordinates of the electron, ζ_a is the orbital expo-

nent, and **a** denotes a set of nonnegative integers

$$\mathbf{a} = (a_x, a_y, a_z). \tag{A.2}$$

The tilde is used to indicate that the function is unnormalized. The normalization constant of the function is given by

$$\mathcal{N}(\zeta_a, \mathbf{a}) = \left(\frac{2\zeta_a}{\pi}\right)^{3/4} (4\zeta_a)^{(a_x+a_y+a_z)/2} \left[(2a_x-1)!!(2a_y-1)!!(2a_z-1)!!\right]^{-1/2}. \tag{A.3}$$

The sum of a_x, a_y and a_z is related to the total angular momentum quantum number, the functions with this sum equal to 0,1,2... being refered to as s,p,d... respectively. The sum is refered to as the angular momentum and **a** as the angular moment index.

It will be useful to introduce the notation

$$\mathbf{1}_i = (\delta_{ix}, \delta_{iy}, \delta_{iz}), \quad i = x, y, z \tag{A.4}$$

with Kronecker's delta. In this notation a Gaussian with angular momentum index $\mathbf{1}_x = (1, 0, 0)$ corresponds to p_x-type Gaussian etc. Components with angular momentum d can be represented by $\mathbf{1}_i + \mathbf{1}_j$ $(i, j = x, y, z)$, where e.g. $\mathbf{1}_x + \mathbf{1}_y$ corresponds to d_{xy}.

We will also use extensively the notation $N_i(\mathbf{a})$ where N_i is meant to take the i-th component of the angular momentum index **a**. $N_i(\mathbf{1}_j)$ thus plays the same role as the Kronecker's delta δ_{ij}.

With these definitions an unnormalized four center overlap integral can be written

$$\langle \mathbf{abcd} \rangle = \int d^3r\, \tilde{g}(\mathbf{r}; \zeta_a, \mathbf{a}, \mathbf{A}) \tilde{g}(\mathbf{r}; \zeta_b, \mathbf{b}, \mathbf{B}) \tilde{g}(\mathbf{r}; \zeta_c, \mathbf{c}, \mathbf{C}) \tilde{g}(\mathbf{r}; \zeta_d, \mathbf{d}, \mathbf{D}). \tag{A.5}$$

Note how the angular momentum index **a** on the left hand side refers to σ_a, **a** and **A** on the right hand side. To obtain the four center overlap integrals (2.68) from the unnormalized ones, one simply multiplies with the corresponding normalization constants.

Differentiating a Cartesian Gaussian with respect to A_i will give two terms, one coming from the derivative of the polynomial and one from the derivative of the

exponential. Gathering these together one obtains

$$\tilde{g}(\mathbf{r};\zeta_a,\mathbf{a}+\mathbf{1}_i,\mathbf{A}) = \frac{1}{2\zeta_a}\frac{\partial}{\partial A_i}\tilde{g}(\mathbf{r};\zeta_a,\mathbf{a},\mathbf{A}) + \frac{N_i(\mathbf{a})}{2\zeta_a}\tilde{g}(\mathbf{r};\zeta_a,\mathbf{a}-\mathbf{1}_i,\mathbf{A}), \tag{A.6}$$

hence

$$\langle \mathbf{a}+\mathbf{1}_i,\mathbf{bcd}\rangle = \frac{1}{2\zeta_A}\frac{\partial}{\partial A_i}\langle \mathbf{abcd}\rangle + \frac{N_i(\mathbf{a})}{2\zeta_a}\langle \mathbf{a}-\mathbf{1}_i,\mathbf{bcd}\rangle . \tag{A.7}$$

To be able to perform the differentiation in the above expression we need a more explicit form for $\langle \mathbf{abcd}\rangle$. Inserting the explicit form of the Cartesian Gaussians

$$\langle \mathbf{abcd}\rangle = \int d^3r\,(x-A_x)^{a_x}(y-A_y)^{a_y}\cdots(z-D_z)^{d_z}\exp[-\zeta_a(\mathbf{r}-\mathbf{A})^2]\cdots\exp[-\zeta_d(\mathbf{r}-\mathbf{D})^2]. \tag{A.8}$$

Combining the exponentials into a single exponent by repeated use of the Gaussian product rule [20]

$$\exp[-\zeta_a(\mathbf{r}-\mathbf{A})^2]\exp[-\zeta_b(\mathbf{r}-\mathbf{B})^2] = \exp[-\xi(\mathbf{A}-\mathbf{B})^2]\exp[-\zeta(\mathbf{r}-\mathbf{P})^2], \tag{A.9}$$

where

$$\xi = \frac{\zeta_a\zeta_b}{\zeta_a+\zeta_b}, \quad \zeta = \zeta_a+\zeta_b \quad \text{and} \quad \mathbf{P} = \frac{\zeta_a\mathbf{A}+\zeta_b\mathbf{B}}{\zeta_a+\zeta_b}, \tag{A.10}$$

one obtains

$$\langle \mathbf{abcd}\rangle = \kappa_{abcd} I_x(a_x b_x c_x d_x) I_y(a_y b_y c_y d_y) I_z(a_z b_z c_z d_z). \tag{A.11}$$

The prefactor κ_{abcd} is defined by

$$\kappa_{abcd} = \exp[-\xi(\mathbf{A}-\mathbf{B})^2]\exp[-\lambda(\mathbf{C}-\mathbf{D})^2]\exp[-\rho(\mathbf{P}-\mathbf{Q})^2] \tag{A.12}$$

where

$$\lambda = \frac{\zeta_c\zeta_d}{\zeta_c+\zeta_d}, \quad \rho = \frac{\zeta\eta}{\zeta+\eta}, \quad \eta = \zeta_c+\zeta_d, \quad \mathbf{Q} = \frac{\zeta_c\mathbf{C}+\zeta_d\mathbf{D}}{\zeta_c+\zeta_d} \tag{A.13}$$

and

$$\mathbf{W} = \frac{\zeta\mathbf{P}+\eta\mathbf{Q}}{\zeta+\eta} = \frac{\zeta_a\mathbf{A}+\zeta_b\mathbf{B}+\zeta_c\mathbf{C}+\zeta_d\mathbf{D}}{\zeta_a+\zeta_b+\zeta_c+\zeta_d}. \tag{A.14}$$

The integral I_x is defined by

$$I_x(a_x b_x c_x d_x) = \int dx\,(x-A_x)^{a_x}(x-B_x)^{b_x}(x-C_x)^{c_x}(x-D_x)^{d_x}\exp[-(\zeta+\eta)(x-W_x)^2], \tag{A.15}$$

and similarly for I_y and I_z. Using the binomial theorem

$$(a+b)^n = \sum_{k=0}^{n}\binom{n}{k}a^k b^{n-k}, \tag{A.16}$$

the integral transforms into

$$\begin{aligned} I_x(a_x b_x c_x d_x) = &\sum_{k_{a_x}=0}^{a_x}\sum_{k_{b_x}=0}^{b_x}\sum_{k_{c_x}=0}^{c_x}\sum_{k_{d_x}=0}^{d_x}\binom{a_x}{k_{a_x}}\binom{b_x}{k_{b_x}}\binom{c_x}{k_{c_x}}\binom{d_x}{k_{d_x}} \\ &\times (W_x-A_x)^{a_x-k_{a_x}}(W_x-B_x)^{b_x-k_{b_x}}(W_x-C_x)^{c_x-k_{c_x}}(W_x-D_x)^{d_x-k_{d_x}} \\ &\times \int_{-\infty}^{\infty} dx\, x^{k_{a_x}+k_{b_x}+k_{c_x}+k_{d_x}}\exp[-(\zeta+\eta)x^2]. \end{aligned} \tag{A.17}$$

The integrand is odd when $k_{a_x}+k_{b_x}+k_{c_x}+k_{d_x}$ is odd, and the integral vanishes. Gradshteyn and Ryzhik [56] provide us with

$$\int_0^{\infty} dx\, x^{2n}\exp(-px^2) = \frac{(2n-1)!!}{2(2p)^n}\sqrt{\frac{\pi}{p}}, \quad (p>0, n=0,1,2,\ldots), \tag{A.18}$$

and hence the integral becomes

$$\begin{aligned} I_x(a_x b_x c_x d_x) = &\sqrt{\frac{\pi}{\zeta+\eta}}\sum_{\substack{k_{a_x}=0\\ k_{a_x}+k_{b_x}+k_{c_x}+k_{d_x}=\text{even}}}^{a_x}\sum_{k_{b_x}=0}^{b_x}\sum_{k_{c_x}=0}^{c_x}\sum_{k_{d_x}=0}^{d_x}\binom{a_x}{k_{a_x}}\binom{b_x}{k_{b_x}}\binom{c_x}{k_{c_x}}\binom{d_x}{k_{d_x}} \\ &\times (W_x-A_x)^{a_x-k_{a_x}}(W_x-B_x)^{b_x-k_{b_x}}(W_x-C_x)^{c_x-k_{c_x}}(W_x-D_x)^{d_x-k_{d_x}} \\ &\times \frac{(k_{a_x}+k_{b_x}+k_{c_x}+k_{d_x}-1)!!}{[2(\zeta+\eta)]^{(k_{a_x}+k_{b_x}+k_{c_x}+k_{d_x})/2}}. \end{aligned} \tag{A.19}$$

Note that we have now actually calculated the four center integral analytically. We will not use this result directly though, but for obtaining the derivative in Equation (A.6).

Differentiation of Equation (A.11) with respect to A_i leads to two terms. One were we differentiate κ

$$\frac{1}{2\zeta_a}\frac{\partial \kappa_{abcd}}{\partial A_i} = \left(\frac{\zeta_a A_i + \zeta_b B_i + \zeta_c C_i + \zeta_d D_i}{\zeta + \eta} - A_i\right)\kappa_{abcd} = (W_i - A_i)\,\kappa_{abcd} \tag{A.20}$$

and the other includes the derivative of I_i which is obtained by use of Equation (A.19):

$$\begin{aligned}\frac{1}{2\zeta_a}\frac{\partial I_i}{\partial A_i} = &\left(\frac{1}{2(\zeta+\eta)} - \frac{1}{2\zeta_a}\right) N_i(\mathbf{a}) I_i(a_i - 1, b_i c_i d_i) \\ &+ \frac{1}{2(\zeta+\eta)}\left[N_i(\mathbf{b}) I_i(a_i, b_i - 1, c_i d_i) + N_i(\mathbf{c}) I_i(a_i b_i, c_i - 1, d_i)\right] \\ &+ \frac{1}{2(\zeta+\eta)}\left[N_i(\mathbf{d}) I_i(a_i b_i c_i, d_i - 1)\right].\end{aligned} \tag{A.21}$$

By combining Equations (A.7), (A.20) and (A.21) we finally obtain our recursive relation for the four center integrals ($i = x, y, z$)

$$\begin{aligned}\langle \mathbf{a} + \mathbf{1}_i, \mathbf{bcd}\rangle = (W_i - A_i)\,\langle \mathbf{abcd}\rangle + \\ \frac{a_i \langle \mathbf{a} - \mathbf{1}_i, \mathbf{bcd}\rangle + b_i \langle \mathbf{a}, \mathbf{b} - \mathbf{1}_i, \mathbf{cd}\rangle + c_i \langle \mathbf{ab}, \mathbf{c} - \mathbf{1}_i, \mathbf{d}\rangle + d_i \langle \mathbf{abc}, \mathbf{d} - \mathbf{1}_i\rangle}{2(\zeta+\eta)}\end{aligned} \tag{A.22}$$

It is not enough to have the recursive relations, we also need the starting point which is the four center integrals of only s-type Gaussians. It should be quite clear from Equations (A.11) and (A.19) that

$$\langle \tilde{s}_a \tilde{s}_b \tilde{s}_c \tilde{s}_d \rangle = \left(\frac{\pi}{\zeta+\eta}\right)^{3/2} \kappa_{abcd}. \tag{A.23}$$

A.2 Recursive Relations

The derivations of other recursive relations follow similar lines as the one in Section A.1 and are discussed in the original paper [27]. In this section we will only collect together in a single place the recursive relations we use. The notation is the same as in last section.

A.2.1 Electron Repulsion Integral

In the Hartree term we need electron repulsion integrals that are written here in terms of unnormalized Cartesian Gaussian functions as

$$\langle \mathbf{ab}|\,|\mathbf{cd}\rangle = \iint d^3r\, d^3r' \,\frac{\tilde{g}(\mathbf{r};\zeta_a,\mathbf{a},\mathbf{A})\tilde{g}(\mathbf{r};\zeta_b,\mathbf{b},\mathbf{B})\tilde{g}(\mathbf{r}';\zeta_c,\mathbf{c},\mathbf{C})\tilde{g}(\mathbf{r}';\zeta_d,\mathbf{d},\mathbf{D})}{|\mathbf{r}-\mathbf{r}'|}. \tag{A.24}$$

Introducing an auxiliary electron repulsion integral

$$\langle \mathbf{ab}|\,|\mathbf{cd}\rangle^{(m)} = \frac{2}{\sqrt{\pi}}\int_0^\infty du \left(\frac{u^2}{\rho+u^2}\right)^m \langle \mathbf{ab}|\,u\,|\mathbf{cd}\rangle\,, \tag{A.25}$$

where m is nonnegative integer and

$$\langle \mathbf{ab}|\,u\,|\mathbf{cd}\rangle = \int d^3r'\,\tilde{g}(\mathbf{r}';\zeta_c,\mathbf{c},\mathbf{C})\tilde{g}(\mathbf{r}';\zeta_d,\mathbf{d},\mathbf{D})\,\langle \mathbf{a}|\,\mathbf{0}_{r'}\,|\mathbf{b}\rangle \tag{A.26}$$

with

$$\langle \mathbf{a}|\,\mathbf{0}_{r'}\,|\mathbf{b}\rangle = \int d^3r\,\tilde{g}(\mathbf{r};\zeta_a,\mathbf{a},\mathbf{A})\tilde{g}(\mathbf{r};\zeta_b,\mathbf{b},\mathbf{B})\exp[-u^2(\mathbf{r}-\mathbf{r}')^2], \tag{A.27}$$

one can obtain the recursive relation ($i = x, y, z$)

$$\begin{aligned}
\langle \mathbf{a}+\mathbf{1}_i,\mathbf{b}|\,|\mathbf{cd}\rangle^{(m)} &= (P_i - A_i)\,\langle \mathbf{ab}|\,|\mathbf{cd}\rangle^{(m)} + (W_i - P_i)\,\langle \mathbf{ab}|\,|\mathbf{cd}\rangle^{(m+1)} \\
&+ \frac{1}{2\zeta}N_i(\mathbf{a})\left(\langle \mathbf{a}-\mathbf{1}_i,\mathbf{b}|\,|\mathbf{cd}\rangle^{(m)} - \frac{\rho}{\zeta}\,\langle \mathbf{a}-\mathbf{1}_i,\mathbf{b}|\,|\mathbf{cd}\rangle^{(m+1)}\right) \\
&+ \frac{1}{2\zeta}N_i(\mathbf{b})\left(\langle \mathbf{a},\mathbf{b}-\mathbf{1}_i|\,|\mathbf{cd}\rangle^{(m)} - \frac{\rho}{\zeta}\,\langle \mathbf{a},\mathbf{b}-\mathbf{1}_i|\,|\mathbf{cd}\rangle^{(m+1)}\right) \\
&+ \frac{1}{2(\zeta+\eta)}N_i(\mathbf{c})\,\langle \mathbf{ab}|\,|\mathbf{c}-\mathbf{1}_i,\mathbf{d}\rangle^{(m+1)} \\
&+ \frac{1}{2(\zeta+\eta)}N_i(\mathbf{d})\,\langle \mathbf{ab}|\,|\mathbf{c},\mathbf{d}-\mathbf{1}_i\rangle^{(m+1)}\,.
\end{aligned} \tag{A.28}$$

Note that the elements with $m = 0$ are the true ERI's.

The ERI over s-type functions is

$$\langle \tilde{s}_a\tilde{s}_b|\,|\tilde{s}_c\tilde{s}_d\rangle^{(m)} = \frac{1}{\sqrt{\zeta+\eta}}K(\zeta_a,\zeta_b,\mathbf{A},\mathbf{B})K(\zeta_c,\zeta_d,\mathbf{C},\mathbf{D})F_m(T) \tag{A.29}$$

where the Boys function is defined by

$$F_m(T) = \int_0^1 dt\, t^{2m} \exp(-Tt^2), \tag{A.30}$$

$$T = \rho(\mathbf{P} - \mathbf{Q})^2 \tag{A.31}$$

and

$$K(\zeta, \zeta', \mathbf{R}, \mathbf{R}') = \sqrt{2}\frac{\pi^{5/4}}{\zeta + \zeta'} \exp\left[-\frac{\zeta\zeta'}{\zeta + \zeta'}(\mathbf{R} - \mathbf{R}')^2\right]. \tag{A.32}$$

With a little help from Gradstheyn and Ryzhik [56] one can obtain the Boys function as

$$F_m(T) = \frac{1}{2m+1}\Phi\left(m + \frac{1}{2}, m + \frac{3}{2}, -T\right), \tag{A.33}$$

where $\Phi(\alpha, \gamma; z)$ is the confluent hypergeometric function. For large values of T we may approximate the Boys function

$$F_m(T) = \int_0^1 dt\, t^{2m} \exp(-Tt^2) \approx \int_0^\infty dt\, t^{2m} \exp(-Tt^2) \quad (T \gg 1). \tag{A.34}$$

Hence [20]

$$F_m(T) \approx \frac{(2m-1)!!}{2^{m+1}}\sqrt{\frac{\pi}{T^{2m+1}}} \qquad (T \gg 1). \tag{A.35}$$

A.2.2 Two Center Overlap Integrals

Two center overlap integrals are needed to obtain the overlap matrix. Two center overlap matrix over unnormalized Cartesian Gaussian are written

$$\langle \mathbf{a}|\mathbf{b}\rangle = \int d^3r\, \tilde{g}(\mathbf{r}; \zeta_a, \mathbf{a}, \mathbf{A})\tilde{g}(\mathbf{r}; \zeta_b, \mathbf{b}, \mathbf{B}). \tag{A.36}$$

The recursive relation for these elements is

$$\langle \mathbf{a} + \mathbf{1}_i|\mathbf{b}\rangle = (P_i - A_i)\langle \mathbf{a}|\mathbf{b}\rangle + \frac{1}{2\zeta}N_i(\mathbf{a})\langle \mathbf{a} - \mathbf{1}_i|\mathbf{b}\rangle + \frac{1}{2\zeta}N_i(\mathbf{b})\langle \mathbf{a}|\mathbf{b} - \mathbf{1}_i\rangle \tag{A.37}$$

and the integral over s functions is given by

$$\langle \tilde{s}_a|\tilde{s}_b\rangle = \left(\frac{\pi}{\zeta}\right)^{3/2} \exp[-\xi(\mathbf{A} - \mathbf{B})^2]. \tag{A.38}$$

A.2.3 Kinetic Energy Integrals

The kinetic energy integral of unnormalized Cartesian Gaussians

$$\langle \mathbf{a}| \hat{T} |\mathbf{b}\rangle = \int d^3r\, \tilde{g}(\mathbf{r};\zeta_a,\mathbf{a},\mathbf{A})(-\frac{1}{2}\nabla^2)\tilde{g}(\mathbf{r};\zeta_b,\mathbf{b},\mathbf{B}) \tag{A.39}$$

is obtained by the recursive relation

$$\begin{aligned}\langle \mathbf{a}+\mathbf{1}| \hat{T} |\mathbf{b}\rangle = (P_i - A_i)\langle \mathbf{a}| \hat{T} |\mathbf{b}\rangle + \frac{1}{2\zeta}N_i(\mathbf{a})\langle \mathbf{a}-\mathbf{1}_i| \hat{T} |\mathbf{b}\rangle \\ + \frac{1}{2\zeta}N_i(\mathbf{b})\langle \mathbf{a}| \hat{T} |\mathbf{b}-\mathbf{1}_i\rangle \\ + 2\xi\left[\langle \mathbf{a}+\mathbf{1}_i|\mathbf{b}\rangle - \frac{1}{2\zeta_a}\langle \mathbf{a}-\mathbf{1}_i|\mathbf{b}\rangle\right].\end{aligned} \tag{A.40}$$

The kinetic energy integral over s functions is

$$\langle \tilde{s}_a| \hat{T} |\tilde{s}_b\rangle = \xi[3 - 2\xi(\mathbf{A}-\mathbf{B})^2]\langle \tilde{s}_a|\tilde{s}_b\rangle. \tag{A.41}$$

A.2.4 Nuclear Attraction Integrals

The nuclear attraction integral over unnormalizes Cartesian Gaussian

$$\langle \mathbf{a}| \hat{U}_{\text{nucl}}(\mathbf{C}) |\mathbf{b}\rangle = \int d^3r\, \frac{\tilde{g}(\mathbf{r};\zeta_a,\mathbf{a},\mathbf{A})\tilde{g}(\mathbf{r};\zeta_b,\mathbf{b},\mathbf{B})}{|\mathbf{r}-\mathbf{C}|} \tag{A.42}$$

is obtained through the recursive relation of auxiliary function

$$\begin{aligned}\langle \mathbf{a}+\mathbf{1}_i|\hat{U}_{\text{nucl}}(\mathbf{C}) |\mathbf{b}\rangle^{(m)} = (P_i - A_i)\langle \mathbf{a}| \hat{U}_{\text{nucl}}(\mathbf{C}) |\mathbf{b}\rangle^{(m)} \\ - (P_i - C_i)\langle \mathbf{a}| \hat{U}_{\text{nucl}}(\mathbf{C}) |\mathbf{b}\rangle^{(m+1)} \\ + \frac{1}{2\zeta}N_i(\mathbf{a})\left(\langle \mathbf{a}-\mathbf{1}_i| \hat{U}_{\text{nucl}}(\mathbf{C}) |\mathbf{b}\rangle^{(m)} - \langle \mathbf{a}-\mathbf{1}_i| \hat{U}_{\text{nucl}}(\mathbf{C}) |\mathbf{b}\rangle^{(m+1)}\right) \\ + \frac{1}{2\zeta}N_i(\mathbf{b})\left(\langle \mathbf{a}| \hat{U}_{\text{nucl}}(\mathbf{C}) |\mathbf{b}-\mathbf{1}_i\rangle^{(m)} - \langle \mathbf{a}| \hat{U}_{\text{nucl}}(\mathbf{C}) |\mathbf{b}\rangle^{(m+1)}\right),\end{aligned} \tag{A.43}$$

where the real nuclear attraction integrals are the ones with $m = 0$. The auxiliary integrals are defined by

$$\langle \mathbf{a}| \hat{U}_{\text{nucl}}(\mathbf{C}) |\mathbf{b}\rangle^{(m)} = \frac{2}{\sqrt{\pi}}\int_0^\infty du\, \left(\frac{u^2}{\zeta+u^2}\right)^m \langle \mathbf{a}| \mathbf{0}_\mathbf{C} |\mathbf{b}\rangle, \tag{A.44}$$

where

$$\langle \mathbf{a}| \, \mathbf{0_C} \, |\mathbf{b}\rangle = \int d^3r \, \tilde{g}(\mathbf{r}; \zeta_a, \mathbf{a}, \mathbf{A}) \tilde{g}(\mathbf{r}; \zeta_b, \mathbf{b}, \mathbf{B}) \exp(-u^2(\mathbf{r} - \mathbf{C})^2). \tag{A.45}$$

The auxiliary integrals over s functions are

$$\langle \tilde{s}_a| \, U_{\text{nucl}}(\mathbf{C}) \, |\tilde{s}_b\rangle^{(m)} = 2 \left(\frac{\zeta}{\pi}\right)^{1/2} \langle \tilde{s}_a|\tilde{s}_b\rangle F_m(U), \tag{A.46}$$

where

$$U = \xi(\mathbf{P} - \mathbf{C})^2. \tag{A.47}$$

Appendix B

The Equality of the Matrix of a Function and the Function of a Matrix in a Complete Basis

We will now prove the assertion made in Section 2.5.1:

$$M[f(n)] = f(M[n]). \tag{2.64}$$

Assume that we can write the function f as a Taylor series

$$f(n) = \sum_m \alpha_m n^m, \tag{B.1}$$

then

$$M[f(n)] = M[\sum_m \alpha_m n^m] = \sum_m \alpha_m M[n^m] = \sum_m \alpha_m (M[n])^m = f(M[n]). \tag{B.2}$$

The last step is obtained by repeated use of the completeness relation of the basis

$$\sum_\phi |\phi\rangle\langle\phi| = \infty, \tag{B.3}$$

such that

$$\begin{aligned}\langle\phi_\mu|\,\hat{n}^m\,|\phi_\beta\rangle &= \sum_{\phi_1\ldots\phi_{m-1}} \langle\phi_\mu|\,\hat{n}\,|\phi_1\rangle\cdots\langle\phi_{m-1}|\,\hat{n}\,|\phi_\nu\rangle \\ &= \sum_{1\cdots(m-1)} M_{\mu 1}[n]M_{1,2}[n]\cdots M_{m-1,\nu}[n] \\ &= \sum_{2\cdots(m-1)} M^2_{\mu 2}[n]\cdots M_{m-1,\nu}[n] = M^m_{\mu\nu}[n].\end{aligned} \tag{B.4}$$

Note that in the proof we have frequently had to use the completeness of the basis. One could fear that if the basis were substantially incomplete the equality of Equation (2.64) would not be very accurate. Experience through comparisons with other calculations and experiments will tell if this is accurate enough but as touched upon in Section 2.5.1 it often turns out to be the case.

Appendix C

Fourier Transform of the Heitler Zeta Function

In this appendix we calculate the Fourier transform of the Heitler zeta function $\zeta(k-p)$. Using the definition given in Equation (3.33) we obtain

$$\int dp\, e^{ipx}\zeta(k-p) = P\int dp\, \frac{e^{ipx}}{k-p} - i\pi e^{ikx} = e^{ikx}\left(P\int_{-\infty}^{\infty} dz\, \frac{e^{-izx}}{z} - i\pi\right). \quad \text{(C.1)}$$

The principal part

$$I_p = P\int_{-\infty}^{\infty} dz\, \frac{e^{-izx}}{z} \quad \text{(C.2)}$$

is calculated in the complex plane, using the Cauchy integral formula. As usual whether we close the integration path in the upper or lower halfplane depends on the sign of x. In the following we assume that $x > 0$ and close in the lower halfplane, giving (cf. Figure C.1)

$$0 = \int_{C_R} dz\, \frac{e^{-izx}}{z} + \int_{C_\varepsilon} dz\, \frac{e^{-izx}}{z} - I_p(R,\varepsilon), \quad \text{(C.3)}$$

where

$$I_p(R,\varepsilon) = \int_{-R}^{-\varepsilon} dz\, \frac{e^{-izx}}{z} + \int_{\varepsilon}^{R} dz\, \frac{e^{-izx}}{z}. \quad \text{(C.4)}$$

In the limit $R \to \infty$ and $\varepsilon \to 0$, $I_p(R,\varepsilon) \to I_p$. In this limit the integral over C_R is zero since the exponential falls fast enough to zero. To calculate the path integral over C_ε we use a nice little lemma [57] that states that if $f(z)$ has a simple pole at $z = \alpha$ with residue a_{-1} and $k = k(\varepsilon,\phi)$ is an arc of the circle $|z-\alpha| = \varepsilon$ that

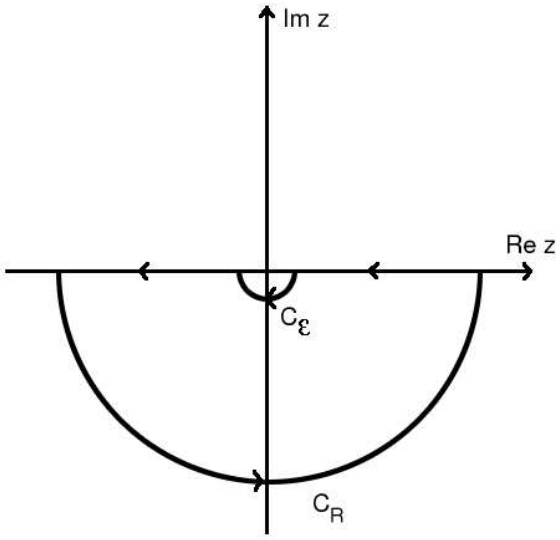

Figure C.1: The contours used when integrating the principal part.

subtends an angle ϕ at the center; then

$$\lim_{\varepsilon \to 0^+} \int_k dz\, f(z) = i\phi a_{-1}. \tag{C.5}$$

Hence

$$I_{C_\varepsilon} = -i\pi, \tag{C.6}$$

the minus coming from the orientation of the path. We therefore obtain

$$I_p = -i\pi. \tag{C.7}$$

Similar calculations for $x < 0$ give

$$I_p = i\pi, \tag{C.8}$$

and therefore

$$I_p = -i\pi\epsilon(x) \tag{C.9}$$

where

$$\epsilon(x) = \begin{cases} -1 & x < 0, \\ 1 & x > 0. \end{cases} \tag{C.10}$$

The Fourier transform of the zeta function follows

$$\int dp\, e^{ipx}\zeta(k-p) = -i\pi e^{ikx}(1+\epsilon(x)) = -2\pi i e^{ikx}\theta(x), \tag{C.11}$$

where $\theta(x)$ is the Heaviside step function.

The exact same steps give

$$\int dp\, e^{ipx}\zeta(k+p) = -i\pi e^{-ikx}(1-\epsilon(x)) = -2\pi i e^{ikx}\theta(-x). \tag{C.12}$$

The case $x = 0$ has to be treated separately. In this case the principal part is zero and we obtain

$$\int_{-\infty}^{\infty} dp\, \zeta(k \pm p) = -i\pi. \tag{C.13}$$

Appendix D

Transformation of the LS equation to a Matrix Equation

In numerical calculations the integral equation for the T-matrix is transformed into a matrix equation. This is done in both the 1D case (Section D.1) and in the 2D/3D case (Section D.2).

D.1 1D Case

In 1D the T-matrix satisfies the integral equation

$$T(k',k) = V(k',k) + \int dp\, V(k',p) G_0(p;E) T(p,k) \tag{D.1}$$

The units of T and V are energy times length, so if we scale all energies in Rydbergs and lengths in units of Bohr radii we obtain the exact same equation except everything is scaled. We will in this appendix only work with scaled sizes, but will not introduce a new notation for it.

In these scaled units the Green's function is

$$G_0(p;k) = \frac{1}{k^2 - p^2 + i\eta}. \tag{D.2}$$

Using the fact [38]

$$\frac{1}{x \pm i\eta} = \frac{P}{x} \mp i\pi\delta(x), \tag{D.3}$$

where P denotes principal value, the Green's function can be rewritten as

$$G_0(p;k) = \frac{P}{k^2 - p^2} - \frac{i\pi}{2k}\left(\delta(p-k) + \delta(p+k)\right) \tag{D.4}$$

Introducing this into the LS equation for the T-matrix

$$\begin{aligned} T(k',k) = V(k',k) &+ P\int_{-\infty}^{\infty} dp\, \frac{V(k',p)T(p,k)}{k^2 - p^2} \\ &- \frac{i\pi}{2k}\left(V(k',k)T(k,k) + V(k',-k)T(-k,k)\right). \end{aligned} \tag{D.5}$$

The integrand in the remaining integral is singular at $p = \pm k$. Since

$$P\int_0^{\infty} dp\, \frac{1}{k^2 - p^2} = 0 \tag{D.6}$$

one can get rid of the singularity of the integrand by a subtraction of a zero [31, 36]. For a general function f we have (assume $k > 0$)

$$\begin{aligned} P\int_{-\infty}^{\infty} dp\, \frac{f(p)}{k^2 - p^2} &= P\int_0^{\infty} dp\, \frac{f(-p)}{k^2 - p^2} + P\int_0^{\infty} dp\, \frac{f(p)}{k^2 - p^2} \\ &= \int_0^{\infty} dp\, \frac{f(-p) - f(-k)}{k^2 - p^2} + \int_0^{\infty} dp\, \frac{f(p) - f(k)}{k^2 - p^2}. \end{aligned} \tag{D.7}$$

The value of the integrand at the singularity can, by use of l'Hôpital's rule, be seen to have become $f'(\pm k)/2k$. Assuming that f' is nonsingular at $\pm k$, the principal value can therefore be skipped as already done. In our case f is a combination of T and V that are smooth functions of energy. Using the above we obtain for the remaining integral in Equation (D.5)

$$\begin{aligned} P\int_{-\infty}^{\infty} dp\, \frac{V(k',p)T(p,k)}{k^2 - p^2} &= \int_0^{\infty} dp\, \frac{V(k',p)T(p,k) - V(k',k)T(k,k)}{k^2 - p^2} \\ &+ \int_0^{\infty} dp\, \frac{V(k',-p)T(-p,k) - V(k',-k)T(-k,k)}{k^2 - p^2}. \end{aligned} \tag{D.8}$$

We perform the integral by putting the upper limit to $p_{\max}$ and dividing the integration interval into $n_{\text{intervals}}$ equal length subintervals

$$\int_0^{\infty} \approx \int_0^{p_{\max}} = \sum_{i=1}^{n_{\text{intervals}}} \int_{p(i)}^{p(i+i)}, \tag{D.9}$$

where

$$p(i) = (i-1)\frac{p_{\max}}{n_{\text{intervals}}} = (i-1)\Delta_{\text{int}}. \tag{D.10}$$

Each subinterval integral is approximated by a four point Gaussian quadrature such that, for a general f

$$\int_{p(i)}^{p(i+i)} dp\, f(p) = \frac{\Delta_{\text{int}}}{2}\sum_{j=1}^{4} w_j f(y_j) = \sum_{j=1}^{4} w'_j f(y_j), \tag{D.11}$$

where

$$w'_j = \frac{\Delta_{\text{int}}}{2} w_j \tag{D.12}$$

and

$$y_j = \frac{\Delta_{\text{int}}}{2} x_j + \frac{2i-1}{2}\Delta_{\text{int}}. \tag{D.13}$$

x_j and w_j are the abscissas and weight factors respectively used in the four point Gaussian scheme were integration limits are from -1 to 1 [58]. We will therefore write

$$\int_0^{\infty} dp\, f(p) \approx \sum_{l=1}^{N_g} w'_l f(y_l), \tag{D.14}$$

where $N_g = 4n_{\text{intervals}}$ is the total number of Gaussian points

Using the above procedure on the integral in Equation (D.8) gives

$$\begin{aligned} P\int_{-\infty}^{\infty} dp\, \frac{V(k',p)T(p,k)}{k^2-p^2} &= \sum_{l=1}^{N_g} w'_l \frac{V(k',p_l)T(p_l,k) - V(k',k)T(k,k)}{k^2-p_l^2} \\ &+ \sum_{l=1}^{N_g} w'_l \frac{V(k',-p_l)T(-p_l,k) - V(k',-k)T(-k,k)}{k^2-p_l^2}, \end{aligned} \tag{D.15}$$

transforming the integral equation for T into

$$\begin{aligned} T(k',k) = V(k',k) &+ \sum_{l=1}^{N_g} w_l' \frac{V(k',-p_l)T(-p_l,k)}{k^2-p_l^2} \\ &+ \sum_{l=1}^{N_g} w_l' \frac{V(k',p_l)T(p_l,k)}{k^2-p_l^2} - \sum_{l=1}^{N_g} \frac{w_l'}{k^2-p_l^2} V(k',-k)T(-k,k) \\ &- \sum_{l=1}^{N_g} \frac{w_l'}{k^2-p_l^2} V(k',k)T(k,k) \\ &- \frac{i\pi}{2k}\left(V(k',k)T(k,k) + V(k',-k)T(-k,k)\right). \end{aligned} \tag{D.16}$$

We put k' on a net

$$k_m = \begin{cases} -p_{N_g-m+1} & m = 1,\ldots,N_g, \\ p_{m-N_g} & m = N_g+1,\ldots,2N_g, \\ -k & m = 2N_g+1, \\ k & m = 2N_g+2. \end{cases} \tag{D.17}$$

It is clear that the weight factors for $-p_l$ equal w_l and the weight factors corresponding to the k_m become

$$v_m = \begin{cases} w'_{N_g-m+1} & m = 1,\ldots,N_g, \\ w'_{m-N_g} & m = N_g+1,\ldots,2N_g. \end{cases} \tag{D.18}$$

With these definitions we obtain for $k' = k_n$

$$\begin{aligned} T(k_n,k) = V(k_n,k) &+ \sum_{m=1}^{2N_g} v_m \frac{V(k_n,k_m)T(k_m,k)}{k^2-k_m^2} \\ &- \frac{1}{2}\sum_{m=1}^{2N_g} \frac{v_m}{k^2-k_m^2}\left(V(k_n,k_{2N_g+1})T(k_{2N_g+1},k) + V(k_n,k_{2N_g+2})T(k_{2N_g+2},k)\right) \\ &- \frac{i\pi}{2k}\left(V(k_n,k_{2N_g+1})T(k_{2N_g+1},k) + V(k_n,k_{2N_g+2})T(k_{2N_g+2},k)\right). \end{aligned} \tag{D.19}$$

Defining

$$D_m = \begin{cases} \frac{v_m}{k^2-k_m^2} & m = 1, \ldots, 2N_g \\ -\frac{1}{2}\sum_{m=1}^{2N_g} \frac{v_m}{k^2-k_m^2} - i\frac{\pi}{2k} & m = 2N_g+1, 2N_g+2, \end{cases} \tag{D.20}$$

the equation for the T-matrix, Equation (D.19), becomes

$$T_{n,2N_g+2} = V_{n,2N_g+2} + \sum_{m=1}^{2N_g+2} V_{nm} D_m T_{m,2N_g+2}. \tag{D.21}$$

This can be rewritten as

$$\sum_m F_{nm} T_{m,2N_g+2} = V_{n,2N_g+2} \tag{D.22}$$

where we have defined

$$F_{nm} = \delta_{nm} - V_{nm} D_m. \tag{D.23}$$

This is an easily solved matrix equation. The matrix element $T_{2N_g+2,2N_g+2}$ is directly related to the transmission amplitude

$$t = 1 + f_E(k \leftarrow k) = 1 - \frac{i\pi}{k} T(k,k) = 1 - \frac{i\pi}{k} T_{2N_g+2,2N_g+2}. \tag{D.24}$$

D.2 2D and 3D Case

We now want to transform Equation (3.103) which, if all energies and lengths are normalized in units of Rydbergs and Bohr radii respectively, can be written

$$T_{mn}(k,k_n) = V_{mn}(k,k_n) + \frac{1}{2\pi}\sum_l \int_{-\infty}^{\infty} dq\,|q| \frac{V_{ml}(k,q) T_{ln}(q,k_n)}{k_l^2 - q^2 + i\eta}. \tag{D.25}$$

The energy E is a parameter in this equation through the energy dependence of k_l. The transverse modes are separated into propagating and evanescent modes depending on the sign of k_l^2. We make this separation explicit by splitting the sum

over transverse modes into two sums

$$T_{mn}(k,k_n) = V_{mn}(k,k_n) + \frac{1}{2\pi}\sum_{l=1}^{N_{\text{prop}}}\int_{-\infty}^{\infty} dq\,|q|\frac{V_{ml}(k,q)T_{ln}(q,k_n)}{k_l^2-q^2+i\eta} - \frac{1}{2\pi}\sum_{l=N_{\text{prop}}+1}^{N_{\text{modes}}}\int_{-\infty}^{\infty} dq\,|q|\frac{V_{ml}(k,q)T_{ln}(q,k_n)}{\kappa_l^2+q^2}, \tag{D.26}$$

where N_{prop} is the number of propagating modes, N_{modes} is the total number of modes used in the calculation and $\kappa_l^2 = 2m\varepsilon_l/\hbar^2 - k_E^2 > 0$. We have assumed that the energy is not equal to one of the transverse eigenenergies, hence the Green's function for the evanescent modes is non-singular for all q, thus allowing η to be ignored.

Using relation (D.4) with $k = k_l$ we obtain for the sum over propagating modes

$$\frac{1}{2\pi}\sum_{l=1}^{N_{\text{prop}}}\int_{-\infty}^{\infty} dq\,|q|\frac{V_{ml}(k,q)T_{ln}(q,k_n)}{k_l^2-q^2+i\eta} = \frac{1}{2\pi}\sum_{l=1}^{N_{\text{prop}}} P\int_{-\infty}^{\infty} dq\,|q|\frac{V_{ml}(k,q)T_{ln}(q,k_n)}{k_l^2-q^2} - \frac{i}{4}\sum_{l=1}^{N_{\text{prop}}}\left[V_{ml}(k,-k_l)T_{ln}(-k_l,k_n) + V_{ml}(k,k_l)T_{ln}(k_l,k_n)\right]. \tag{D.27}$$

The principal part integration is done using the prescription given in Equations (D.7) and (D.14), leading to

$$\begin{aligned}\frac{1}{2\pi}\sum_{l=1}^{N_{\text{prop}}} P\int_{-\infty}^{\infty} dq\,|q|\frac{V_{ml}(k,q)T_{ln}(q,k_n)}{k_l^2-q^2} = &\\ \frac{1}{2\pi}\sum_{l=1}^{N_{\text{prop}}}\sum_{j=1}^{N_g} w_j' p_j \frac{V_{ml}(k,-p_j)T_{ln}(-p_j,k_n)}{k_l^2-p_j^2} &\\ -\frac{1}{2\pi}\sum_{l=1}^{N_{\text{prop}}}\sum_{j=1}^{N_g} w_j' k_l \frac{V_{ml}(k,-k_l)T_{ln}(-k_l,k_n)}{k_l^2-p_j^2} &\\ +\frac{1}{2\pi}\sum_{l=1}^{N_{\text{prop}}}\sum_{j=1}^{N_g} w_j' p_j \frac{V_{ml}(k,p_j)T_{ln}(p_j,k_n)}{k_l^2-p_j^2} &\\ -\frac{1}{2\pi}\sum_{l=1}^{N_{\text{prop}}}\sum_{j=1}^{N_g} w_j' k_l \frac{V_{ml}(k,k_l)T_{ln}(k_l,k_n)}{k_l^2-p_j^2}.&\end{aligned} \tag{D.28}$$

In analogy with the 1D case we reorder the p_j such that

$$q_j = \begin{cases} -p_{N_g-j+1} & j = 1, \ldots, N_g, \\ p_{j-N_g} & j = N_g+1, \ldots, 2N_g, \end{cases} \tag{D.29}$$

and

$$v_j = \begin{cases} w'_{N_g-j+1} & j = 1, \ldots, N_g, \\ w'_{j-N_g} & j = N_g+1, \ldots, 2N_g. \end{cases} \tag{D.30}$$

Using this in the equation for the principal part (D.28) the sum over the propagating modes becomes

$$\begin{aligned} &\frac{1}{2\pi}\sum_{l=1}^{N_{\text{prop}}}\int_{-\infty}^{\infty} dq\,|q|\frac{V_{ml}(k,q)T_{ln}(q,k_n)}{k_l^2-q^2+i\eta} = \sum_{l=1}^{N_{\text{prop}}}\sum_{j=1}^{2N_g}\frac{v_j|q_j|}{2\pi}\frac{V_{ml}(k,q_j)T_{ln}(q_j,k_n)}{k_l^2-q_j^2}+ \\ &\sum_{l=1}^{N_{\text{prop}}}\left(\frac{-k_l}{4\pi}\sum_{j=1}^{2N_g}\frac{v_j}{k_l^2-q_j^2}-\frac{i}{4}\right)\left(V_{ml}(k,-k_l)T_{ln}(-k_l,k_n)+V_{ml}(k,k_l)T_{ln}(k_l,k_n)\right). \end{aligned} \tag{D.31}$$

In the evanescent part of Equation (D.26) there is no singularity and the Gaussian quadrature (D.14) can be applied directly

$$\begin{aligned} &-\frac{1}{2\pi}\sum_{l=N_{\text{prop}}+1}^{N_{\text{modes}}}\int_{-\infty}^{\infty} dq\,|q|\frac{V_{ml}(k,q)T_{ln}(q,k_n)}{\kappa_l^2+q^2} \\ &=-\frac{1}{2\pi}\sum_{l=N_{\text{prop}}+1}^{N_{\text{modes}}}\int_{0}^{\infty} dq\,q\frac{V_{ml}(k,-q)T_{ln}(-q,k_n)+V_{ml}(k,q)T_{ln}(q,k_n)}{\kappa_l^2+q^2} \\ &=-\frac{1}{2\pi}\sum_{l=N_{\text{prop}}+1}^{N_{\text{modes}}}\sum_{j=1}^{N_g} v_j p_j\frac{V_{ml}(k,-p_j)T_{ln}(-p_j,k_n)+V_{ml}(k,p_j)T_{ln}(p_j,k_n)}{\kappa_l^2+p_j^2} \\ &=\sum_{l=N_{\text{prop}}+1}^{N_{\text{modes}}}\sum_{j=1}^{2N_g}\frac{-v_j|q_j|}{2\pi}\frac{V_{ml}(k,p_j)T_{ln}(p_j,k_n)}{\kappa_l^2+p_j^2}. \end{aligned} \tag{D.32}$$

Noting that $\kappa_l^2+p_j^2 = -(k_l^2-p_j^2)$ we can combine the evanescent part (D.32) and

Table D.1: The map between the index μ and the number of the transverse mode l and wavenumber k.

μ	l	k
1	1	q_1
2	1	q_2
$\vdots$	$\vdots$	$\vdots$
$2N_g$	1	q_{2N_g}
$2N_g+1$	2	q_1
$\vdots$	$\vdots$	$\vdots$
$2N_{\text{modes}}N_g$	N_{modes}	q_{2N_g}
$2N_{\text{modes}}N_g+1$	N_{prop}	$-k_{N_{\text{prop}}}$
$\vdots$	$\vdots$	$\vdots$
$2N_{\text{modes}}N_g+N_{\text{prop}}$	1	$-k_1$
$2N_{\text{modes}}N_g+N_{\text{prop}}+1$	1	k_1
$\vdots$	$\vdots$	$\vdots$
$2N_{\text{modes}}N_g+2N_{\text{prop}}$	N_{prop}	$k_{N_{\text{prop}}}$

the propagating part (D.31) to obtain for our T-matrix LS equation the form

$$T_{mn}(k,k_n)=V_{mn}(k,k_n)+\sum_{l=1}^{N_{\text{modes}}}\sum_{j=1}^{2N_g}\frac{v_j|q_j|}{2\pi}\frac{V_{ml}(k,q_j)T_{ln}(q_j,k_n)}{k_l^2-q_j^2}+$$
$$\sum_{l=1}^{N_{\text{prop}}}\left(\frac{-k_l}{4\pi}\sum_{j=1}^{2N_g}\frac{v_j}{k_l^2-q_j^2}-\frac{i}{4}\right)\left(V_{ml}(k,-k_l)T_{ln}(-k_l,k_n)+V_{ml}(k,k_l)T_{ln}(k_l,k_n)\right). \tag{D.33}$$

This is still an equation with two indices but in numerical calculation it is preferable to work with equations with only one index. We therefore define the map $\mu\leftrightarrow(l,k)$ given in Table D.2. As in the 1D case we define a matrix D

$$D_\mu=\begin{cases}\frac{v_j|q_j|}{2\pi}\frac{1}{k_l^2-q_j^2} & \mu=1,\ldots,2N_{\text{modes}}N_g,\\ \frac{-k_l}{4\pi}\sum_{j=1}^{2N_g}\frac{v_j}{k_l^2-q_j^2}-\frac{i}{4} & \mu=2N_{\text{modes}}N_g+1,\ldots,2N_{\text{modes}}N_g+2N_{\text{prop}}.\end{cases} \tag{D.34}$$

Note that if there is only one propagating mode and no evanescent modes the matrix D reduced to the one given in the 1D case (cf. Equation (D.20)) except for a factor $|q_j|/2\pi$ or $k_l/2\pi$. This is exactly the factor that enters the LS equation for the T-

matrix (D.25), because of the different normalization in the 2D/3D case. Denoting $(m, k) = \mu_0$ and $(n, k_n) = \nu_0$, using the map in Table D.2 and the above definition of the D matrix, the LS equation (D.33) is transformed into

$$T_{\mu_0\nu_0} = V_{\mu_0\nu_0} + \sum_{\mu} V_{\mu_0\mu} D_{\mu} T_{\mu\nu_0}. \tag{D.35}$$

This is the exact same form as obtained in the 1D case in Equation (D.21), and is solved by the same means.

Bibliography

[1] G. E. Moore, *Cramming more components onto integrated circuits*, Electronics **38**, 114 (1965).

[2] G. E. Moore, in *2003 IEEE International Solid-State Circuits Conference. Digest of Technical Papers.* (2003), vol. 1, pp. 20–23.

[3] Richard P. Feynman, *The Pleasure of Finding Things Out - The Best Short Works of Richard P. Feynman* (Allen Lane, The Penguin Press, 1999), chap. There's Plenty of Room at the Bottom, pp. 117–140.

[4] A. Aviram and M. A. Ratner, *Molecular rectifiers*, Chem. Phys. Lett. **29**, 277 (1974).

[5] M. A. Reed, C. Zhou, C. J. Muller, T. P. Burgin, and J. M. Tour, *Conductance of a Molecular Junction*, Science **278**, 252 (1997).

[6] A. M. Rawlett, T. J. Hopson, L. A. Nagahara, R. K. Tsui, G. K. Ramachandran, and S. M. Lindsay, *Electrical measurements of a dithiolated electronic molecule via conducting atomic force microscopy*, Appl. Phys. Lett. **81**, 3043 (2002).

[7] J. Reichert, R. Ochs, D. Beckmann, H. B. Weber, M. Mayor, and H. v. Löhneysen, *Driving Current through Single Organic Molecules*, Phys. Rev. Lett. **88**, 176804 (2002).

[8] S. Kubatkin, A. Danilov, M. Hjort, J. Cornil, J. Brédas, N. Stuhr-Hansen, P. Hedegård, and T. Bjørnholm, *Single-electron transistor of a single organic molecule with access to several redox states*, Nature **425**, 698 (2003).

[9] R. H. M. Smit, Y. Noat, C. Untiedt, N. D. Lang, M. C. van Hemert, and J. M. van Ruitenbeek, *Measurement of the conductance of a hydrogen molecule*, Nature **419**, 906 (2002).

[10] W. Tian, S. Datta, S. Hong, R. G. Reifenberger, J. I. Henderson, and C. P. Kubiak, *Resistance of molecular nanostructures*, Physica E **1**, 304 (1997).

[11] M. Di Ventra and N. D. Lang, *Transport in nanoscale conductors from first principles*, Phys. Rev. B **65**, 045402 (2001).

[12] M. Brandbyge, J. Mozos, P. Ordejón, J. Taylor, and K. Stokbro, *Density-functional method for nonequilibrium electron transport*, Phys. Rev. B **65**, 165401 (2002).

[13] Y. Imry and R. Landauer, *Conductance viewed as transmission*, Rev. Mod. Phys. **71**, S306 (1999).

[14] Robert G. Parr and Weitao Yang, *Density-Functional Theory of Atoms and Molecules* (Oxford University Press, 1989).

[15] R. M. Dreizler and E. K. U. Gross, *Density Functional Theory - An approach to the Quantum Many-Body Problem* (Springer-Verlag Germany, 1990).

[16] P. Hohenberg and W. Kohn, *Inhomogeneous Electron Gas*, Phys. Rev. **136**, B864 (1964).

[17] W. Kohn and L. J. Sham, *Self-Consistent Equations Including Exchange and Correlation Effects*, Phys. Rev. **140**, A1133 (1965).

[18] J. C. Slater, *A Simplification of the Hartree-Fock Method*, Phys. Rev. **81**, 385 (1951).

[19] Attila Szabo and Neil S. Ostlund, *Modern Quantum Chemistry - Introduction to Advanced Electronic Structure Theory* (Dover Publications, Inc., New York, 1996).

[20] Trygve Helgaker, Poul Jørgensen, and Jeppe Olsen, *Molecular Electronic-Structure Theory* (John Wiley & Sons Ltd., 2000).

[21] S. F. Boys, *Electronic wave functions. I. A general method of calculation for the stationary states of any molecular system*, Proc. Roy. Soc. (London) **A200**, 542 (1950).

[22] E. R. Davidson and D. Feller, *Basis Set Selection for Molecular Calculations*, Chem. Rev. **86**, 681 (1986).

[23] Warren J. Hehre, Leo Radom, Paul v. R. Schleyer, and John A. Pople, *Ab Initio Molecular Orbital Theory* (John Wiley & Sons, Inc., 1986).

[24] R. Ditchfield, W. J. Hehre, and J. A. Pople, *Self-Consistent Molecular-Orbital Methods. IX. An Extended Gaussian-Type Basis for Molecular-Orbital Studies of Organic Molecules*, J. Chem. Phys. **54**, 724 (1971).

[25] W. J. Hehre, R. Ditchfield, and J. A. Pople, *Self-consistent Molecular Orbital Methods. XII. Further Extensions of Gaussian-Type Basis Sets for Use in Molecular Orbital Studies of Organic Molecules*, J. Chem. Phys. **56**, 2257 (1972).

[26] P. C. Hariharan and J. A. Pople, *The Influence of Polarization Functions on Molecular Orbital Hydrogenation Energies*, Theoret. chim. Acta (Berl.) **28**, 213 (1973).

[27] S. Obara and A. Saika, *Efficient recursive computation of molecular integrals over Cartesian Gaussian functions*, J. Chem. Phys. **84**, 3963 (1986).

[28] Y. C. Zheng and J. Almlöf, *Density functionals without meshes and grids*, Chem. Phys. Lett. **214**, 397 (1993).

[29] G. Berghold, J. Hutter, and M. Parrinello, *Grid-free DFT implementation of local and gradient-corrected XC functionals*, Theor. Chem. Acc. **99**, 344 (1998).

[30] J. E. Almlöf and Y. C. Zheng, *Recent Advances in Density Functional Methods - Part II* (World Scientific, 1997), vol. 1 of *Recent Advances in Computational Chemistry*, chap. A Grid-Free Implementation of Density Functional Theory, pp. 15 – 40.

[31] Rubin H. Landau, *Quantum Mechanics II - A Second Course in Quantum Theory* (John Wiley & Sons, Inc., 1996), 2nd ed.

[32] Claude Cohen-Tannoudji, Bernard Diu, and Franck Laloë, *Quantum Mechanics*, vol. 1 (John Wiley & Sons, 1977).

[33] Supriyo Datta, *Electronic Transport in Mesoscopic Systems* (Cambridge University Press, 2002).

[34] W. Heitler, *The quantum theory of radiation* (Dover Publications, Inc., New York, 1984).

[35] V. E. Barlette, M. M. Leite, and S. K. Adhikari, *Integral equations of scattering in one dimension*, Am. J. Phys. **69**, 1010 (2001).

[36] M. I. Haftel and F. Tabakin, *Nuclear Saturation and the Smoothness of Nucleon-Nucleon Potentials*, Nuclear Physics **A158**, 1 (1970).

[37] Eugen Merzbacher, *Quantum Mechanics* (John Wiley & Sons, Inc., 1998), 3rd ed.

[38] Henrik Bruus and Karsten Flensberg, *Introduction to Many-body Quantum Theory in Condensed Matter Physics* (Lecture Notes, University of Copenhagen and Technical University of Denmark, 2002).

[39] M. Büttiker, Y. Imry, R. Landauer, and S. Pinhas, *Generalized many-channel conductance formula with application to small rings*, Phys. Rev. B **31**, 6207 (1985).

[40] P. F. Bagwell, *Evanescent modes and scattering in quasi-one-dimensional wires*, Phys. Rev. B **41**, 10354 (1990).

[41] G. Cattapan and E. Maglione, *Coupled-channel integral equations for quasi-one-dimensional systems*, Am. J. Phys. **71**, 903 (2003).

[42] David K. Ferry and Stephen M. Goodnick, *Transport in Nanostructures* (Cambridge University Press, 2001).

[43] John H. Davies, *The Physics of Low-Dimensional Semiconductors - An Introduction* (Cambridge University Press, 2000).

[44] Y. B. Levinson, M. I. Lubin, and E. V. Sukhorukov, *Short-range impurity in a saddle-point potential: Conductance of a microjunction*, Phys. Rev. B **45**, 11936 (1992).

[45] S. A. Gurvitz and Y. B. Levinson, *Resonant reflection and transmission in a conducting channel with a single impurity*, Phys. Rev. B **47**, 10578 (1993).

[46] V. Vargiamidis and O. Valassiades, *Shape effects on scattering in three-dimensional quantum wires*, J. Appl. Phys. **92**, 302 (2002).

[47] B. J. van Wees, H. van Houten, C. W. J. Beenakker, J. G. Williamson, L. P. Kouwenhoven, D. van der Marel, and C. T. Foxon, *Quantized Conductance of Point Contacts in Two-Dimensional Electron Gas*, Phys. Rev. Lett. **60**, 848 (1988).

[48] J. U. Nöckel and A. D. Stone, *Resonance line shapes in quasi-one-dimensonal scattering*, Phys. Rev. B **50**, 17415 (1994).

[49] J. M. van Ruitenbeek, A. Alvarez, I. Piñeyro, C. Grahmann, P. Joyez, M. H. Devoret, D. Esteve, and C. Urbina, *Adjustable nanofabricated atomic size contacts*, Rev. Sci. Instrum. **67**, 108 (1996).

[50] H. B. Weber, J. Reichert, F. Weigend, R. Ochs, D. Beckmann, M. Mayor, R. Ahlrichs, and H. v. Löhneysen, *Electronic transport through single conjugated molecules*, Chem. Phys. **281**, 113 (2002).

[51] W. Tian, S. Datta, S. Hong, R. Reifenberger, J. I. Henderson, and C. P. Kubiak, *Conductance spectra of molecular wires*, J. Chem. Phys. **109**, 2874 (1998).

[52] J. Chen, M. A. Reed, A. M. Rawlett, and J. M. Tour, *Large On-Off Ratios and Negative Differential Resistance in a Molecular Electronic Device*, Science **286**, 1550 (1999).

[53] N. D. Lang, *Resistance of Atomic Wires*, Phys. Rev. B **52**, 5335 (1995).

[54] M. Di Ventra, S. T. Pantelides, and N. D. Lang, *First-Principles Calculation of Transport Properties of a Molecular Device*, Phys. Rev. Lett. **84**, 979 (2000).

[55] G. C. Liang, A. W. Gosh, M. Paulsson, and S. Datta, *Electrostatic potential profiles of molecular conductors*, Phys. Rev. B **69**, 115302 (2004).

[56] I. S. Gradshteyn and I. M. Ryzhik, *Table of Integrals, Series, and Products* (Academic Press, Inc. San Diego, 1994), 5th ed.

[57] Norman Levinson and Raymond M. Redheffer, *Complex Varibles* (Holden-Day, Inc., 1970).

[58] Milton Abramowitz and Irene A. Stegun, *Handbook of Mathematical Functions* (Dover Publications, Inc., New York, 1965).